



**Identification and functional characterization of TGF- β inducible,
immunosuppressive miRNAs in human CD8⁺ T cells**

**Identifizierung und funktionelle Charakterisierung von TGF- β
induzierbaren, immunsuppressiven miRNAs in humanen CD8⁺ T Zellen**

Doctoral thesis for a doctoral degree at the Graduate School of Life Sciences, Julius-
Maximilians-Universität Würzburg,

Section: **Infection and immunity**

submitted by

Anoop Chandran P.

from

Trivandrum, India

Würzburg 2014

Submitted on:

Office stamp

Members of the *Promotionskomitee*:

Chairperson: Prof. Dr. Thomas Hünig

Primary Supervisor: Prof. Dr. Jörg Wischhusen

Supervisor (Second): Prof. Dr. Utz Fischer

Supervisor (Third): Prof. Dr. Gunter Meister

Date of Public Defence:

Date of Receipt of Certificates:

Affidavit

I hereby confirm that my thesis entitled '**Identification and functional characterization of TGF- β inducible, immunosuppressive miRNAs in human CD8⁺ T cells**', is the result of my own work. I did not receive any help or support from commercial consultants. All sources and/or materials applied are listed and specified in the thesis.

Furthermore, I confirm that this thesis has not yet been submitted as part of another examination process neither in identical nor in similar form.

Place: Würzburg

Date :

Signature

Acknowledgements

First and foremost I thank Prof. Dr. Jörg Wischhusen, for giving me the opportunity to work on my PhD, for the wonderful atmosphere, for the kind words and helping hands that he provided throughout my research in his lab, for his understanding and attempts to sharpen my strengths, for his tolerance towards my shortcomings and his honesty in pointing out my weaknesses, for sharing his passion for science and above all for being such a wonderful mentor.

I thank Prof. Dr. Gunter Meister, for the technical support during my miRNA research, for providing me various miRNA reagents, for his valuable comments and guidance during my doctoral research and for opening the doors to his lab during my research stays at the Max Planck Institute of Biochemistry, Martinsried. I also want to thank Prof. Dr. Utz Fischer for co-supervising my doctoral research and his critical comments and suggestions during my supervisory committee meetings.

My sincere thanks to Prof. Dr. Johannes Dietl for providing me the opportunity and the necessary assistance to work at the Frauenklinik, Würzburg.

I also thank Dr. Lasse Weinmann, Stefanie Schwinn, Dr. Matthias Wöfl and Dr. Andreas Keller for their help and support throughout my PhD.

I want to thank Prof. Dr. Thomas Hünig and all my colleagues at the GP Immunomodulation for teaching me the language 'Immunology'.

I extend my warmest gratitude towards Markus Junker and Dr. Ahmed Seida, two of my loving colleagues. Among ourselves we, shared meaningful discussions, offered helping hands throughout our tough times and above all for the wonderful friendship we cherish. I thank all my colleagues including Birgitt Fischer, Itsaso Montalban, Valentin Bruttel, Dr. Roland Stein, Evi Horn, Dr. Sebastian Häusler, Anna Schmidt, Lina Gerloff, Dr. Tina Schäfer, Dr. Dirk Pühringer, Dr. Joachim Diessner, Franziska Grän and Igor Vögele for all their support and for showing me that colleagues can be friends and friends can work together. I also want to thank my ex-colleagues Dr. Yvonne Dombrowski and Monica Ossadnik for helping me during the beginning of my PhD research.

I want to thank Dr. Stephan Schröder-Köhne and the entire administrative staff of the GSLS, Würzburg for offering a wonderfully moulded PhD study program, for the smooth and professional handling of administrative procedures and for their help and support right from my entry and all throughout my stay in Würzburg.

I thank my dear father Premachandran Nair and my mother Ambika KV for their love and unconditional support, for sacrificing their well being trying to save up for my good future, for letting me go when it was time for my higher education and for smiling at me even though they miss my presence at all times.

I want to thank my Valiyamma, Ammumma and my entire family for all their love and prayers.

I thank my wife Vrinda who lovingly stood beside me throughout our long distance relationship while I was in Würzburg and she was in India and Tübingen, for selflessly understanding me at all levels, for living alone on weekdays, for cooking wonderful food on weekends and above all for giving me our precious little Vaiga. Finally, I want give a big hug to my daughter Vaiga for coming like a bundle of joy, for her never ending, never tiring smile and for the new meaning you have brought into our lives.

Contents

1	SUMMARY	1
2	ZUSAMMENFASSUNG	2
3	INTRODUCTION	3
3.1	CD8 ⁺ T cells.....	3
3.2	Transforming growth factor- β (TGF- β).....	10
3.3	microRNAs (miRNAs)- biogenesis and action.	14
4	MATERIALS AND METHODS	23
4.1	Isolation of PBMCs.....	23
4.2	Cell culture	24
4.3	<i>In vitro</i> activation of CD8 ⁺ T cells.....	25
4.4	miRNA microarrays	26
4.5	Generation of small RNA libraries from CD8 ⁺ T cells	26
4.6	NK cell mRNA microarrays	27
4.7	Identification of new miRNAs	28
4.8	Quantification of miRNAs by qRT-PCR.....	28
4.9	Quantification of mRNAs by qRT-PCR	29
4.10	PCR amplifications	30
4.11	Transfection of CD8 ⁺ T cells	31
4.12	Antagomirs and mimics.....	32
4.13	Priming and generation of Melan-A- and STEAP-specific T cells	33
4.14	Reporter vectors and cloning	34
4.15	Transfection of HEK293T cells and dual reporter gene assays	36

4.16	Degranulation assay.....	37
4.17	Quantification of proteins in cell lysate.....	37
4.18	Immunoblot analysis.....	37
4.19	Surface staining for NKG2D receptor expression.....	38
4.20	Intracellular staining for IFN- γ and CD107a/LAMP1	38
4.21	ELISA	39
4.22	CD8 ⁺ T cell cytotoxicity assay	40
4.23	Statistics.....	40
5	RESULTS.....	41
5.1	miR-23a cluster is induced by TGF- β in CD8 ⁺ T cells.....	41
5.2	Comparison of miRNA arrays and deep sequencing.....	47
5.3	qRT-PCR validation of miRNA regulations.....	50
5.4	The 3'UTRs of LAMP1 and IFN- γ contain binding sites for members of the miR-23a cluster	53
5.5	The miR-23a cluster inhibits LAMP1 surface expression on activated CD8 ⁺ T cells.....	58
5.6	miR-23a cluster inhibits IFN- γ expression in activated CD8 ⁺ T cells.....	61
5.7	miRNAs from the miR-23a cluster inhibit IFN- γ expression in Melan-A-specific CD8 ⁺ T cells.....	65
5.8	The miR-23a cluster inhibits the cytotoxic activity of antigen-specific CD8 ⁺ T cells.....	69
5.9	Regulation of NKG2D surface expression by TGF- β	71
6	DISCUSSION	77
6.1	Induction of the miR-23a cluster by TGF- β and functional characterization of its immunomodulatory functions.....	77
6.2	Regulation of NKG2D/DAP10 surface expression by TGF- β	83
7	PUBLICATIONS:	84

8	ABBREVIATIONS	86
9	REFERENCES	87
10	CURRICULUM VITAE	102

1 Summary

While TGF- β is able to regulate miRNA expression in numerous cell types, TGF- β -dependent changes in the miRNA profile of CD8⁺ T cells had not been studied before. Considering that TGF- β suppresses CD8⁺ T cell effector functions in numerous ways, we wondered whether induction of immune-regulatory miRNAs could add to the known transcriptional effects of TGF- β on immune effector molecules. In this study, we used miRNA arrays, deep sequencing and qRT-PCR to identify miRNAs that are modulated by TGF- β in human CD8⁺ T cells. Having found that the TGF- β -dependent downregulation of NKG2D surface expression in NK cells and CD8⁺ T cells does not go along with a corresponding reduction in mRNA levels, this pathway appeared to be a possible target of TGF- β -inducible miRNAs. However, this hypothesis could not be confirmed by miRNA reporter assays. Instead, we observed that DAP10 transcription is suppressed by TGF- β which in turn negatively affects NKG2D surface expression. In spite of promising preliminary experiments, technical difficulties associated with the transfection of primary NK cells and NK cell lines unfortunately precluded the final proof of this hypothesis.

Instead, we focused on the TGF- β -induced changes in the miRNome of CD8⁺ T cells and confirmed the induction of the miR-23a cluster members, namely miR-23a, miR-27a and miR-24 by three different techniques. Searching for potential targets of these miRNAs which could contribute to the immunosuppressive action of TGF- β in T cells, we identified and confirmed a previously unknown regulation of IFN- γ mRNA by miR-27a and miR-24. Newly generated miRNA reporter constructs further revealed that LAMP1 mRNA is a target of miR-23a. Upon modulation of the miR-23a cluster in CD8⁺ T cells by the respective miRNA antagomirs and mimics, significant changes in IFN- γ expression confirmed the functional relevance of our findings. Effects on CD107a/LAMP1 expression were, in contrast, rather minimal. Still, overexpression of the miR-23a cluster attenuated the cytotoxic activity of antigen-specific CD8⁺ T cells. Taken together, these functional data reveal that the miR-23a cluster not only is induced by TGF- β , but also exerts a suppressive effect on CD8⁺ T-cell effector functions, even in the absence of TGF- β signaling.

2 Zusammenfassung

Obwohl bekannt war, dass TGF- β die miRNA Expression in zahlreichen Zelltypen moduliert, waren TGF- β abhängige Veränderung des miRNA Profils in CD8⁺ T Zellen noch nicht untersucht worden. Da TGF- β die Effektorfunktionen von CD8⁺ T Zellen aber in vielfältiger Weise inhibiert, fragten wir uns, ob die transkriptionellen Effekte, die TGF- β bekanntermaßen auf Immuneffektormoleküle ausübt, noch durch die Induktion immunregulatorischer miRNAs ergänzt werden. Daher nutzten wir miRNA Arrays, Genomsequenzierungstechniken und Echtzeit-PCR um miRNAs zu identifizieren, welche in humane CD8⁺ T Zellen von TGF- β moduliert werden. Die Beobachtung, dass die TGF- β -abhängige Herunterregulation der NKG2D Oberflächenexpression in Natürlichen Killerzellen und CD8⁺ T Zellen nicht mit einer entsprechenden Verringerung der mRNA Menge einhergeht, ließ zudem vermuten, dass dieser Signalweg über miRNAs reguliert werden könnte. Nach verschiedenen miRNA Reporterassays musste diese Hypothese jedoch verworfen werden. Stattdessen zeigte sich, dass TGF- β die Transkription von DAP10 inhibiert was wiederum die Oberflächenexpression von NKG2D limitieren sollte. Trotz viel versprechender initialer Experimente scheiterte der letztgültige Beweis dieser Hypothese aber an der ungenügenden Transfizierbarkeit von primären NK Zellen sowie von NK Zelllinien.

Daher konzentrierten wir uns im Weiteren auf die durch TGF- β induzierten Veränderungen im miRNom von CD8⁺ T Zellen und konnten mit drei verschiedenen Techniken die Induktion des miR-23a Clusters (mit den einzelnen miRNAs miR-23a, miR-27a und miR-24) bestätigen. Auf der Suche nach potentiellen immunregulatorisch relevanten Zielgenen dieser miRNAs konnten wir erstmals eine Regulation von IFN- γ durch miR-27a und miR-24 nachweisen. Zu diesem Zweck generierte miRNA Reporterkonstrukte zeigten zudem, dass LAMP1 durch miR-23a reguliert wird. Nach Modulation des miR-23a Clusters durch die entsprechenden miRNA Antagomir und Surrogat-Konstrukte konnten wir auch in CD8⁺ T Zellen signifikante Veränderungen der IFN- γ Expression nachweisen und somit die funktionelle Relevanz unserer Befunde bestätigen. Die Effekte auf die Expression von CD107a/LAMP1 waren hingegen nur minimal. Trotzdem führte die Überexpression des miR-23a Clusters zu einer Verringerung der zytotoxischen Aktivität von antigenspezifischen CD8⁺ T Zellen. Zusammen genommen belegen diese funktionellen Untersuchungen, dass das miRNA-23a Cluster, welches durch TGF- β induziert wird, zur Hemmung der Effektorfunktionen in CD8⁺ T Zellen beiträgt, und zwar sowohl in Gegenwart als auch in Abwesenheit von TGF- β .

3 Introduction

3.1 CD8⁺ T cells

CD8⁺ T cells are important effectors of our adaptive immune response towards virus (and other pathogens) infected cells, damaged cells as well as against tumor cells.

3.1.1 Birth of a CD8⁺ T cell

It all begins in the bone marrow where the hematopoietic stem cells reside. These multipotent cells give rise to pluripotent lymphoid progenitors which migrate through the blood stream and reach the thymus. In the thymus they lose their B cell potency through activation of Notch1 signaling (1). The resulting bi-potent (NK and T cell) progenitors (2) eventually give up their NK cell potency to form double negative (DN- no CD4 or CD8) T cell precursors. DN T cells then assemble a pre- T cell receptor (TCR) which contains either α and β (in almost 95% of cases) or, more rarely, γ and δ chains. The transition from the expression of pre-TCR to mature TCR involves recombination at the TCR- α locus while undergoing 6-8 cell divisions. At this stage, there is low surface expression of the TCR along with CD3/ ζ . Co-receptor expression also begins by the expression of CD8 followed by CD4 resulting in a double positive (DP) T cell. DPs then prepare to audition for their survival in front of cortical thymic epithelial cells (cTECs).

Their verdict to live is almost entirely based on the avidity/affinity of the TCRs towards the cTEC MHC-self peptide complexes. DPs with TCRs which do not interact or interact very poorly with the cTEC MHC-self peptide complexes lack necessary survival signals and die by neglect. If the TCRs show an intermediate affinity for cTEC MHC-self peptide complexes, they are induced to differentiate into mature single positive cells through positive selection. At the same time, cells which interact too strongly with the cTEC MHC-self peptide complexes are potentially dangerous if allowed to travel to peripheral organs as they can cause autoimmunity and are thus induced to undergo apoptosis (negative selection) (3-5).

DPs differentiate into single positive cells by complicated silencing of the transcription of one of the co-receptors (CD4 or CD8). This process has been extensively reviewed by Littman et al. (6). Several hypotheses had been devised to explain this process, from an instruction model, to a selection model as well as a default model. In short, the instruction model proposed that the DP cells were instructed by the appropriate MHCs to terminate the expression of one specific co-receptor. The selection model stated that the DP cells randomly

selected either a CD4 or CD8 co-receptor and then waited for their chance of survival. Studies contradicting and supporting the 2 hypotheses surfaced (7-10). The default model however proposed that the DP cells chose to keep CD4 expression unless the TCR recognized a Class I MHC (Figure 1).

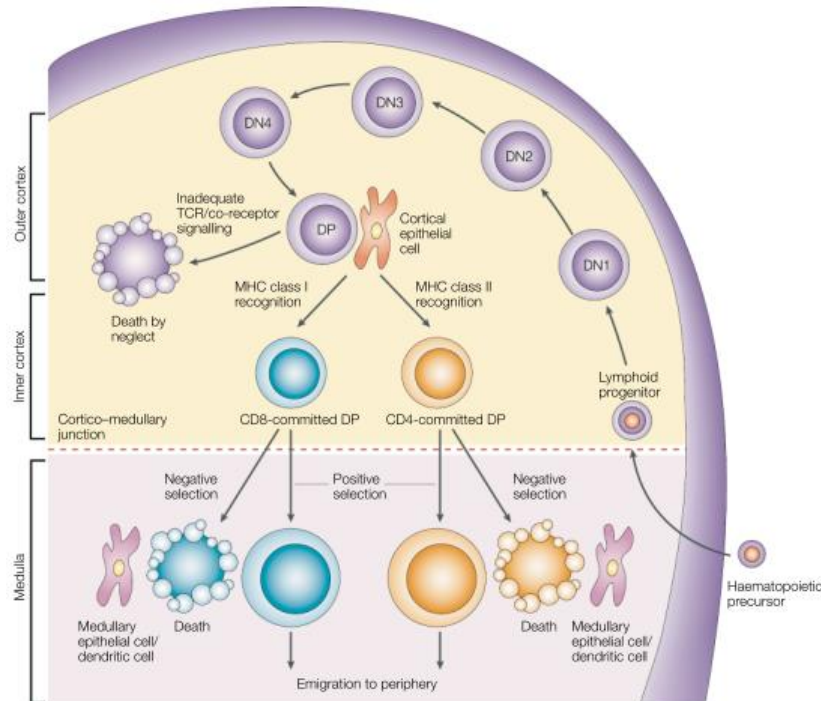


Figure 1: T cell development in the thymus. Lymphoid progenitors enter the lymph nodes and progressively differentiate through various DN stages to DP, finally ending up as single positive T cells. (Image source: Germain R, Nature Reviews Immunology, 2002)

However, later studies shed light on a new model where the DP cells gradually lose the expression of both co-receptors only to recover them to first express CD4 and later on CD8 (hence a $CD4^{high}$, $CD8^{low}$ stage) to progress towards a single positive stage. This model has been reviewed by Germain R (3).

3.1.2 Activation of a $CD8^{+}$ T cell

A $CD8^{+}$ T cell that is formed in the thymus emigrates into circulation and homes to the lymph nodes by the interaction of L-selectin with CCR7 (11). It is in the peripheral T cell area within the lymph nodes that the dendritic cells (DCs) deliver them the first kiss with their cognate antigen (12, 13). Upon activation, the naïve $CD8^{+}$ T cells divide and differentiate into a phenotypically and functionally heterogeneous population of effector cells. Cytotoxic T cells (CTLs) are short-lived yet functionally more potent effector cells. They are thought to be derived from naïve cells that received a high level stimulation. On the other hand, those cells that received a low stimulation are likely the long-lived memory precursor effector cells (14,

15). Other studies have revealed that a single naïve CD8⁺ T cell can give rise to both CTLs and memory cells during the initial rounds of cells division through an asymmetric distribution of the transcription factor T-bet and proteasomal machinery, whereby the cells which receive more T-bet and less proteasomes become the short lived effectors (16, 17). Upon adequate antigenic stimulation, a naïve CD8⁺ T cell can undergo about 19 cell divisions in a week (18). Memory cells that persist in circulation or in secondary lymphoid organs can respond quickly and more effectively to repeated exposure to the antigen. CD28 receptor on T cells can interact with B7-1 and B7-2 receptors on antigen presenting cells to provide co-stimulation. T cells can also receive a negative activation stimulus from B7-1 and B7-2 through its CTLA4 receptors (19). A scheme summarizing the various signals a T cell receives from a DC or an antigen presenting cell (APC) and the signaling pathways that get kick-started are shown in **Figure 2**.

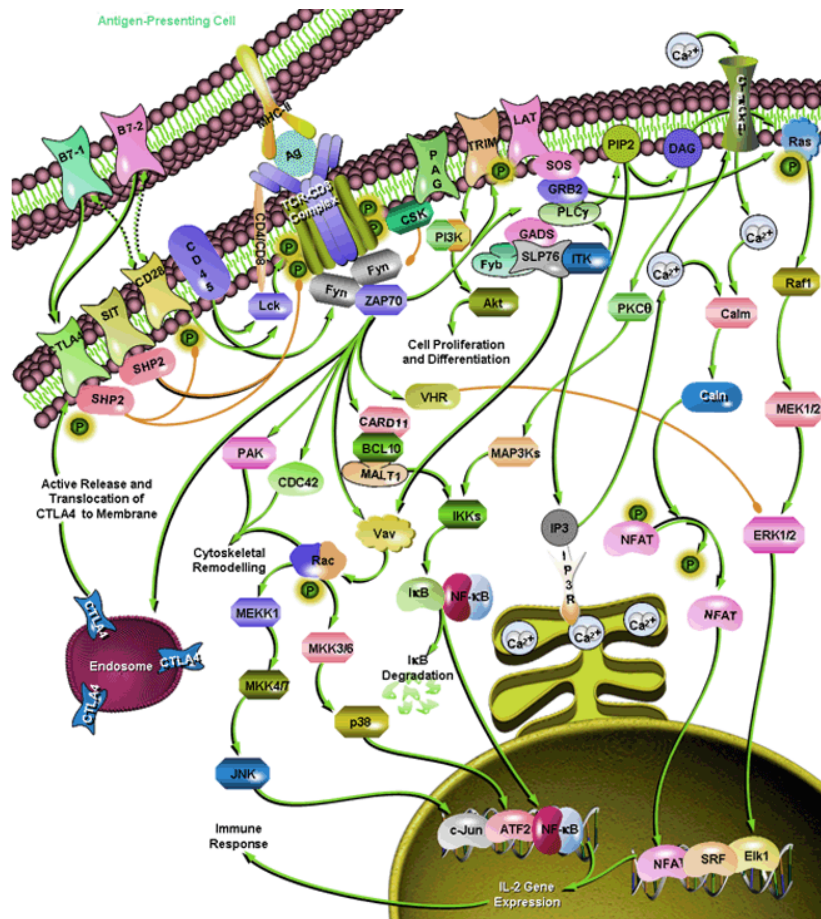


Figure 2: T cell activation by an APC and the various signaling pathways. (Image source: http://www.sabiosciences.com/pathway.php?sn=TCR_Signaling).

In addition to TCR and CD28 co-stimulation, a CD8⁺ T cell can get further stimulated by IL-12, Type I Interferons as well as co-stimulated by 4-1BB, CD27 and OX-40 (14, 15, 20). IL-2 is yet another CD8⁺ T cell activation cytokine, which signals via the CD25 receptor, whose

amounts are critical, where higher amounts favor CTL phenotypes and lower amounts favor a memory phenotype (21, 22). This is the reason why *in vitro* stimulation of T cells using anti-CD3 and anti-CD28 immobilized on beads efficiently activate and expand them. Once activated and expanded, the CD8⁺ T cells upregulate CXCR3 to exit the lymph nodes to migrate towards the site of infection or action (23).

3.1.3 Functions of CD8⁺ T cells

Based on expression of CCR7, circulating CD8⁺ memory T cells can be further divided into two functionally distinct subsets with distinct functional properties: CCR7⁺ central memory cells (T_{CM}) express lymph-node homing receptors and lack immediate effector function, but efficiently stimulate dendritic cells and differentiate into CCR7⁻ effector memory cells (T_{EM}) cells upon secondary stimulation. CCR7⁻ effector memory cells express receptors for migration to inflamed tissues and display immediate effector function (24). The major effector function of an activated CD8⁺ T cell is to kill its target cell which presents its cognate peptide on a self MHC class I molecule. The target cells are usually virus infected cells, cells with intracellular pathogens and tumor cells. Target cell lysis is achieved through 3 mechanisms, death-receptor mediated, lytic granule mediated, and cytokine mediated.

3.1.3.1 Death receptor mediated killing

Activated CD8⁺ T cells express death ligands like Fas ligand (CD178) which can engage Fas receptor (CD95) on target cells and initiate caspase dependent cell death through FADD (Fas associated death domain). FADD activates Caspase 8 which in turn directly kicks on a cascade of effector caspases (in type I cells). In so-called type II cells, Fas-mediated apoptosis is further amplified by activation of caspase 9 via BID, BAX and release of mitochondrial cytochrome (followed by Caspase 3) activation (25). Either mechanism can lead to the death of the target cell (**Figure 3**) – unless the cell is protected by anti-apoptotic proteins like Bcl-2, Bcl-xL, FLIP, IAP, XIAP etc. which are often overexpressed in cancer cells. The same mechanism and thus also the same anti-apoptotic strategies apply to cell death induction via TNF-related apoptosis-inducing ligand (TRAIL) (26, 27).

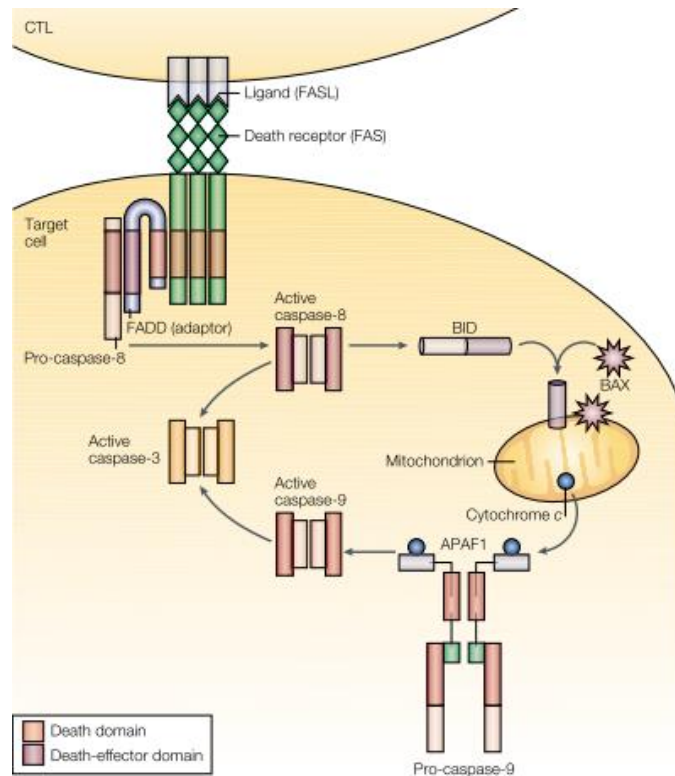


Figure 3: Target cytotoxicity through Fas by CTLs. FasL on CTLs engages Fas on the target cells and initiates Caspase mediated apoptosis. (Image source: Bleackley et al, Nature Reviews Immunology, 2002.)

3.1.3.2 Granule mediated killing

Upon activation via the TCR, a CD8⁺ T cell starts to armor itself by stocking up cytotoxic granules. These granules where all the components bath in an acidic pH contain predominantly perforin, granzymes, calreticulin and granulysin (28). These granules are surrounded by several proteins including lysosomal membrane proteins LAMP1 and LAMP2. When a granule-loaded CTL encounters a target cell, it forms an immunological synapse where the TCR interacts with the cognate peptide presented on the MHC of the target cell. This sets the stage for a granule attack. Microtubule rearrangement and directional procession of the granules then follow which result in the secretion of granule components into the synapse. Perforin and granzymes (mainly A and B) form the fatal duo. It is a matter of debate how granzymes enter the target cells. A role for mannose-6-phosphate receptor (which is involved in granzyme packaging into granules) has been proposed by various studies but later studies showed that it was not essential. This dichotomy was later revealed to be due to the use of monomeric granzymes, which does not require mannose-6-phosphate receptor for target cell entry, in those experiments. Under physiological conditions, granzyme B is released complexed to proteoglycans whose entry into target cells can be mediated by mannose-6-phosphate (29, 30). Another widely accepted mechanism is that perforin forms pores on the

target cell through which the granzymes enter (31). These 2 mechanisms are depicted in **Figure 4**.

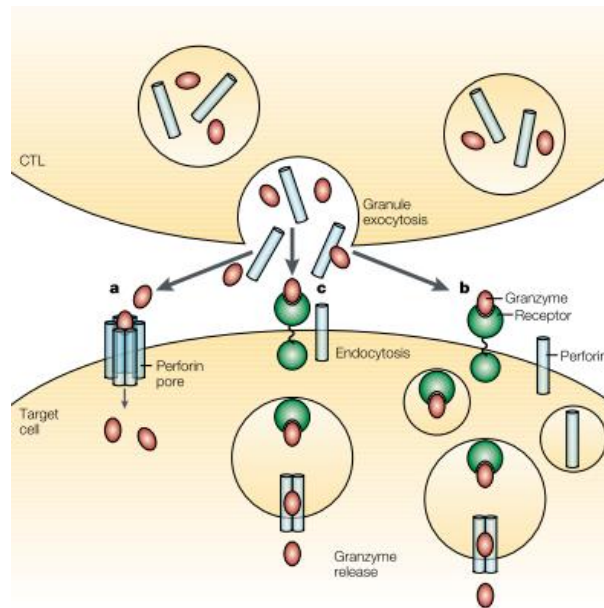


Figure 4: Release of cytotoxic granules and entry of granzymes into the target cell. (Image source Bleackley et al, Nature Reviews Immunology, 2002.)

The best characterized granzymes are the most expressed A and B forms. Granzyme B can cleave proteins after aspartate residues and activates the caspase cleavage cascade by activating caspase 3 and 8 to inflict target cell apoptosis (32-34) as depicted in **Figure 5**.

Cytotoxic granule mediated killing is faster because of the quick release of pre-formed granules. However some studies indicate that there are pre-existing distinct granules in CTLs that store Fas ligand which can be exposed quickly. This would result in 2 waves of Fas ligand exposure (35).

Such potent cytolytic molecules can potentially harm the T cells during storage and delivery. The granule essentially prevents such a catastrophe by maintaining an acidic pH (about 5.5). Calreticulin plays an important role by interacting with perforin monomers keeping them apart within the granules and is later dissociated after exocytosis enabling perforin pore formation (36). Another study highlighted the importance of serine protease inhibitor 6 which maintains granule integrity by inhibiting granzyme B activity within granules (37).

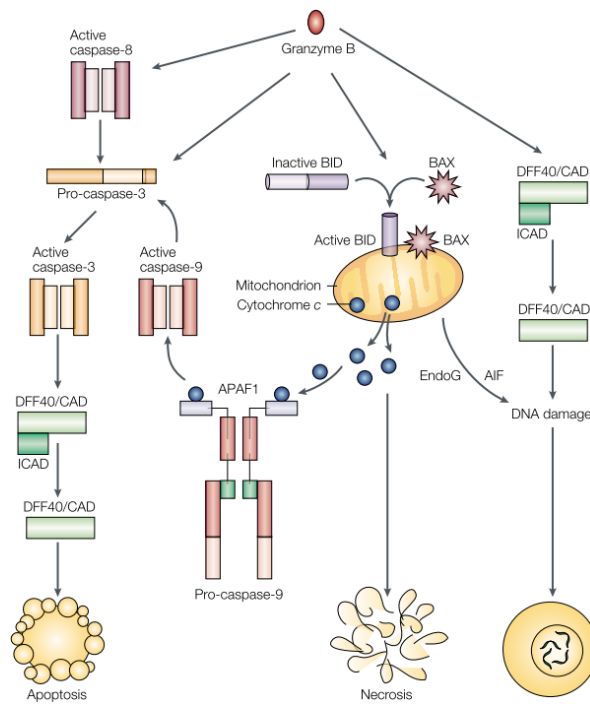


Figure 5: Initiation of caspase dependent and independent cell death by granzyme B. Once internalized by the target cell, granzyme B cleaves caspase 3 and 8 to initiate apoptosis. It can also initiate a BID, BAX and mitochondrial cytochrome mediated cell death pathway. (Image source Bleackley et al, Nature Reviews Immunology, 2002.)

Structural integrity and stability of the cytotoxic granules is also contributed by heavily glycosylated proteins that line the granules, namely LAMP (lysosome associated membrane protein) 1 and 2 (38). LAMP1 (also called CD107a) is a highly abundant lysosomal protein with its N terminal directed towards the granular lumen and spanning the granule membrane once. Intriguingly, the function of LAMP1 and LAMP2 within the lytic granules is largely unknown. Several studies indicate the protective function of LAMP1 and LAMP2 on the granule membrane from the acid hydrolases within, due to their extensive glycosylation. LAMP1 deletion in mice however led to a compensatory effect by an increase in LAMP2 production and almost no effect on lysosomal functions (39). Double (LAMP1 and LAMP2) knockout was however embryonically lethal in mice (40). Still, the importance of LAMP1 in cytotoxic granules was recently uncovered when researchers demonstrated that silencing of LAMP1 resulted in impaired granule mediated NK cell cytotoxicity (41). This was due to the inefficient delivery of perforin rather than granzymes into the granules. In the same study using time lapse imaging, LAMP1 was shown to play a vital role in granule mobility as well.

3.1.3.3 Cytokine mediated toxicity

Upon TCR activation, downstream signaling mediated through T-bet and eomesodermin (Eomes) drives the synthesis of various effector molecules, including Interferon-gamma (IFN- γ) and TNF- α . It has to be noted that T cells that are activated need not elicit all of the aforementioned toxicity mechanisms. For instance, virus specific CTLs are good producers of IFN- γ but show poor granule expression. This non-cytolytic control is particularly important in the clearance of virus infections with minimal self tissue damage. The only member of the type II class of interferons, IFN- γ inhibits viral replication within cells. It also exerts potent anti-proliferative, anti-angiogenic as well as pro-apoptotic anti-tumor effects (42-44). IFN- γ also induces MHC-class I expression on tumor cells which makes them susceptible to CD8⁺ T cell mediated killing (45). The efficacy of IFN- γ in clearing tumors has recently been demonstrated where the adoptive transfer of tumor specific CD4⁺ T cells induced tumor regression in a patient with epithelial cancer (46).

Uncontrolled T cell activation as well as inefficient contraction of an immune response after an infection has been cleared can be detrimental to our body. Hence several immune inhibitory check points are placed during an immune response. One of the cytokines that play an important role in preventing autoimmune responses and restoring homeostasis after infection is TGF- β .

3.2 Transforming growth factor- β (TGF- β)

In 1983, TGF- β was first purified from human platelet extract (47). Since then, a large group of structurally related cell regulatory proteins have been discovered and have formed a group called the TGF- β superfamily named after the founding member. This superfamily has been broadly grouped into 4 major sub-families, the decapentaplegic-Vg-related (DVR) related subfamily (including the bone morphogenetic proteins and the growth & differentiation factors), activins & inhibins, TGF- β s and a group encompassing various other divergent members (48, 49). It is believed that the TGF- β system originated about one billion years ago, before the divergence of arthropods from vertebrates, and has then adapted over the years to regulate newly emerged systems in higher organisms (50). In mammals, TGF- β exists in 3 homologous isoforms, TGF- β -1, 2 and 3 which are encoded by different genes (51). The term TGF- β is widely used (including in the study described in my thesis) to refer to TGF- β 1. Right from its discovery TGF- β was a bit of a mystery molecule because of the large spectrum of divergent effects it had on several cell types, many of them depending on the

cellular context. It could inhibit and promote cell growth, suppress pre-malignant cells but promote metastatic ones, enhance pluripotency as well as promote differentiation, etc. This lead to the expectation of a complicated pathway until the relatively simple pathway mediated by SMAD proteins was uncovered.

TGF- β is synthesized in a pre-pro-form. While the pre-region holds a signal peptide, the pro-TGF- β is processed in the Golgi by a furin-like peptidase (52) where the N-terminus pro-peptide of the immature protein is removed. A homodimer of the resulting latency associated protein (LAP) is non-covalently associated with a homodimer of mature TGF- β and is called latent TGF- β or the small latent complex (SLC). The SLC is either secreted as itself or associated with latent TGF- β -binding protein (LTBP) as a large latent complex (LLC). LTBP enables the targeting of TGF- β to the extracellular matrix (53). Latent TGF- β cannot bind to its receptors unless it is liberated from LAP and LTBP. *In vitro*, this can be achieved using extremes of pH, heat, or several proteases (53). *In vivo*, proven mechanisms for activation include proteolytic activation by transglutaminase, conformational change of LAP through physical interaction with thrombospondin and mechanical traction via $\alpha\beta 6$ integrins on epithelial cells (54-56). Having said so, very little is known about the expression of TGF- β , transcription of its message and protein synthesis. The vast untranslated regions (UTRs) in the TGB- β mRNA point towards post transcriptional regulations that are yet to be uncovered in different cellular contexts (57). In our immune system, TGF- $\beta 1$ is the predominant isoform that is expressed.

TGF- β mediates its effects through the type I (ALK5) and type II (TGF β RII) receptors. The active form of TGF- β binds TGF β RII. While TGF- $\beta 1$ and TGF $\beta 3$ bind to TGF β RII with high affinity, strong binding of TGF- $\beta 2$ to TGF β RII occurs in the presence of membrane bound betaglycan, also known as TGF β RIII (58). The active TGF- β dimer binds to the tetrameric ALK5 and TGF β RII receptor complex to initiate cell signaling (59). Ligand binding brings the type II receptor close to the type I receptor which then becomes activated. Activated type I receptor phosphorylates intracellular Smad proteins. p-Smads then localize to the nucleus and cause the transcriptional regulation of target genes (60). Smads can be grouped into three categories: 5 receptor-associated Smads (R-Smad-1, 2, 3, 5, and 8), 1 common Smad (Co-Smad-4), and two inhibitory Smads (I-Smad-6 and 7). R-Smads are sequestered in the cytoplasm in the absence of signaling. However, when they are phosphorylated by ALK-5, R-Smad-2 and 3 associate with Co-Smad4 and translocate into the nucleus (61) to bind to SBE (Smad-binding element). Smad-7, on the other hand, works downstream of ALK5 to inhibit TGF- β signaling. Instead of getting phosphorylated by ALK5, Smad-7 competes with R-

Smads for ALK-5 binding and recruits Smurf-containing E3 ubiquitinase complexes to degrade ALK5 (62, 63). Activated Smad protein complexes bind to DNA weakly, but they mostly associate with several other transcription factors to increase DNA affinity. This ability to associate with other molecules is responsible for the plethora of effects TGF- β has on various cells types (64, 65). The Smad-transcription factor complexes then recruit histone acetyl transferase (HAT)-coactivators (e.g., CBP/p300) or histone-deacetylase (HDAC) corepressors (e.g., Sno/Ski) to activate or repress target genes, respectively (65, 66). These signaling effects are summarized in **Figure 6**.

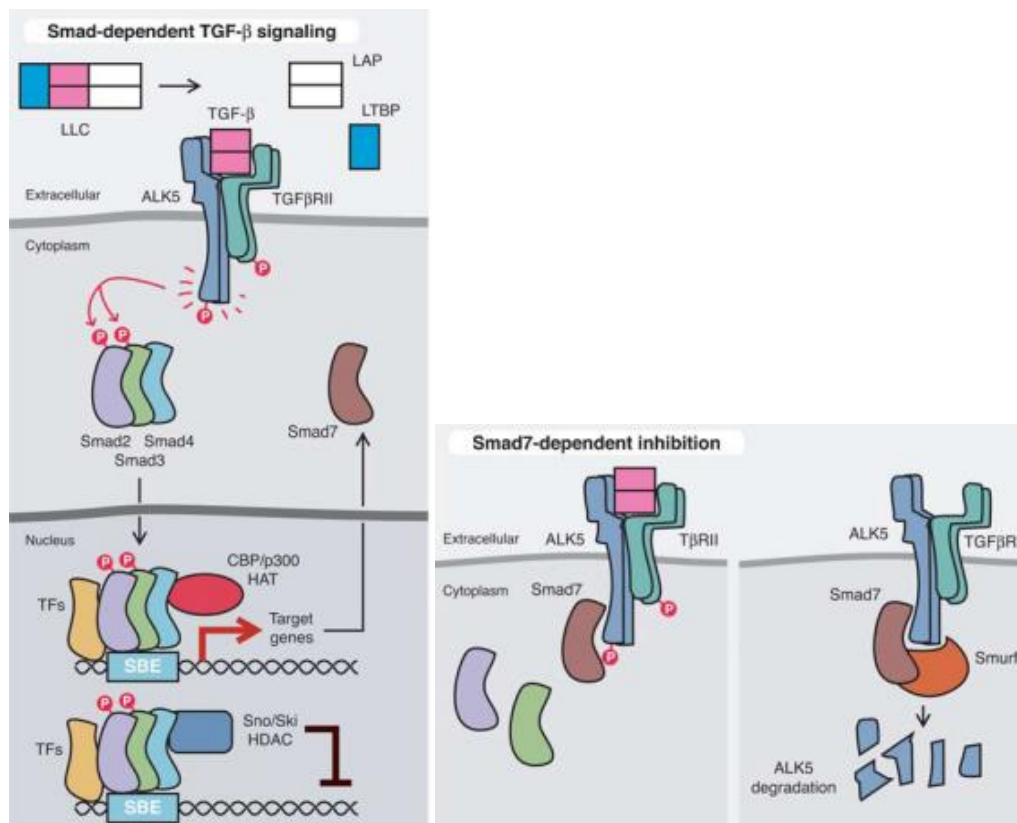


Figure 6: TGF- β signaling from membrane to nucleus. The figure on the left shows the pathway described above that involves the phosphorylation of R-Smads, association with co-Smads, nuclear translocation and transcriptional activation of genes. The figure on the right shows the inhibition of TGF- β signaling by Smad-7 through competition with R-Smads for ALK5 binding and ALK5 degradation. (Image source: Li et al, Annual. Rev. Immunology. 2006)

3.2.1 Effect of TGF- β on T cells

We may state that the overall effect of TGF- β on T cells is to bring about suppression of immune responses, but this statement needs a lot of clarification into the individual effects that TGF- β has on various T cell populations. TGF- β inhibits T cell proliferation and this is done predominantly by targeting IL-2 transcription. TGF- β also inhibits T cell proliferation

by inhibiting c-myc, cyclinD2, CDK4 and cyclin E expression in T cell lines and primary CD4⁺ T cells (67-69). However, activated T cells lower the expression of TGF- β receptor II and hence their proliferation is hardly affected by TGF- β .

This effect can be rescued by the addition of IL-10 which increases TGF- β receptor II expression (70). The inhibition of IL-2 by TGF- β is one of the important ways in which TGF- β prevents autoimmunity as evidenced by the hyperproliferation of thymocytes in TGF- β deficient mice. TGF- β can inhibit the differentiation of CD4⁺ T cells into either Th1 or Th2 phenotypes, which under controlled homeostatic conditions is a way to curb the reckless differentiation of those cell types that might result in autoimmunity and allergic reactions. TGF- β blocks Th1 differentiation predominantly by inhibiting T-bet (71) and by blocking IFN- γ production. TGF- β can transcriptionally activate IL-10 production which is largely anti-inflammatory (72).

My study focused on TGF- β -dependent, potentially miRNA-mediated effects on CD8⁺ T cells. As already mentioned, CD8⁺ T cells are our body's prime fighting front against intracellular pathogens (viruses) and tumors through mechanisms already described above. TGF- β inhibits the CD8⁺ T cell cytotoxic machinery in a number of ways. TGF- β critically targets the 5 faced 'cytotoxic program' of CD8⁺ T cells, namely, perforin, granzyme A, granzyme B, IFN- γ and FasL (73). It has been shown conclusively that TGF- β directly represses the transcription of granzyme B and IFN- γ through Smad signaling and subsequent binding to their respective TGF- β responsive ATF1/CREB binding sites (73). The non-direct inhibitory effects of TGF- β can be attributed in part to the reduction of T-bet expression in these cells (74). Reduced T-bet expression in TGF- β treated CD8⁺ T cells also counts for reduced IFN- γ production, though a mutualistic relationship between IFN- γ and T-bet expression makes it hard to determine in which way the repression occurs.

3.2.2 Tumors and TGF- β

As mentioned above, CD8⁺ T cells with their cytotoxic program are key mediators of our adaptive defense against neoplastic growth in our body. Since tumor outgrowth occurs in the presence of our immune system, tumors must have evolved several methods of immunosuppression and the TGF- β mediated mode stands out. In the initial tumor stages, TGF- β prevents cell proliferation, differentiation, survival, adhesion and metastatic progression (75). However, since tumors are genetically unstable, they often overcome or evolve beyond the suppressive effects of TGF- β . This is done predominantly by turning

insensitive towards TGF- β signaling through downregulation or mutation of TGF- β receptors and by harboring defects in the downstream signaling pathway (75). TGF- β is secreted by various tumors and is often a homeostatic response to the pre-malignant abnormal expansion of cells. Once the tumor has dealt with the anti-neoplastic effect of TGF- β , it uses the cytokine to its advantage. TGF- β induces EMT (epithelial to mesenchymal transition), a pathological step in tumorigenesis which has been demonstrated in breast cancer (76). As described earlier, immunosuppression by TGF- β is a key weapon in the armory of the tumor. In this context, inhibition of the activation receptor NKG2D on NK cell and CD8⁺ T cells is significant. The mechanisms behind TGF- β mediated NKG2D downregulation has not been deduced yet. Our studies have revealed that even when NKG2D mRNA expression is not significantly downregulated the protein level expression of NKG2D can be inhibited by TGF- β in a dose-dependent manner (77). Microarray and qRT-PCR data, however, showed that the expression of DAP10 (HCST or hematopoietic cell signal transducer) mRNA was inhibited when TGF- β was added to NK cells. Being aware that in human cells NKG2D signals exclusively through DAP10 and that the hexameric receptor complex on the cell surface consists of one NKG2D homodimer and 2 DAP10 homodimers (78, 79), DAP10 was brought into focus. All human CD8⁺ T cells constitutively express DAP10 while only activated CD8⁺ T cells in mice express it. It has been shown that resting NK cells in DAP10 deficient mice express little or no NKG2D on the cell surface (80). Based on our preliminary mRNA and protein data, we developed the hypothesis that TGF- β downregulates NKG2D receptor by targeting DAP10. The reasons bringing us towards this conclusion and the difficulties in proving it will be explained in the results section.

3.3 microRNAs (miRNAs)- biogenesis and action.

My thesis exposes the ability of TGF- β to suppress CD8⁺ T cells through a different, still primitively explored mechanism- the induction of immunosuppressive microRNAs (miRNAs). While a major part of our genome gets transcribed, only 2% gets translated into functional proteins. This very fact leaves us with the task to characterize a whole lot of untranslated RNA (non-coding RNA or ncRNA) molecules to fully understand the complex physiological and pathological events that take place in our body. So far, among the several discovered small ncRNAs like siRNA, piRNA, rasiRNA, tasiRNA, tncRNA, hcRNA, and scnRNA, the best studied are the miRNAs. miRNAs were first described in *Caenorhabditis elegans* by Victor Ambros and Gary Ruvkun's groups in 1993 (81).

miRNAs are transcribed by RNA polymerase II or RNA polymerase III into pri-miRNAs which are polyadenylated and capped (82-84). pri-miRNAs can be transcribed under the control of their own promoter independent of other genes or they can arise after intronic cleavage of mRNAs. Co-expression of different miRNAs is quite common (85) The miR-23a/miR-27a/miR-24-2 cluster (miR-23a cluster) is transcribed by RNA polymerase II by binding to its upstream promoter. These pri-miRNAs often undergo sequence editing of adenosine to inosine by ADARs (Adenosine Deaminases Acting on RNAs) (86, 87). This process greatly influences their further downstream processing in a positive or negative manner depending on the sequence of the pri-miRNAs. The pri-miRNA is then cleaved by RNase III enzyme Drosha with the aid of its binding precision partner DGCR8 or Pasha to form the pre-miRNA. It has been shown that TGF- β and BMPs induce miRNA maturation by regulating the activity of the Drosha-Pasha complex by recruiting RNA helicase DDX5 to enhance the processing of certain miRNAs (88).

Pre-miRNA is then transported out of the nucleus into the cytoplasm by Exportin 5 (XPO5) in combination with Ran-GTP (89). The timely uninterrupted transport of pre-miRNAs to the cytoplasm is crucial for the prevention of nuclear degradation of the pre-miRNAs. Cytoplasmic pre-miRNAs that show a high degree of complementarity in their double stranded region are nicked on the 3' arm by Argonaute 2 (AGO2) which possibly eases strand dissociation (90). The RNase III enzyme Dicer then chops the pre-miRNA to generate approximately 22 bp RNA duplexes with 2 nucleotide overhangs at the 3' end. Two proteins namely TRBP (Tar RNA binding protein) and PACT (protein activator of PKR) facilitate the binding and functioning of Dicer. Although different from the functional RISC (RNA induced silencing complex), the miRNA processing and RISC assembling is mediated by the RISC loading complex (RLC) comprising of all the above mentioned proteins (AGO2, Dicer, TRBP and PACT). After the formation of the 22 nucleotide duplex, Dicer, TRBP and PACT dissociate from the complex. The duplex then unwinds with the help of several helicases and the strand with its 5' end at the less stable base pair end of the duplex is loaded onto the RISC complex which includes the AGO2 protein. The events from pri-miRNA transcription to mature miRNA/RISC complex formation are summarized in **Figure 7**.

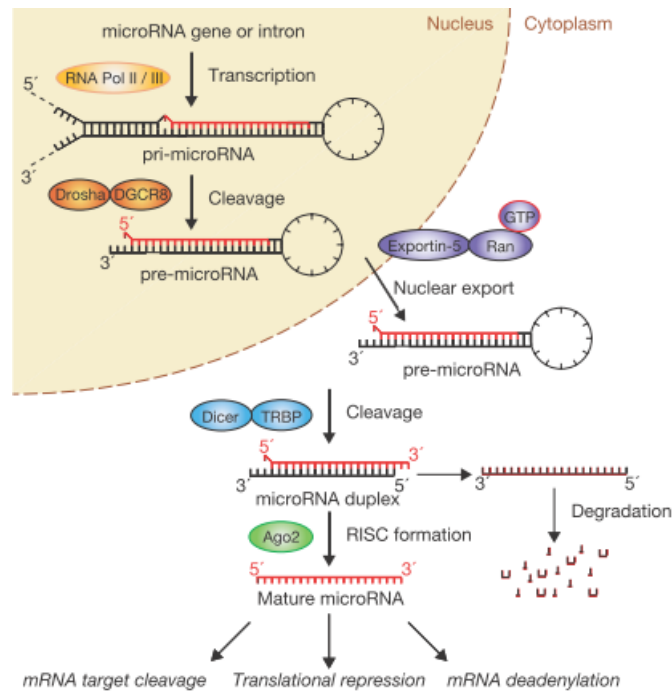


Figure 7: miRNA processing pathway. Mature miRNA synthesis via processing of pri- and pre-forms by the various protein complexes are depicted. (Image source: Julia Winter, Sven Diederichs et al., Nature Cell Biology March 2009)

RISC is a generic term for miRNA/siRNA containing protein complexes that are capable of targeting mRNAs to effect translational inhibition. Common feature of all RISC complexes are the presence of an Argonaute family protein which binds and places the regulatory short RNA (or guide strand) in a conformation that enables base pairing with target mRNAs. Several other proteins may be present alongside Argonaute that can complement its function. The guide strand binds with its 5' end (usually 2nd -8th bases) to target mRNAs by Watson-Crick base pairing (91, 92). The consequence of this base pairing is translational repression of the mRNA. Only at near perfect complementarity does the slicing activity of Argonaute (AGO2 in humans) cut the mRNA to destroy the reading frame (93). However, such extensive base pairing is uncommon in the case of mammalian miRNAs and more often miRNAs pair with their 2nd -7th bases to the 3'UTR of an mRNA (referred as the 'seed region') to initiate translational repression (94). Several modes of action have been described to explain how translational repression is carried out by miRNAs. This has been extensively reviewed in *Cell* (95). It has been shown that for miRNAs to inhibit translation, mRNAs need to have an intact 7-methylguanylate (m⁷G) cap and a poly A tail (96). miRNAs can inhibit translation initiation by utilizing the m⁷G binding motif of Argonaute proteins (97). Evidence for a possible interference during translation comes from the co-sedimentation of miRNAs with polyribosomes (98).

3.3.1 miRNA quantification, profiling and functional characterization

In order to understand the involvement of miRNAs in various biochemical processes and pathways it is necessary to quantify their expression. Since they are not translated, miRNAs are quantified on RNA level. Advanced biochemical methods enable the isolation of intact miRNAs from a wide variety of sources like, formalin fixed paraffin embedded (FFPE) sections, fresh tissues, tumor cell lines, immune cells, whole blood, serum and several other body fluids. miRNA profiles from several body fluids have been identified as potential biomarkers for diseases (99-101). Most miRNA isolation procedures are similar to established RNA isolation methods but include an additional small RNA enrichment process involving silica columns or stringent precipitation steps. miRNAs have been found to be extremely stable even when isolated from FFPE sections, when compared to mRNAs, making them attractive tools in clinical studies. 3 approaches are widely used for miRNA quantifications,

- 1) Microarrays (miRNA arrays)
- 2) Quantitative real time PCR (qRT-PCR)
- 3) Next generation sequencing (NGS) or Deep sequencing or high throughput sequencing.

3.3.1.1 miRNA arrays

miRNA arrays or miRNA microarrays were one of the first strategies to quantify and profile miRNA expression. Although several variations exist, the backbone of the technique is the hybridization of miRNAs onto probes immobilized on array chips. miRNAs in samples may be fluorescently labeled to enable detection. Even here, LNA probes can be used to solve hybridization temperature variability. One major advantage of arrays is that one can immobilize the same probe to different regions of the array and get replicate hybridization signals which enable statistical evaluation of binding intensity and minimize error rates. However, a certain sequence specific bias towards hybridization of the fluorophores and the interference by other cellular RNAs are drawbacks. Some of the commercially available miRNA microarray platforms are (or, in some cases, were) Geniom Biochip miRNA (febit GmbH now CBC, GmbH), GeneChip miRNA array (Affymetrix), GenoExplorer (Genosensor), MicroRNA microarray (Agilent), miRCURY LNA microRNA array (Exiqon), NCode miRNA array (Invitrogen), Nanostring OneArray (Phalanx Biotech), Sentrix array matrix and BeadChips (Illumina), μ ParaFlo biochip array (LC Biosciences) and miRXplore microarrays (Miltenyi biotech) (102).

3.3.1.2 qRT-PCR

This approach converts miRNAs to cDNA followed by qPCR amplification and detection. It can be easily established in laboratories with qPCR expertise. High throughput quantification of up to several hundreds of miRNAs using qRT-PCR is possible through the employment of multi well plates and auto micro sampling techniques. However, massively parallel miRNA quantifications are hindered by the fact that miRNAs vary in their hybridization temperatures. Recently, the use of Locked Nucleic Acid (LNA) probes has made substantial progress in improving miRNA hybridizations. 2 commonly used strategies of miRNA qRT-PCR are shown in **Figure 8**.

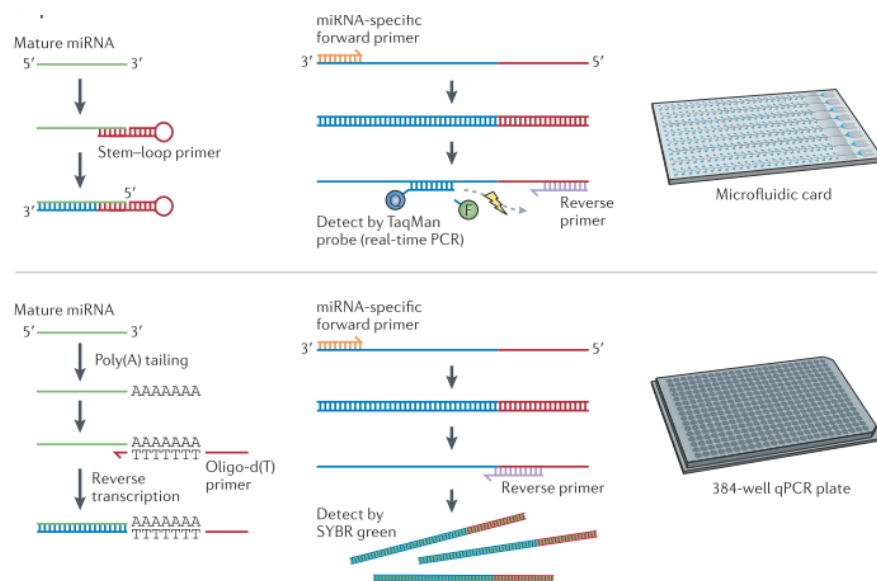


Figure 8. Schemes of miRNA qRT-PCR quantification. The top panel shows the use of stem loop primers to generate miRNA cDNA which is followed by qPCR and TaqMan probe mediated detection of amplification. The bottom panel shows the approach used to quantify miRNAs in my doctoral thesis. miRNAs are elongated by adding a poly-A tail (polyadenylation). Then an anchored oligo dT primer with a known sequence is used to generate the cDNA. Using the cDNA as template, a miRNA specific primer is used to amplify and quantify the respective miRNAs using qPCR. (Image source: Pritchard et al. Nature Reviews Genetics, 2012)

3.3.1.3 Deep Sequencing or Next Generation sequencing

NGS has emerged a powerful tool for miRNA profiling with extremely high throughput and massively parallel sequencing capabilities. Although this is the costliest of the 3 techniques mentioned here, recent advancements in instrumentation and ability to include several samples into a single sequencing reaction have made it more affordable as a routine profiling approach. The major advantage of deep sequencing is the fact that alongside known miRNAs, novel miRNAs can be discovered. miRNAs are converted to cDNA and are cloned and

expanded to create a library which are then sequenced. Prior to sequencing, cDNA from unique samples can be bar-coded using known adaptor sequences which can be identified and sorted after sequencing. This enables several samples to be mixed and sequenced together. In addition to the earlier mentioned cost effectiveness, this strategy also minimized sequencing errors and biases across different sequencing runs. NGS can successfully resolve miRNAs that differ by even one nucleotide. In my study, we were able to distinguish human miR-23a (AUCACAUGCCAGGGAUUUCC) and miR-23b (AUCACAUGCCAGGGAUUACC). Drawbacks of NGS include sequencing errors (which can be critical considering the short length of miRNAs) and the relatively cumbersome bioinformatic analysis and data mining from the sequenced reads which often requires help from statisticians. Some of the available sequencers are (Ion Torrent (Life Technologies), Genome Sequencer 20 (454 Life Sciences), MiSeq, Solexa and HiSeq 2000 (Illumina), SOLiD (Life Technologies) and GS Junior 454 (Roche) (102-104).

3.3.1.4 Tools for miRNA target prediction

Once miRNAs are quantified or profiled, the next step towards determination of their function is to identify mRNAs that they can potentially target. As described earlier, the imperfect complementarity of miRNA-mRNA base pairing enables literally thousands of mRNAs to be potentially targeted. It has been predicted that a single miRNA can target over 300 mRNAs in a cell. There are several tools available at present to predict mRNA-miRNA interactions. These tools use several parameter to make such predictions, which include base pairing between the 3' UTR of mRNAs and the miRNA seed region, nucleotide composition of flanking sequence, thermodynamic stability or free energy of miRNA binding, evolutionary conservation of binding sites, sterical accessibility of the miRNA towards mRNA secondary structures as well as expression of particular genes in the host, cell or tissue type (105). Some of the common miRNA target prediction tools and their links are listed in **Table 1**.

Table 1: List of common miRNA target prediction tools		
Database	Feature	Link
Targetscan	Sequence complementarity	http://www.targetscaan.org/
MiRanda	Sequence complementarity	http://www.microrna.org/microrna/home.do
RNA Hybrid	Favourability of hybridization	http://bibiserv.techfak.uni-bielefeld.de/rnahybrid/
PicTar	Sequence complementarity	http://pictar.mdc-berlin.de/
PITA	Target site accessibility	http://genie.weizmann.ac.il/pubs/mir07/index.html
DIANA-microT 3.0	Round up of several parameters	http://diana.imis.athena-innovation.gr/DianaTools/index.php?r=microT_CDS/index
miRDB	Support vector machine learning approach	http://mirdb.org/miRDB/

3.3.1.5 Tools for miRNA functional analysis

No matter how strong or how probable a predicted miRNA-mRNA interaction may be, there are several other unpredictable factors that determine whether the miRNA is able to inhibit mRNA translation in a physiological setting. In order to establish that an interaction is indeed possible within a live cell, luciferase reporter gene assays are commonly used. Here, miRNA-interactable RNA regions of genes (usually the complete or part of the 3'UTR of suspected target mRNAs) are cloned downstream of luciferase (firefly luciferase from *Photinus pyralis*). These reporter constructs are then transfected into cells that express the miRNA. Relevant controls that either lacks the 3'UTR of the target gene or that contain 3'UTRs with mutations within the miRNA interacting region are also transfected in parallel. Reduced reporter activity in wild type constructs when compared to the mutated construct indicates miRNA interference in the cloned regions. To determine whether a particular miRNA is interfering with the reporter, co-transfection of reporter constructs along with specific miRNA inhibitors (antisense 2'-O-methyl – modified oligoribonucleotides or antagomirs) or miRNA mimics are used. Once a specific miRNA-mRNA interaction is functionally determined, antagomirs and mimics can be used to further understand the control of the miRNA over the expression of that particular gene or its signaling pathways in relevant cells. miRNA mimics are double stranded and mimic the miRNA duplex, hence their transient expression is only suitable only for short term cellular assays. For long term in vitro and in vivo assays, DNA plasmids that can continuously generate the miRNA under endogenous, viral or tissue specific promoters are used (106).

3.3.2 miRNAs in cancer

Several miRNAs are deregulated in almost all cancers. Defects in miRNA processing machinery have been reported to play a role in the prognosis of cancers. In a significant

cohort of non-small cell lung cancer patients, the expression of dicer was shown to be downregulated which correlated with poor operative survival (107). In general, miRNAs that target tumor suppressors can drive tumorigenesis and those that target oncogenes and growth factors may be suppressive to the tumor (108). let-7 miRNA acts as a tumor suppressor by inhibiting the expression of Ras and mutations in let-7 have been shown to control cell proliferation in human cell lines and cancers (109). Nearly 50% of human miRNAs have been shown to lie within fragile sites of our genome (110). These fragile sites are often the first to take the hit of agents that cause genomic instability. Clustered miRNAs miR-15a and miR-16-1, which can target the anti-apoptotic gene Bcl-2, lie within a genomic region that is often deleted in B-CLL (B cell chronic lymphocytic leukemia), prostate cancer and multiple myeloma. These 2 miRNAs have thus been implicated as a tumor suppressors as their suppression (or deletion) increases the anti-apoptotic gene Bcl-2 which then drives tumorigenesis (111, 112). Similarly, miR-143 and miR-145 act as tumor suppressors and are downregulated in colorectal and breast cancers (113, 114). miR-155 has been implicated as a promoter in several lymphomas and breast cancers while miR-21 plays the role of an anti-apoptotic factor driving glioblastomas (113, 115, 116). One well recognized oncogenic miRNA cluster, the miR-17-92 cluster which includes miR-17-5p, miR-18a, miR-19a, miR-19b, miR-20a, miR-92-1 is induced by oncogenic Myc and is upregulated in B cell lymphomas where the members function co-operatively as oncogenes (117).

3.3.2.1 As cancer markers

Since miRNA expression is closely related to genomic instability, miRNA profiles are potential aids to predict the presence, type and stage of several cancers. Cytosolic miRNAs are packaged into exosomes and expelled into circulation. Circulating miRNAs within blood are a promising and minimally invasive marker for cancer diagnosis (118, 119). In blood and tissue from colorectal cancer patients, the expression of miR-23a was shown to increase along with disease progression suggestive of its diagnostic potential (120). Our group has shown the predictive power of miRNA profiles in whole blood from ovarian cancer patients where it was possible to discriminate healthy and serous subtype ovarian cancer samples with an accuracy of > 85% (99). However poor consensus among various studies still limits the full predictive potential of miRNA profiles.

3.3.2.2 As therapeutic targets

All miRNAs that act as tumor suppressors or tumor promoters are potential candidates as cancer therapeutic targets. However the critical hurdle to cross is the delivery of miRNA

modulators into the patients' cancer cells. Viral based miRNA delivery methods are the most effective way to transfer miRNAs *in vitro* but the immunogenicity of such a technique hinders its application in patients. However, in immunotherapy, this technique holds untapped potential. Nano technology has successfully delivered miRNAs and inhibitors to cancer cell lines. Lipid nanocapsule-locked nucleic acid complexes targeting miR-21 were able to sensitize glioblastoma cells to irradiation (121). A neutral lipid emulsion containing either miR-34a or let-7b significantly reduced lung tumor growth in mice (122). Much of the research on miRNA *in vivo* delivery systems focuses on minimizing toxicity. However the field of miRNAs use in cancer therapy is definitely gaining pace towards translational research.

3.3.3 Scope of my PhD thesis

The major part of my study that is elaborated describes the profiling of miRNA changes that occur in human CD8⁺ T cells upon initiation or blocking of TGF- β signaling, which lead to the identification of the miR-23a cluster. Reporter gene assays and functional assays showed that this cluster can inhibit LAMP-1 and IFN- γ as well as repress antigen specific cytotoxicity in CD8⁺ T cells. These findings reveal a previously unidentified mechanism by which TGF- β inhibits CD8⁺ T cell effector functions. On a broader perspective, immune regulatory miRNAs are exciting targets in clinical research. Whether inhibition of the miR-23a cluster can augment T cell responses against tumors and other infections has to be tested in suitable animal models. I also studied the mechanism of NKG2D downregulation in NK cells upon TGF- β treatment. While we initially suspected an involvement of miRNAs, this could not be confirmed. Instead, we arrived at a hypothesis suggesting that TGF- β dependent downregulation of the signaling counterpart of NKG2D, namely DAP10, could prevent the assembly of a complete NKG2D receptor complex and thus reduce NKG2D surface levels. This hypothesis is based on a number of experiments which showed that DAP10 mRNA is downregulated by TGF- β . Further, I contributed to various other studies which were published and which are summarized towards the end of my thesis.

4 Materials and methods

4.1 Isolation of PBMCs

Blood was drawn from healthy donors and mixed with acid citrate dextrose solution to a final concentration of 10% to prevent clotting. 50 ml of citrated-blood was then diluted with 90 ml PBS. 15 ml Biocoll lymphocyte separation medium was added to centrifugation tubes (50 ml). The citrated-blood-PBS mixture was gently layered over the Biocoll. The tube was then centrifuged for 20 minutes at 600 rpm (in a centrifuge from Jouan/Thermo Electron GmbH, 63303 Dreieich, Germany) with very low acceleration and deceleration at room temperature. 5 ml fluid was removed from the top to remove the platelets. The tube was again centrifuged for another 30 minutes at 1400 rpm with very low acceleration and deceleration at room temperature. PBMCs that accumulated at the interphase of Biocoll and serum were harvested into another tube and were washed twice with PBS.

4.1.1 Purification of CD8⁺ T cells and NK cells from PBMCs

Untouched CD8⁺ T cells were purified from PBMCs using the human CD8⁺ T cell isolation kit and NK cells were purified using human NK cell isolation kit (Miltenyi Biotec) on LS columns as instructed by the manufacturer. Cells and buffers were maintained at 4°C throughout the purification procedure. The following volumes were used for 10⁸ PBMCs: PBMCs were harvested by centrifuging them at 300 g for 10 minutes. Subsequently, they were resuspended in 400 µl of MACS buffer (PBS pH 7.2 with 0.5% BSA and 2 mM EDTA). 100 µl of CD8⁺ T cell Biotin-Antibody Cocktail was added, mixed well and incubated for 5 minutes. 300 µl of MACS buffer was added followed by 200 µl CD8⁺ T cell (or NK cell) Microbead Cocktail and the mixture was incubated for 10 minutes. Cells were diluted with 10 ml of MACS buffer, centrifuged at 300 g for 10 minutes and resuspended in 500 µl MACS buffer.

A MACS LS column was mounted on a magnetic holder and was rinsed using 3 ml of MACS buffer. The cell suspension was added to the column and the eluate, which contained untouched CD8⁺ T cells (or NK cells), was collected. The column was further rinsed 3 times using 3 ml of MACS buffer.

The purity of the isolated CD8⁺ T cells and NK cells were determined using flow cytometry. This method yielded consistently between 85% - 95% CD8⁺ T cells and NK cells (**Figure 9**).

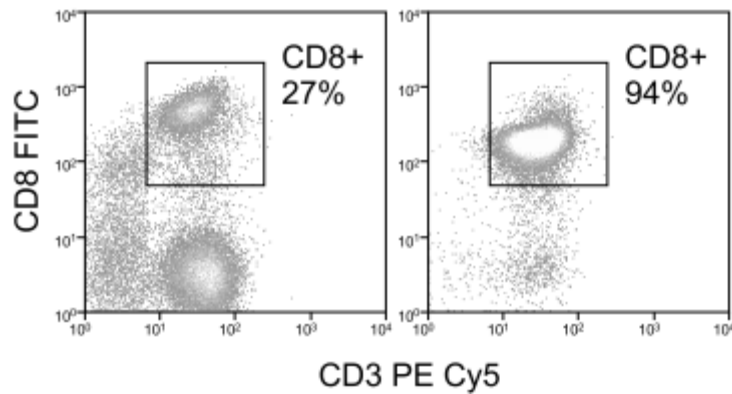


Figure 9. Purity of CD8⁺ T cells enriched using CD8⁺ T cell isolation kit. PBMCs (left) and purified CD8⁺ T cells (right) were stained with CD8 FITC and CD3 PE-Cy5 antibodies (Immunotools) and were analyzed using a flow cytometer.

4.1.2 Isolation of murine CD8⁺ T cells

Murine CD8⁺ T cells were isolated, activated and treated with TGF- β by Katerina Andreev under the supervision of Prof. Dr. Susetta Finotto. In brief, spleens from Balb/cJ hCD2- Δ kT β RII (123) and Balb/cJ wild-type mice were passed through a cell strainer and red cells were lysed by hypotonic solution as previously described (124). CD8⁺ T cells were purified from splenocytes using magnetic anti-mouse CD8 microbeads (Miltenyi Biotech, Bergisch Gladbach, Germany), according to the manufacturer's instructions. Using FITC-conjugated anti-mouse CD8 antibody (clone 53-6.7, BD Biosciences, Heidelberg, Germany), the purity of the isolated CD8⁺ T cells was confirmed to be between 88% and 93%.

4.2 Cell culture

4.2.1 PBMCs

PBMCs were maintained in RPMI 1640 with 10% fetal bovine serum (FBS), 100 units/ml penicillin, 0.1 mg/ml streptomycin and 50 μ M sodium pyruvate.

4.2.2 CD8⁺ T cells isolated from PBMCs

Human CD8⁺ T cells used for miRXploreTM arrays and deep sequencing were cultured in X-VIVOTM 15 medium (Lonza, Basel, Switzerland). For functional experiments, CD8⁺ T cells were cultured in RPMI 1640 with 10% FBS, 100 units/ml penicillin, 0.1 mg/ml streptomycin and 50 μ M sodium pyruvate.

4.2.3 Antigen specific CD8⁺ T cells

Melan-A specific and STEAP specific CD8⁺ T cells were cultured in CellGro DC Medium (CellGenix, Freiburg, Germany) supplemented with 5 % human serum (Biochrom), 30 IU/ml IL-2 (Peprotech) and 5 ng/ml IL-15 (Peprotech).

4.2.4 Cell lines

HEK293T cells were cultured in DMEM (high glucose), 10% FBS, 100 units/ml penicillin, 0.1 mg/ml streptomycin and 50 μ M sodium pyruvate. FM55 cells were cultured in RPMI 1640 with the same supplements. These adherent cell lines were grown until they were 80% confluent and were thereafter split into thinner densities after detaching them using Trypsin/EDTA solution (PAA). NKL cells were cultured in the same medium used for FM55 additionally supplemented with 20 IU/ml rh-IL-2 (Catalog no. 200-02, Peprotech) while NK-92 cells were cultured in IMDM medium (+25mM HEPES) (PAA) supplemented with FBS (10% final), horse serum (10% final), 100 units/ml penicillin, 0.1 mg/ml streptomycin, 2 mM L-glutamine, 50 μ M sodium pyruvate and 100 IU/ml rh-IL-2 (Peprotech).

4.2.5 Manual cell counting

Cells were washed once with PBS. 20 μ l of cell suspension was diluted with 20 μ l of 0.1% Trypan blue solution and the cells were counted using a Neubauer counting chamber. Total cell numbers were determined as follows:

$$\text{Total cell count} = \frac{\text{no. cells in 4 quadrants} \times 2 \times 10000 \times \text{total volume of cell suspension}}{4}$$

4.3 *In vitro* activation of CD8⁺ T cells

Human CD8⁺ T cells were activated using the T cell activation/expansion kit (Miltenyi Biotec). Anti-biotin MACSiBead particles were coupled to anti-CD2, anti-CD3, and anti-CD28 antibodies as follows.

100 μ l MACSiBead particles solution was mixed with 20 μ l each of anti-CD2, anti-CD3, and anti-CD28 antibodies. Then 40 μ l of MACS buffer was added. The resulting mixture had a concentration of 10⁵ beads / μ l and was incubated at 4°C for at least 4 h with slight agitation. CD8⁺ T cells were then stimulated with this mixture at a 1:2 bead/T cell ratio.

4.4 miRNA microarrays

Human CD8⁺ T cells were isolated as stated above from 5 different donors and were activated with activation/expansion beads for 24 h. Then, the cells were either left untreated (control) or treated with TGF- β 1 (5 ng/ml) (Peprotech) or the TGF- β receptor 1 kinase inhibitor SD-208 (1 μ M) (Tocris, Bristol, UK) (125). After 15 min, aliquots were drawn to check for phosphorylation of SMAD2/3. 24 h later, the cells were centrifuged at 400 g for 10 minutes, snap-frozen in liquid N₂ (-195°C) and shipped to Miltenyi Biotec. Cells belonging to the same group were pooled from each donor and the total RNA was isolated and purified (Trizol reagent). Bioactivity of TGF- β was assessed via SMAD2/3 phosphorylation at 15 min and via downregulation of NKG2D after 24 h (126). RNA from the control and SD-208 groups were fluorescently labeled with Hy3 and the TGF- β group was labeled with Hy5. 1.5 μ g of the fluorescently labeled total RNA was then mixed in pairs (TGF- β with control and TGF- β with SD-208 group) and hybridized overnight to miRXploreTM microarrays using the a-HybTM hybridization station. Fluorescence signals were detected using a laser scanner (Agilent). For each spot of the microarray images, mean signal and mean local background intensities were obtained using the ImaGene^R software (Biodiscovery). Normalized mean Hy5/Hy3 ratio of 4 replicates of each miRNA was calculated using miRXplorer software (Miltenyi Biotec).

4.5 Generation of small RNA libraries from CD8⁺ T cells

CD8⁺ T cells from 5 different donors were treated in exactly the same way as for the miRNA arrays. Small RNA libraries were generated by Vertis Biotechnology AG (Freising-Weihenstephan, Germany) as described earlier (127). Briefly, RNA was isolated and resolved on a denaturing 12.5% polyacrylamide gel. RNA molecules that were 15-30 bases long were then concentrated by ethanol precipitation. RNAs were then polyadenylated and 5' adapter sequences were ligated onto them. The 5' adapter sequence used for each group was 5'-GCCTCCCTCGCGCCATCAGCTNNNNGACCTTGGCTGTCCTCA-3', where NNNN represents a 'bar code' sequence for the 3 groups (GCTC for RNA from the TGF- β 1-treated group, CCGA for the SD-208-treated group and GTAT for the control group).

Then, cDNA synthesis was performed using an oligo(dT)-linker primer and M-MLV-RNase H- reverse transcriptase. cDNAs were PCR-amplified in 22 cycles. The resulting 120 - 135 bp amplification products were confirmed by polyacrylamide gel electrophoresis (PAGE). cDNA pools were mixed in equal amounts, gel fractionated and electro-eluted from 6% PAA-gels. After isolation with Nucleospin Extract II (Macherey and Nagel) cDNA

pools were dissolved in 5 mM Tris/HCl, pH 8.5 at a concentration of 10 ng/μl and used in single-molecule sequencing. Massively parallel sequencing was performed by 454 Life Sciences (Branford, USA) using the Genome Sequencer 20 system.

4.5.1 Analysis of deep sequencing results

By identifying the ‘bar code’, sequences from control, TGF-β and SD-208 groups were separately filed in ‘.xls format. The following steps were then performed using Pearl scripts written by Jiayun Zhu (Research Group, Prof. Dr. Gunter Meister), that were modified according to the nature and number of reads in each group. The 5’ adapter sequence and the polyA tail were removed. The resulting 25 base sequences were screened for unrecognizable bases (sequencing errors, designated as N) and these bases were removed. The sequences were then arranged in descending order according to base count. In the next steps 2 groups were combined in one file, side-by-side, for comparison. We combined the control and the TGF-β group and the SD-208 and the TGF-β group. The number of same reads was then counted for each group and was assigned to each read. The sequences were then arranged in descending order according to read counts. Since 454 sequencing results typically show abnormal ‘A’ inserts within reads, we eliminated all ‘A’s in all the reads, however one row with the parental sequence was maintained during the analysis. Then the sequences were annotated by comparing them against all miRNAs in the miRBase (www.mirbase.org). Usage of a non-stringent comparison and possibility of sequencing errors, the annotated sequences were further cross-checked manually, one at a time, for abnormal base repeats (e.g. CCC could be sequenced as CC or CCCC), rather short sequenced due to the removal of ‘A’s, as well as for unannotated sequences that were left out due to shortened reads. After this step, the number of reads for each miRNA in the various groups was determined. To facilitate comparison between the different data sets, miRNA counts were normalized to 10⁴ reads and ratios were calculated for each individual miRNA by dividing the number of normalized reads in the TGF-β treated group by the number of reads in either the control or the SD-208 treated group.

4.6 NK cell mRNA microarrays

(performed by Yvonne Dombrowski)

NK cells were isolated from 6 healthy donors and were treated with 5 ng/ml TGF-β or left untreated for 24 h. Cells from each donor for the same treatment were pooled at 4°C, snap

frozen in liquid N₂ and were shipped to Miltenyi Biotec. RNA was isolated and quality controlled. RNA from the control group was fluorescently labeled with Cy3 and the TGF-β group was labeled with Cy5. 825 ng of the corresponding Cy3- and Cy5-labeled fragmented cRNA were combined and hybridized overnight (17 h, 65 °C) to Agilent Whole Human Genome Oligo Microarrays. Fluorescence signals were detected by the DNA microarray scanner (Agilent Technologies) and the corresponding Cy5/Cy3 fluorescence ratios were calculated to indicate gene regulations.

4.7 Identification of new miRNAs

Unannotated miRNAs with about 50 or more read counts were aligned against the human genome. The chromosomal location of sequences that showed 100% homology were then determined and 40-50 bases either upstream or downstream were retrieved. This stretch of RNA was then folded using the RNAfold WebServer, Institute for Theoretical Chemistry, University of Vienna (<http://rna.tbi.univie.ac.at/cgi-bin/RNAfold.cgi>).

4.8 Quantification of miRNAs by qRT-PCR

Isolation of miRNAs for qRT-PCR was optimized by comparing various available kits in the market. Best results were obtained when the RNA was isolated and the miRNA fraction was enriched using the Absolutely RNA/miRNA Kit (Agilent Technologies, Böblingen, Germany). 10⁶ cells were used per isolation and the miRNAs were eluted using 50 µl of RNase-free water. The isolated miRNAs were then 3'-poly-adenylated using the E. coli polyadenylase enzyme (Agilent Technologies).

Polyadenylation reaction		Reaction conditions	
miRNA elute	10 µl	37°C	45 min
EPAP buffer (5X)	4 µl	95°C	5 min
rATP (10 mM)	1 µl	4°C	hold
RNase free water	4 µl		
PAP enzyme	1 µl		
Total	= 20 µl		

Several available reverse transcriptases were tested in parallel for their efficiency to reverse transcribe the poly-adenylated miRNAs. Affinityscript reverse transcriptase (Agilent

Technologies) proved to be the best and thus cDNA synthesis was henceforth performed with the High specificity miRNA First Strand Synthesis Kit (Agilent Technologies) with an anchored oligo-dT primer with a universal recognition sequence (URT-primer).

miRNA cDNA synthesis reaction		Reaction conditions	
Affinity script RT buffer (10X)	2 μ l	55°C	5 min
Polyadenylation reaction	10 μ l	25°C	15 min
dNTP mix (10 nM)	0.8 μ l	42°C	45 min
URT primer	1 μ l	95°C	5 min
Affinity script/ RNase block enzyme	1 μ l	4°C	hold
Total	= 20 μ l		

miRNA expression was quantified using ABsolute™ QPCR SYBR Low ROX mix (Thermo Scientific) together with miRNA specific forward primers and a URT specific primer. Our protocol was adapted from a previous study (128).

Primers	Sequence
URT primer	5'-AACGAGACGACGACAGACTTTTTTTTTTTTTTTT
URT specific primer	5'-AACGAGACGACGACAGACTTT
miR-23a	5'-ATCACATTGCCAGGGATTCC
miR-27a	5'-TTCACAGTGGCTAAGTTCCGC
miR-24	5'-TGGCTCAGTTCAGCAGGAACAG
U6	5'-CGCTTCGG-CAGCACATATAC
SNORD70	5'-ATTCGTCACTACCACTGAGA

The resulting C_T values for the respective miRNAs were then quantified by the $\delta\delta C_T$ method using U6 ribosomal RNA as internal control. For murine CD8⁺ T cells, the same miRNA-specific primers could be used. Here, however, SNORD70 was chosen as internal control.

4.9 Quantification of mRNAs by qRT-PCR

Up to 5×10^6 cells were lysed using 500 μ l of peqGOLD TriFast (Peqlab Biotechnology) and total RNA was isolated following the manufacturer's instructions. RNA purity (A260/A280) and concentration were determined using a spectrophotometer. In short, 2 μ l of the total RNA fraction was diluted in 198 μ l (dd) H₂O; the absorbance was measured at 260 and 280 nm against (dd) H₂O control. The concentration was calculated using the formula:

$C [\mu\text{g} / \text{ml}] = \text{OD } 260 \text{ nm} \times \text{dilution factor} \times 40$. The purity of the isolated RNA was estimated by dividing the value obtained for the absorbance at 260 nm by the absorbance measured at 280 nm. Ratio of OD 260 nm /OD 280 nm close to 1.8 indicated good purity. 0.5 μg of total RNA was reverse transcribed into cDNA using iScriptTM synthesis kit (Biorad).

cDNA synthesis reaction		Reaction conditions	
5x iScript Reaction Mix	4 μl	Temperature	Incubation period
iScript reverse transcriptase	1 μL	25°C	5 min
RNA template	0.5 μg	42°C	30 min
Nuclease-free water	to 20 μl	85°C	5 min

mRNA expression was quantified by SybrGreen based real time PCR using Absolute Blue qPCR low ROX mix (Thermo Scientific) on an ABI 7500 Fast thermocycler (Applied Biosystems, Life Technologies).

q-PCR reaction mix		Thermal cycling conditions	
2 x Absolute Blue QPCR SYBR Green lowRox mix	7.5 μl	Temperature	Incubation time
Forward primer (1.1 μM)	1 μl	50°C	2 min
Reverse primer (1.1 μM)	1 μl	95°C	15 min
Water	0.5 μl	95°C	40 cycles/ 15 sec
cDNA (prediluted 1:20 in water)	5 μl	60°C	1 min 40 cycles
Total	15 μl	Dissociation curve	
		95°C	15 s dissociation curve
		60°C	1 min
		95°C	15 sec

Primers	Sequence
NKG2D (Forward)	5' -TCTCGACACAGCTGGGAGATG
NKG2D (Reverse)	5' -GACATCTTTGCTTTTGCCATCGTG
DAP10 (Forward)	5' -TCCATCTGGGTCACATCCTCTTCC
DAP10 (Reverse)	5' -GAGTGATGATCTCTCTCCTG GAGTCGTCTGAGCTG
18S (Forward)	5' -CGGCTACCACATCCAAGGAA
18S (Reverse)	5' -GCTGGAATTACCGCGGCT

4.10 PCR amplifications

Amplification of 3'UTRs for cloning reporter constructs was performed using Crimson longAmp Polymerase Kit (NEB) on CD8⁺ T cell cDNA.

Component	Volume
5 x Crimson LongAmp Taq	5 μ l
10 mM dNTP	0.75 μ l
10 μ M forward primer	1 μ l
10 μ M reverse primer	1 μ l
cDNA	1 μ l
(dd) H ₂ O	to 25 μ l
AmpliAmp Polymerase	0.5 μ l

Temperature	Incubation time
94°C	3 min
Denaturing (94°C)	30 sec 35 cycles
Annealing (55°C-65°C)	30 sec 35 cycles
Extension (72°C)	45 sec 35 cycles
72°C	10 min
4°C	Hold

4.11 Transfection of CD8⁺ T cells

Our laboratory is equipped to safety level S1 which does not allow us to perform viral transductions. Primary immune cells are very difficult to transfect with non-viral methods. Since this study routinely involved the modulation of miRNA levels in primary CD8⁺ T cells, we decided to optimize a non-viral and relatively homogenous method of transfecting these cells with least variability between successive transfections. We tested several commercially available transfection reagents in parallel using FAM labeled anti-miRNA control (Ambion, Life Technologies) for their efficiency in transfecting primary CD8⁺ T cells.

Based on our observations (**Table 2**), we decided to nucleofect CD8⁺ T cells using the T cell nucleofection reagent. Although high transfection rates were obtained using TRANS-IT TKO, the reagent was highly toxic to CD8⁺ T cells. Briefly, 2-5x10⁶ CD8⁺ T cells were washed with PBS and MACS buffer (2 mM EDTA and 0.5% BSA in PBS; pH 7.2) before being nucleofected either with 1 μ g of plasmid DNA or with 300 nM miRNA mimics, antagomirs or control RNA. Immediately after nucleofection [performed with Amaxa[®]'s Human T cell Nucleofector[®] kit (VPA-1002, Lonza) and program U-014], the cells were transferred into fresh, warm medium (37°C).

Reagent (supplier)	Transfection efficiency
control	0%
Dreamfect (OZ Biosciences)	35-45%
Attractene (Qiagen)	high toxicity
TRANS-IT (Mirus)	2-4%
Hi-Perfect (Qiagen)	50-55%
RNA iMAX (Life Technologies)	5-10%
Dharmafect (Thermo Scientific)	5-10%
GeneSilencer (Genlantis)	0-1 %
ICA fectin (Eurogentec)	0-1%
TRANS-IT TKO (Mirus)	75-85%
Amaxa nucleofection (Lonza)	70-80%

Table 2. Efficiency of various transfection reagents while transfecting CD8⁺ T cells. Purified CD8⁺ T cells were transfected with FAM- anti-miRNA negative control RNA using the above listed transfection reagents following instructions provided by the respective suppliers. Untransfected cells served as control. The respective percentages of FAM positive cells were determined by flow cytometry and are indicated in the above table.

4.12 Antagomirs and mimics

Antagomirs are synthetic anti-sense 2'-O-Methyl RNA oligos which are perfectly complementary to the target miRNA which they inhibit.

Antagomir for miR-23a (ant-23a): r[2'-OMe](GGAAAUCCUGGCAAUGUGAUU)dT

Antagomir for miR-27a (ant-27a): r[2'-OMe](GCGGAACUUAGCCACUGUGAAU)dT

Antagomir for miR-24 (ant-24): r[2'-OMe](CUGUCCUGCUGAACUGAGCCAU)dT

Antagomir for miR-9 (ant-9): r[2'-OMe](UCAUACAGCUAGAUAAACCAAAGA)dT

Since deep sequencing and qRT-PCR both showed that miR-9 was not expressed in CD8⁺ T cells, antagomirs against this miRNA served as control in our experiments. miRNA mimics and control RNA were obtained from commercial providers: mimic-23a: Syn-hsa-miR-23a miScript miRNA Mimic (Cat.no:MSY0000078), mimic-27a: Syn-hsa-miR-27a miScript miRNA Mimic (Cat.no:MSY0000084, Qiagen, Hilden, Germany), mimic-24: hsa-miR-24 miRIDIAN Mimic (Cat.no: C-300496-05-0005, Dharmacon RNAi Technologies, Thermo Scientific) and control RNA: All stars negative control RNA (Cat.no. 1027280, Qiagen).

The efficacy of the antagomirs and mimics to deregulate miR-23a cluster was tested and is shown in **Figure 10**.

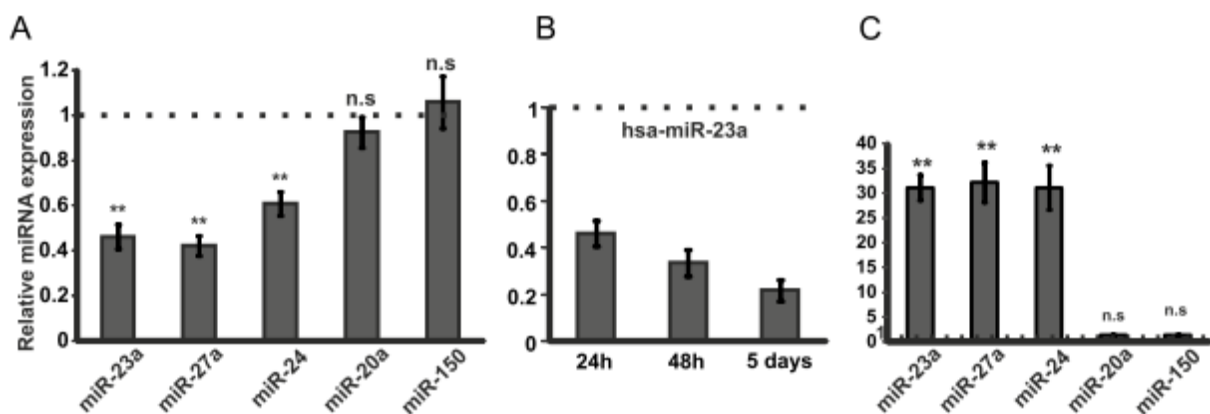


Figure 10. Efficacy of antagomirs and mimics in CD8⁺ T cells after nucleofection. (A) CD8⁺ T cells were nucleofected with an antagomir cocktail (antagomirs against miR-23a, miR-27a and miR-24, 100 nM each) or without any antagomirs and the expression of these miRNAs was quantified 24 h later by qRT-PCR. miR-20 and miR-150 were also quantified to control for off-target effects. U6 snRNA was used as internal control. Expression values were normalized to the mock-nucleofected control. (B) The expression of miR-23a in CD8⁺ T

cells was monitored over 5 days after nucleofection with an antagomir against miR-23a. For functional assays in this study, the maximum duration of experiments involving antagomirs was 60 h after nucleofection. (C) CD8⁺ T cells were either mock-transfected or nucleofected with a cocktail of miRNA mimics (containing 100 nM each of mimics for miRNA-23a, miR-27a and miR-24) and the expression of these miRNAs was quantified 24h later by qRT-PCR. U6 snRNA was used as internal control. Further, miR-20 and miR-150 were quantified to control for off-target effects. The displayed expression values were normalized to the group nucleofected without any mimics. p-values were determined using Student's *t*-test (ns- not significant, * *p*<0.05, ** *p*<0.01, *** *p*<0.001).

4.13 Priming and generation of Melan-A- and STEAP-specific T cells

The detailed priming protocol has been previously described (129) and was performed at the Department of Pediatric Hematology, Oncology and Stem Cell Transplantation, Children's Hospital, University of Würzburg Medical School under the supervision of Dr. Matthias Wölfl. Briefly, DCs were generated from plastic-adherent monocytes. After 72 h of culture in GM-CSF/IL-4-containing DC medium (Cellgenix, Freiburg, Germany), DCs were matured in medium containing 100 ng/ml IL-4 (Peprotech), 800 IU/ml GM-CSF (Peprotech), 10 ng/ml LPS, and 100 U/ml IFN- γ (Peprotech) plus Melan-A-peptide (26-35(A27L)) (ELAGIGILTV, 2.5 μ g/ml) (JPT, Berlin, Germany). After 16 h, DCs were irradiated (30 Gy) and co-incubated with CD45RO⁻, CD57⁻ naïve CD8⁺ T cells at a 1:4 ratio in medium containing 5% AB serum and 10 ng/ml IL-21 (Peprotech). Fresh medium, IL-7 (Peprotech), and IL-15 (Peprotech) were added on days 3, 5, and 7 of culture, before evaluation on day 10-12. The percentage of Melan-A specific T cells was determined by MHC-multimer staining (Immudex, Copenhagen, Denmark). When further purification was required, antigen-specific T cells were stained with appropriate Dextramer-APC conjugates (Immudex) and enriched using magnetic anti-APC Beads (Miltenyi) according to the manufacturer's instructions.

To obtain STEAP-specific T cell clones, cells from an HLA-A02:01⁺ donor were primed and expanded similar to Melan-A-specific T cells, using the STEAP peptide MLAVFLPIV (292.2L) (JPT, Berlin, Germany). The cells were then purified using a Dextramer-APC conjugate and clones were obtained via limiting dilution: To this aim, 0.3-3 Dextramer enriched T cells per well were seeded in 96 well plates and cultured together with 200,000 feeder cells/well (PBMCs from three different, HLA- mismatched donors at a 1:1:1 ratio) and 30 ng/ml soluble OKT3 (OrthocloneTM, Janssen-Cilag, Neuss, Germany) in CellGro DC Medium (CellGenix, Freiburg, Germany) supplemented with 5 % human serum (Biochrom), 30 IU/ml IL-2 (Peprotech) and 5 ng/ml IL-15 (Peprotech). This medium was also used for subsequent culture. After 14 days, specific T cell clones were identified by dextramer staining

and restimulated on irradiated feeder cells with OKT3. Cells were then used for experiments or stored at -185°C. When thawed, cells were restimulated on irradiated feeder cells with OKT3. Experiments were done at least 10 days after restimulation. In order to restimulate the antigen specific T cells using monocytes pulsed with peptides, CD14 positive cells were purified from PBMCs using magnetic beads (Miltenyi Biotec). These cells were then fed with 100 ng/ml IL-4 (Peprotech), 800 IU/ml GM-CSF (Peprotech) and the respective peptide (1 µg/ml) for 24 h before they were mixed with T cells.

4.14 Reporter vectors and cloning

miRNA binding to the 3' UTR of putative targets was analyzed with a dual reporter plasmid pMIR-RL (**Figure 11**) encoding both *Renilla reniformis* and *Photinus pyralis* (firefly) luciferase (130).

Briefly, *Renilla reniformis* luciferase is constitutively expressed under the SV-40 promoter and is used to normalize for transfection efficiency. Transcription of firefly (*Photinus pyralis*) luciferase is driven by the weaker HSV-TK promoter. To render this signal susceptible to inhibition by miRNAs, the 3'UTR of the gene of interest was fused to the firefly luciferase sequence.

For amplification of the 3'UTRs of LAMP1 and IFN-γ, cDNA from CD8⁺ T cells was used as template and amplified with the following primers (containing restriction sites for either Spe1 or Pme1):

LAMP1 3'UTR forward: CGCTACTAGTGGGCCTCTGTTTCCTTTCTCT

LAMP1 3'UTR reverse: CGCTGTTTAAACAGCTGGTCCCGTGTACAATC

IFN-γ 3'UTR forward: CGCTACTAGTGGTTGTCCTGCCTGCAATA

IFN-γ 3'UTR reverse: CGCTGTTTAAACTTCCATTTGGGTACAGTCACAG

Amplified 3' UTRS were run in a 1.5% agarose gel and were excised and eluted using the innuPREP Gel Elution kit (Analytic Jena). pMIR-LAMP1-3'UTR (LAMP1-3'UTR) and pMIR-IFN-γ-3'UTR (IFN-γ 3'UTR) were then generated by cloning the obtained PCR products into the Pme1 and Spe1 restriction sites of pMIR-RL plasmid using the T4 DNA ligase (Roche) (**Figure 11**).

3'UTR sequences containing mutations in miR-27a and miR-24 binding sites for IFN-γ (IFN-γ-mut UTR) and mutations in miR-23a binding sites for LAMP1 (LAMP1-mut UTR) (compare **Figure 21**) were chemically synthesized (Genewiz, Sigma Aldrich). These mutated 3' UTRs were then fused to the firefly luciferase gene in the pMIR-RL plasmid between the

PmeI and SpeI restriction sites to generate the pMIR-IFN- γ -mut 3'UTR and pMIR-LAMP1-mut 3'UTR constructs, respectively.

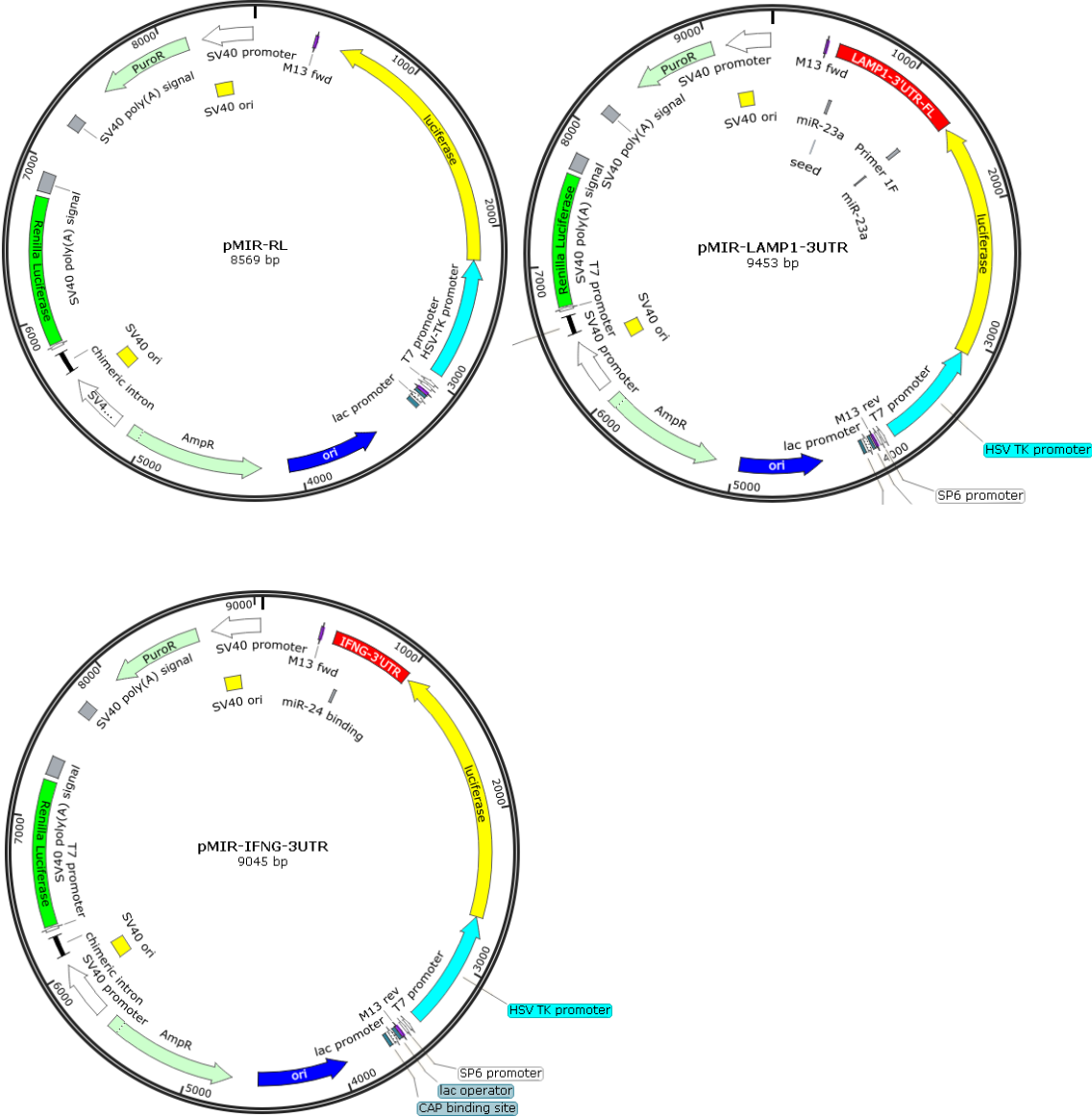


Figure 11: pMIR RL, pMIR-LAMP1-3'UTR, pMIR-IFNG-3'UTR vector maps (created using Snapgene viewer).

4.15 Transfection of HEK293T cells and dual reporter gene assays

1×10^4 HEK293T cells/well were seeded in a 96 well flat bottom plate (TPP, Trasadingen, Switzerland) and adhered overnight. Transfection with pMIR-LAMP1-3'UTR, pMIR-IFN- γ -3'UTR, pMIR-LAMP1-mut 3'UTR, pMIR-IFN- γ -mut 3'UTR or pMIR-RL either alone or in combination with miRNA mimics, miRNA antagomirs or control RNA (All Stars Negative Control siRNA from Qiagen) was performed, using the X-treme GENE siRNA Transfection Reagent (Roche Applied Science, Mannheim, Germany). Briefly, 100 μ l of transfection complex were prepared with 1 μ g of plasmid DNA and 200 nM miRNA mimics, antagomirs or control RNA and 30 μ l were added per well. After the specified incubation time, supernatant was removed and the cells were lysed using 60 μ l of Reporter Lysis Buffer (Promega). After one freeze-thaw cycle at -20°C , firefly and *Renilla* luciferase activities were measured using a non-commercial dual luciferase assay system (131).

Firefly luciferase buffer		Renilla luciferase buffer	
Ingredient	concentration	Ingredient	concentration
Glycylglycine	25 mM	Sodium chloride	1.1 M
K ₂ HPO ₄ (pH 8.0)	15 mM	Na ₂ EDTA	2.2 mM
EGTA	4 mM	KH ₂ PO ₄	0.22 M
ATP	2 mM	BSA	0.44 mg/ml
DTT	1 mM	NaN ₃	1.3 mM
MgSO ₄	15 mM	Coelenterazine	1.43 μ M
Coenzyme A	0.1 mM		
D-Luciferin	75 μ M		

In short, 25 μ l of cell lysate were transferred into each well of an opaque 96 well plate (Lumitrac 200, Greiner Bio-One, Frickenhausen, Germany) and luciferase activities were measured on an Orion Microplate Luminometer (Berthold Detection Systems, Pforzheim, Germany) using automated consecutive injection. Background values were obtained from untransfected cells. Relative light units (RLU), i.e. the ratio of background-subtracted firefly to *Renilla* luciferase signals were normalized to the reporter plasmid without 3'UTR (pMIR-RL) or to the control RNA transfected group.

4.16 Degranulation assay

In order to quantify degranulation, anti-CD107a/LAMP1-PE (clone: H4A3, BioLegend) or a PE-conjugated, isotype-matched control antibody (clone: MOPC21, BioLegend) was added directly to CD8⁺ T cells. After 1 h, 2 μ M monensin (BioLegend) was added. 4 h later, the cells were washed and stained with anti-CD8 PE-Cy5 (clone: HIT8 α , BioLegend) and anti-CD3 APC (BioLegend) antibodies and the expression of CD107a on CD8⁺ T cells was measured by flow cytometry.

4.17 Quantification of proteins in cell lysate

Total protein concentration in cell lysates used for immunoblotting was determined by Bradford assay. 50 μ l of distilled water was loaded in every well of a 96-well plate, then 1 μ l of protein lysate or Protein standard (HSA) was loaded in triplicate. For the standard row, protein concentrations of 1, 2, 4, 6, 8, 10 and 12 μ g/ml were used. Thereafter, Rotiquant Bradford reagent was diluted by 1:3.75 with distilled water, and then 200 μ l of this solution were added to each well. After 20 min at room temperature, total protein concentration was determined in an ELISA reader by measuring the absorbance at 595 nm.

4.18 Immunoblot analysis

Total LAMP1, DAP10 and phospho-SMAD-2/3 in cells were analyzed by immunoblot. In short, cells were collected by centrifugation, washed with PBS and lysed in protein lysis buffer containing 50 mM Tris-HCl (tris(hydroxymethyl)aminomethane-hydrochloric acid) pH 8.0 (Sigma-Aldrich Chemie GmbH, Steinheim, Germany), 120 mM sodium chloride, 5 mM EDTA, 2 μ g/ml Aprotinin, 10 μ g/ml Leupeptin, 1 mM PMSF, 10 nM sodium fluoride (all purchased from Carl Roth, Karlsruhe, Germany), 0.5% Nonidet P-40 and 1 mM sodium orthovanadate (both from Applichem GmbH, Darmstadt, Germany). 10-20 μ g proteins were separated on a 10% polyacrylamide (Carl Roth) gel under reducing conditions, transferred to a PVDF membrane (Carl Roth) which was blocked in PBS containing 5% skimmed milk powder and 0.05% Tween20 (both from Carl Roth) and incubated overnight at 4°C with either 0.5 μ g/ml LAMP1 antibody (clone H4A3, BioLegend), 0.5 μ g/ml DAP10/HCST (# AP16996PU-N, Acris Antibodies, Herford, Germany) or with, 1:1000 dilution of p-SMAD 2/3 antibody (#8828- Cell Signaling). GAPDH (clone EPR1977Y, Epitomics, Burlingame CA.) or β -actin (clone: 2F1-1, Biolegend) served as relevant loading controls. Proteins were

visualized using horseradish peroxidase-coupled species specific secondary antibodies (anti-mouse, anti-goat or anti-rabbit IgG secondary antibody from KPL, Wedel, Germany) and homemade enhanced chemiluminescence (ECL) solution. ECL solution was prepared by mixing 0.25 mg/ml Luminol (Carbosynth Ltd, Berkshire, UK) in 0.1 M Tris-HCL (pH 8.6) with 1.1 mg/ml para-hydroxycoumaric acid (Sigma-Aldrich) and 30% hydrogen peroxide (Carl Roth) at a 10:1:0.003 ratio.

4.18.1 Buffers used for immunoblotting:

Blocking Buffer: 5% skim milk powder in PBS-T. *PBS-T:* PBS + 0.05% Tween20. *Protein loading buffer (5x):* 100 mM Tris-HCl pH 6.8, 4% SDS, 0.2% Bromophenol blue, 0% Glycerol, 10% β -Mercaptoethanol. *Gel running buffer:* 25 mM Tris, 193 mM Glycin, 0.5% SDS pH 8.8. *Gel to PVDF transfer buffer:* 25 mM Tris, 192 mM Glycin, 20% Methanol.

4.19 Surface staining for NKG2D receptor expression

Cells were harvested and washed once with PBS and again with FACS buffer (PBS+ 2% FBS). Unspecific antibody binding was blocked with 0.5% normal rabbit serum. PE conjugated Anti-human NKG2D antibody (mouse monoclonal; clone: BAT221; Miltenyi Biotec) or an isotype control was added and incubated for 30 min on ice. Cells were then washed twice with PBS and analyzed on a FACSCalibur™ (BD Biosciences).

4.20 Intracellular staining for IFN- γ and CD107a/LAMP1

Cells were treated with 2 μ M monensin for 4 h. Afterwards, they were harvested by centrifugation and washed with ice cold PBS. All downstream processes were performed on ice. Unspecific antibody binding was blocked with 0.5% normal rabbit serum for 15 mins. Cells were then stained with PE-Cy5-conjugated anti-CD8 (Biolegend) and APC-labeled anti-CD3 (Biolegend) antibodies. They were fixed in 4% paraformaldehyde solution for 15 min and washed with PBA buffer (1% BSA in PBS). Cells were permeabilized by incubating them for 15 min in 0.5% Saponin (Carl Roth) (in PBA buffer). After one wash, intracellular stainings were performed with PE-labeled anti-IFN- γ (clone 4S.B3, Biolegend) in permeabilization buffer or with anti-CD107a/ LAMP1 antibodies and analyzed on a FACSCalibur™ (BD Biosciences).

4.21 ELISA

To quantify secreted IFN- γ , cells were centrifuged at 300g for 10 minutes and the supernatant was transferred to a fresh 1.5 ml tube. This tube was centrifuged at 15,000 g for 10 minutes and the supernatant was collected and stored at 4°C until use. In order to quantify intracellular IFN- γ , cells were harvested by centrifugation at 300g for 10 minutes. Protease-free buffer was prepared by mixing 2 μ g/ml aprotinin, 10 μ g/ml leupeptin and 1 nM PMSF in PBS and the cells were lysed in this buffer by 4 freeze-thaw cycles at -20°C. Secreted and intracellular IFN- γ was quantified by ELISA. The antibodies (capture and detection) and IFN- γ standard were from the IFN- γ high sensitivity human ELISA set (Immunotools, Friesoythe, Germany). Briefly, anti-human IFN- γ capture antibody was diluted (1: 2000) in coating buffer (100 mM Na₂CO₃, pH 9.6) and was coupled to a Maxisorp™ 96 well plate (Nunc, Roskilde, Denmark). The plate was incubated at 4°C overnight and was washed 5 times with wash buffer (0.01% Tween 20 in PBS). Unspecific antibody binding was then blocked by incubating the plate in blocking buffer (1% BSA in PBS) for 1 h at room temperature followed by 5 washes with wash buffer. IFN- γ standard concentrations (ranging from 0.078 ng/ml up to 5 ng/ml) and a blank control were prepared in dilution buffer (1% BSA and 0.05% Tween 20 in PBS) and 100 μ l from each were pipetted in duplicates into the plate. 100 μ l of cell supernatants were also added into separate wells in duplicates. The plate was then incubated for 1 h at room temperature and washed 5 times with wash buffer. Biotinylated anti-human IFN- γ detection antibody mixed (1: 2000) in dilution buffer was added for 1 h at room temperature and the plate was washed 5 times with wash buffer. The plate was further incubated for 30 min with Streptavidine-HRP (Immunotools) diluted (1:7500) in dilution buffer. After washing 5 times with wash buffer, substrate solution* was added for 20 minutes to enable color development. The reaction was stopped using 2N sulphuric acid. Absorbance was measured at 450 nm in a Sunrise microplate reader (Tecan, Crailsheim, Germany) and cytokine concentrations were determined based on the standard row using the Magellan analysis software (Tecan).

* Substrate solution: 5 ml of 42 mM TMB (3,5,3',5'-tetramethylbenzidine) solution in DMSO and 500 ml of 0.1 M sodium acetate solution were mixed. Into 10 ml of this solution, 2 μ l hydrogen peroxide was added and used as substrate solution.

4.22 CD8⁺ T cell cytotoxicity assay

10⁴ FM55 melanoma cells were seeded per well in a 96 well plate in complete RPMI 1640 medium. On the next day, 10⁴ Melan-A-specific CD8⁺ T cells were added for 4h. Then, CellEventTM Caspase 3/7 Green detection reagent (Life technologies) was added to a final concentration of 4 μM and incubated for additional 30 minutes. The cells were then harvested using Accutase (Sigma Aldrich) and stained with anti-CD8β-PE-Cy7 (Biolegend) to discriminate between CD8⁺ T cells and (Melan-A-expressing) tumor cell targets. From the latter subset, the percentage of cells showing caspase 3/7 activity was analyzed by flow cytometry (Attune[®], Life technologies). To assess the effect of the miR-23a cluster on the cytotoxic activity of a CD8⁺ T cell clone, STEAP-specific T cells were nucleofected with miRNA mimics or control RNA and 10⁴ MCF-7 breast cancer cells were seeded 10⁴ in a 96 well plate. On the following day, the tumor cells were loaded with the STEAP peptide (5 μg/ml) in the presence of IFN-γ (10 ng/ml). 24 h later, 10⁴ STEAP-specific CD8⁺ T cells were added and the cytotoxic activity was assessed as described above.

4.23 Statistics

P values for the microarrays were calculated with the miRXplorer software based on a comparison between the mean ratio of 4 replicates and the error of the respective mean ratio with the Gaussian error function. To calculate the cumulative effect of miRNA induction for miR-23a, -27a, and -24, the CT values obtained from qRT-PCR were transformed to z-scores before standard ANOVA was performed for the 4 respective groups. Unless mentioned otherwise, significance was determined by Student's t test, and P < 0.05 was considered significant.

5 Results

5.1 miR-23a cluster is induced by TGF- β in CD8⁺ T cells

5.1.1 miRNA microarrays

We determined TGF- β mediated regulation of the CD8⁺ T cell miRNome using an overlap approach employing miRNA microarrays and next generation sequencing. For this, we prepared 3 groups of cells. Cells were activated for 24 h using T cell activation beads (described above) and treated with either 5 ng/ml TGF- β , 1 μ M SD-208 or were left untreated (control group). SD-208, a TGF- β receptor 1 kinase inhibitor, blocks TGF- β signaling and was included in order to account for endogenous TGF- β signaling. In order to exclude the interference of bovine TGF- β in FBS, we cultured the cells in X-Vivo15 medium which is serum-free. We confirmed the induction of the TGF- β signaling pathway upon TGF- β treatment in these cells by analyzing SMAD 2/3 phosphorylation 15 minutes after treatment (**Figure 12A**) and the down regulation of NKG2D receptor 24 h after treatment (**Figure 12B**) (132). Data from representative donors is shown.

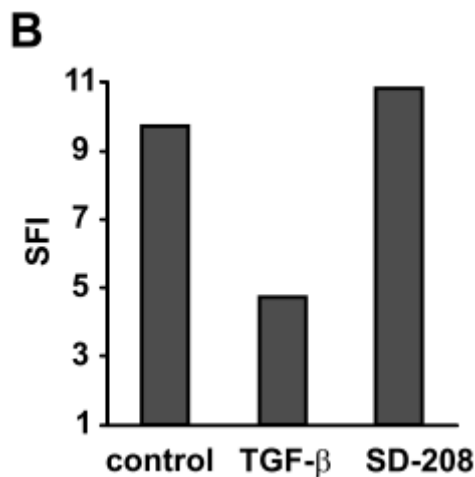
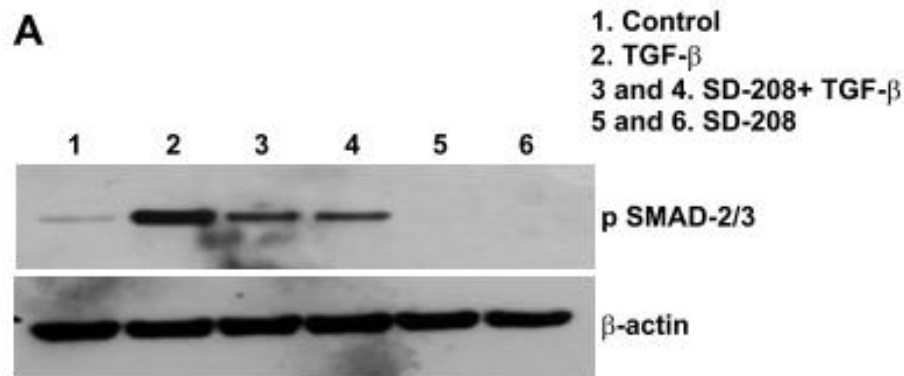


Figure 12. Validation of TGF- β signaling. (A) CD8⁺ T cells were activated for 24 h using T cell activation beads and then treated with 5 ng/ml TGF- β or 1 μ M SD-208 for 15 minutes. In order to control the potency of SD-208, some cells from this donor were also pre-treated for 10 minutes with 1 μ M SD-208 followed by the addition of 5 ng/ml TGF- β for 15 minutes. Untreated cells served as control. Cells were lysed and 5 μ g of total protein lysate was separated in a poly acrylamide gel under reducing conditions. The amount of phospho-SMAD 2/3 was determined by immunoblotting. β -actin was used as loading control. (B) CD8⁺ T cells were activated for 24 h and treated with either 5 ng/ml TGF- β , 1 μ M SD-208 or were left untreated (control group) for 24 h. NKG2D expression on the cell surface was quantified by flow cytometry. Specific fluorescence indices (SFI) were calculated by taking the ratio between the median fluorescent signal obtained with the specific antibody staining to that obtained with the isotype antibody.

After confirming that TGF- β signaling had occurred, cells from 5 donors per treatment group were individually snap-frozen in liquid nitrogen and shipped to Miltenyi Biotec on dry ice. Cells belonging to the same treatment group were pooled across the different donors and total RNA was isolated. Cells were pooled in order to even out donor dependent variations as well as to obtain a sufficient quantity of RNA for hybridization. Quality of RNA was checked on the Agilent 2100 Bioanalyzer platform (Agilent Technologies). The results of the Bioanalyzer run were visualized in a gel (Figure 13A) and an electropherogram (Figure 13B). The 2 prominent peaks in the electropherogram indicate 28S and 18S ribosomal RNA. Peaks between 25 and 200 nucleotides confirmed the presence of 5S ribosomal RNA, transfer RNAs and miRNAs.

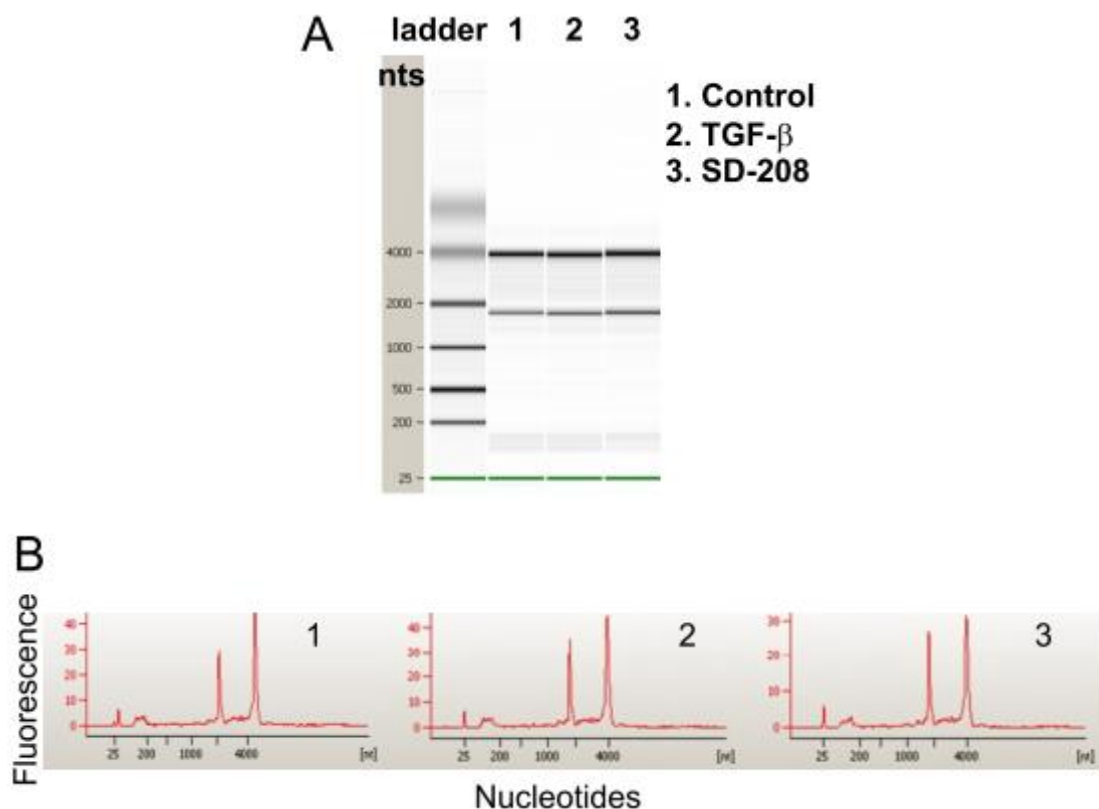


Figure 13. Visualization of total RNA. (A) Gel image where the first lane shows an RNA molecular weight ladder (in nucleotides, nts). The lowest migrating green band is an internal standard. (B) Electropherogram after RNA isolation.

Fluorescence signals from the microarrays were detected using a laser scanner (Agilent) and the false-color images are shown (**Figure 14**). A red spot indicates that the Hy5 signal was higher than the Hy3 signal, a green spot indicates the opposite and a yellow spot indicates similar Hy5 and Hy3 signal intensities.

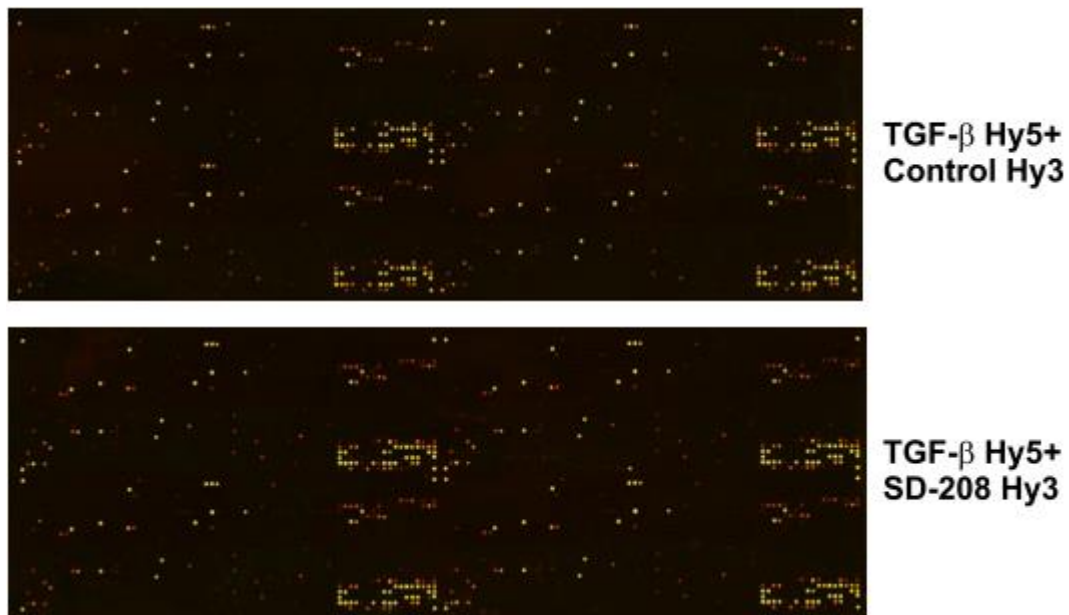


Figure 14. Hy5/Hy3 false-color image after scanning of the microarrays. Using the PIQOR™ Analyzer, mean Hy5/Hy3 ratios for all miRNAs were calculated to obtain the miRNA variations in the TGF-β group relative to both the control and SD-208 treated group.

5.1.2 Next generation sequencing (deep sequencing or libraries)

CD8⁺ T cells from 5 donors were prepared and treated exactly as done for the microarrays. As described in the methods section, from the annotated reads the normalized read numbers for each miRNA were derived and the fold changes of the miRNAs in the TGF-β group relative to the control and the SD-208 group were determined. These changes differed from the ratios obtained from the microarrays. We believe that these variations are due to the inherent differences between the 2 techniques. Such discordances and their reasons have been reported previously (133, 134). Reads that were still not annotated as a known miRNA could have been fragments of longer RNAs, sequencing errors or more interestingly, previously unidentified miRNAs.

5.1.3 Identification of new miRNAs

15-25 base long RNA reads showing no less than 50 reads per sequence were aligned against the human genome (both + and -). Sequences that showed 100% homology were chosen as primary candidates for new miRNAs. Some of the sequences aligned to multiple chromosomes, which was not surprising considering the short size of miRNAs and the fact that similar sequence miRNAs occur throughout the genome. Then, 50-100 bases either upstream or downstream of the sequences were retrieved and the secondary structures were analyzed for their characteristic stem loop formation shown by miRNA precursors. Since pri-miRNAs and polycistronic miRNA transcripts can have multiple stem loops and since their fragments could also be within the sequences reads, we included such secondary structures also among the potential candidates. To this end, sequences were folded *in silico* using the RNAfold WebServer. Options to obtain minimum free energy (MFE) of folding and secondary structure of folding were included in the query along with the sequence. Some of the secondary structures that looked similar to miRNA precursors with sufficiently favorable MFE are shown below.

Sequence A: TCCCACCGCTGCCACC

a. Location: Chromosome 14 (Start = 56043519 Stop = 56045534)

Folding region:

AAGGCCCGCAGCAGCACACAAGCCAGAGGGGAGGGTGGCAGCGGTGGGAG

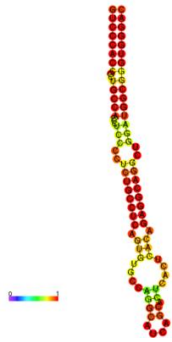


MFE: -22.29 kcal/mol

b. Location: Chromosome 3 (Start = 34575158 Stop = 34577173)

Folding region:

GTCCCACCGCTGCCACCCTCCCCTCTGCCTCAGTGTGCCAGGCATCAGCACTCACTCACAGAGGCA
GGCTGGATGGCGGGTGGGAC

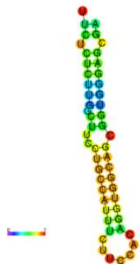


MFE: -45.08 kcal/mol

c. Location: Chromosome 7 (Start = 6148710 Stop = 6150725)

Folding region:

TTCTCTCTGGCTTCTGCCATTTCTTCCACAGGTGGCAGCGGTGGGAGCGA



MFE: -18.59 kcal/mol

This sequence had been annotated as miR-1280 after we had sequenced the libraries. However, its miR status was later withdrawn citing the probability that it could be a t-RNA fragment.

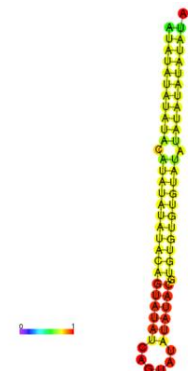
Sequence B: CTCCCACTGCTTCAACT

a. Location: Chromosome X (Start = 835965 Stop = 837981)

Folding region:

ATATATATATACATATATATACAGTATATCAGTATATATACGTGTGTGTATATATATATATATAT
GTAATAAGCATCCAAGAAAACAGAGCTGCTTCAGTTGAAGCAGTGGGAGGCT

(Region ahead of the miRNA sequence shows this folding. Folded Region shown in Green)

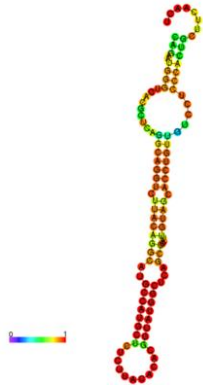


MFE: -24.86 kcal/mol

b. Location: Chromosome 9 (Start= 10820180 Stop= 10820196)

Folding region:

CAGAATGGGTCACGCTCAGGCAGGTCTTACAGGCATGCCATGCTCTCTTACACACGGTATGGCTCA
GCTGATTGTAGCACCTGTTGTCCTCCCACTGCTTCAACT

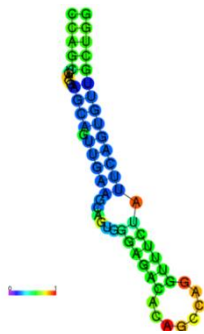


MFE: -34.29 kcal/mol

c. Location: Chromosome 5 (Start= 12327573 Stop= 12327557)

Folding region:

CCAGCTGAGGAGCAGTTGAAGCAGTGGGAGACACAGCCAGGTTTCTATTCAGTGTTGCTGG



MFE: -16.94 kcal/mol.

Sequence C: TTCTCACTACTGCACTTGAA

Location: Chromosome 2 (Start = 34096014 Stop = 34098032)

Folding region:

CTTCAATGAACATACATGATTTGAGAAAACAAAAGGTGACAATGTATCTTTTTATTTTAAACCA
GTCAAGTGCAGTAGTGAGAAG



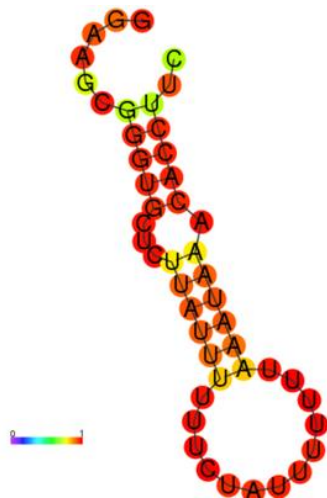
MFE: -15.46 kcal/mol.

This sequence showed 80% homology to the stem loop of cer-miR-248.

Sequence D : GAAGCGGGTGCTCTTATTTT

Location: Chromosome 10 (Start = 18075498 Stop = 18075517)

Folding region: GGAAGCGGGTGCTCTTATTTTTTCTATTTTTTTAAATAAACACCTTC



MFE: -5.9 kcal/mol

This sequence was previously investigated by our collaborators. It was mapped downstream of a tRNA sequence. No activity was detected in reporter gene assays as well as no binding to Ago proteins was observed. Hence it is unlikely to be a functional miRNA.

5.2 Comparison of miRNA arrays and deep sequencing

Significantly ($p < 0.05$) regulated miRNAs from the arrays were compared to their regulation in the libraries and are listed in **Table 3**.

miRNA	Array		Library	
	TGF- β / control	TGF- β / SD208	TGF- β / control	TGF- β / SD208
hsa-let-7b	1.306	1.936	0.330	0.368
hsa-miR-101	1.345	4.054	0.776	0.748
hsa-miR-140-5p	1.362	2.896	1.854	1.023
hsa-miR-146a	2.278	2.064	0.734	1.039
hsa-miR-150	0.749	0.373	0.670	0.620
hsa-miR-15a	1.458	4.557	0.806	0.948
hsa-miR-16	1.011	0.859	0.872	0.796
hsa-miR-17	1.457	0.879	0.996	0.781
hsa-miR-181a	1.649	1.558	0.831	0.682
hsa-miR-21	1.301	3.563	1.057	1.358
hsa-miR-22	1.660	1.881	0.834	1.047
hsa-miR-23a	1.502	1.184	1.150	1.707
hsa-miR-23b	1.953	1.314	1.071	1.008
hsa-miR-24	1.043	1.226	1.400	1.254
hsa-miR-25	3.092	1.779	1.085	0.906
hsa-miR-26b	4.418	2.220	0.990	1.051
hsa-miR-27a	1.878	2.484	1.134	1.636
hsa-miR-27b	2.251	4.355	0.777	0.793
hsa-miR-30b	1.467	1.138	0.660	1.254
hsa-miR-30c	1.860	1.752	0.821	1.243
hsa-miR-30d	1.223	1.183	1.104	0.842
hsa-miR-361-5p	2.421	3.392	1.300	1.249
hsa-miR-93	2.330	7.078	1.448	0.942
hsa-let-7a	0.981	0.765	1.545	0.813
hsa-let-7f	1.360	1.165	1.247	0.896
hsa-miR-103	0.798	0.858	1.185	1.019
hsa-miR-107	0.793	0.846	1.351	1.295
hsa-miR-142-3p	1.161	2.859	0.921	0.996
hsa-miR-19a	1.209	1.891	2.142	14.369
hsa-miR-20a	1.138	1.282	0.944	0.819
hsa-miR-20b	1.014	1.418	0.461	0.334

hsa-miR-106b	0.885	1.247	1.221	1.570
hsa-miR-335	0.790	1.517	0.212	1.105
hsa-miR-29b	1.319	2.545	0.801	0.891
hsa-miR-92a	1.604	1.608	0.881	0.854
hsa-miR-342-3p	0.730	0.455	1.155	0.777
hsa-let-7i	1.249	1.512	1.812	1.351
hsa-miR-142-5p	1.133	1.871	0.422	0.609
hsa-miR-191	0.772	0.645	1.050	0.966
hsa-miR-212	1.055	2.137	0.456	0.884
hsa-miR-26a	0.733	0.595	0.911	0.892
hsa-miR-29c	1.571	1.992	0.821	1.144
hsa-miR-30e	1.269	2.257	1.005	1.263
hsa-miR-30e*	1.111	1.490	1.327	1.253
hsa-miR-769-5p	1.000	3.376	0.741	0.276
hsa-miR-320b	1.568	2.274	2.307	1.934

Table 3. miRNA fold changes in the libraries and arrays. We selected miRNAs that showed statistically significant ($p < 0.05$) regulations and were at least 20% up or down regulated in the TGF- β group relative to the SD-208 treated group in the arrays and compared the fold changes of these miRNAs in the libraries.

To visualize the overlap between the arrays and libraries, we generated a Venn diagram from the miRNAs in table 1 (**Figure 15**).

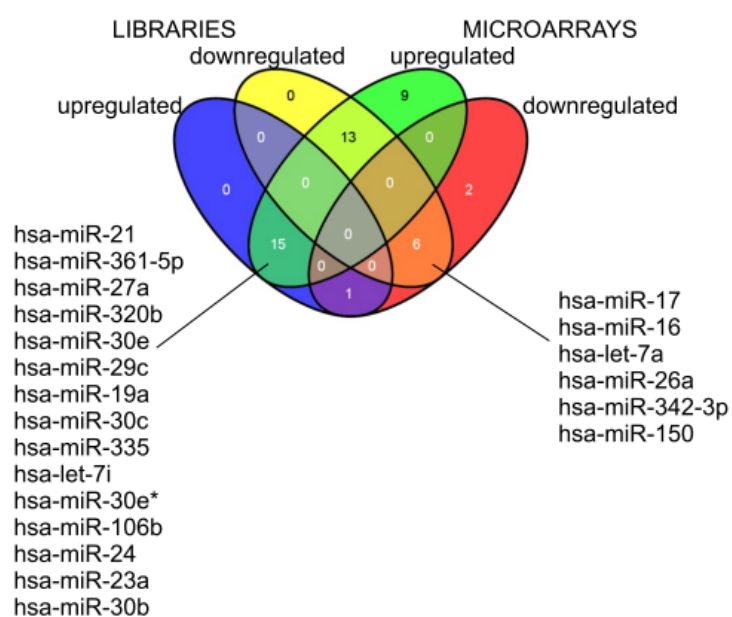


Figure 15. Library vs array. The Venn diagram shows the overlap of regulations between the TGF- β treated group and the SD-208 treated group in the libraries and arrays. miRNAs which were at least 20% up or down regulated were included in the comparison. The Venn diagram was generated using the freely available online tool Venny (135).

As one can observe, several miRNAs showed discordant regulations in the arrays and libraries. A comparison between the 2 platforms is, however, not the major focus of this study, so we searched for the overlap between the two techniques in order to obtain reliable candidates for further validation. Hence, 13 miRNAs which were significantly regulated in the arrays ($p < 0.05$ for TGF- β vs. SD-208 treated groups) and which also showed somewhat similarly directed (up or down) regulations in the miRNA libraries are shown in (Table 4) and were selected for further validation by qRT-PCR.

Table 4.

miRNA		Array		Library	
		TGF- β / control	TGF- β / SD208	TGF- β / control	TGF- β / SD208
1	hsa-miR-21	1.30	3.56	1.06	1.36
2	hsa-miR-361-5p	2.42	3.39	1.30	1.25
3	hsa-miR-140-5p	1.36	2.90	1.85	1.02
4	hsa-miR-27a	1.88	2.48	1.13	1.64
5	hsa-miR-320b	1.57	2.27	2.31	1.93
6	hsa-miR-30e	1.27	2.26	1.01	1.26
7	hsa-miR-19a	1.21	1.89	2.14	14.37
8	hsa-let-7i	1.25	1.51	1.81	1.35
9	hsa-miR-30e*	1.11	1.49	1.33	1.25
10	hsa-miR-24	1.04	1.23	1.40	1.25
11	hsa-miR-23a	1.50	1.18	1.15	1.71
12	hsa-miR-26a	0.73	0.59	0.91	0.89
13	hsa-miR-150	0.75	0.37	0.67	0.62

5.3 qRT-PCR validation of miRNA regulations

CD8⁺ T cells from 3 different donors were isolated and activated for 24 h. The cells were then treated with either 5 ng/ml TGF- β , 1 μ M SD-208 or were left untreated for 24 h. We did not

pool the individual groups from various donors. miRNA cDNA was prepared using a universal reverse primer as described in the methods section.

The efficiency of our technique to robustly amplify mature miRNAs was tested. Sybr green based quantification enabled validation of end product purity through the dissociation curve. A single curve indicated one specific product (**Figure 16A**). In order to confirm that we were indeed amplifying the mature miRNA and not the stem loop precursor, we amplified miRNAs arising from the 5' end and 3' end of the stem loop precursor and analyzed the products on a gel. If the templates were the stem loop precursors, then the amplicons from miRNAs in the 5' end should be longer than the ones from the 3' end and this was not the case (**Figure 16B**). Each miRNA amplicon was nearly 50 bases long because of the addition of the poly-A tail and subsequent binding of the URT primer.

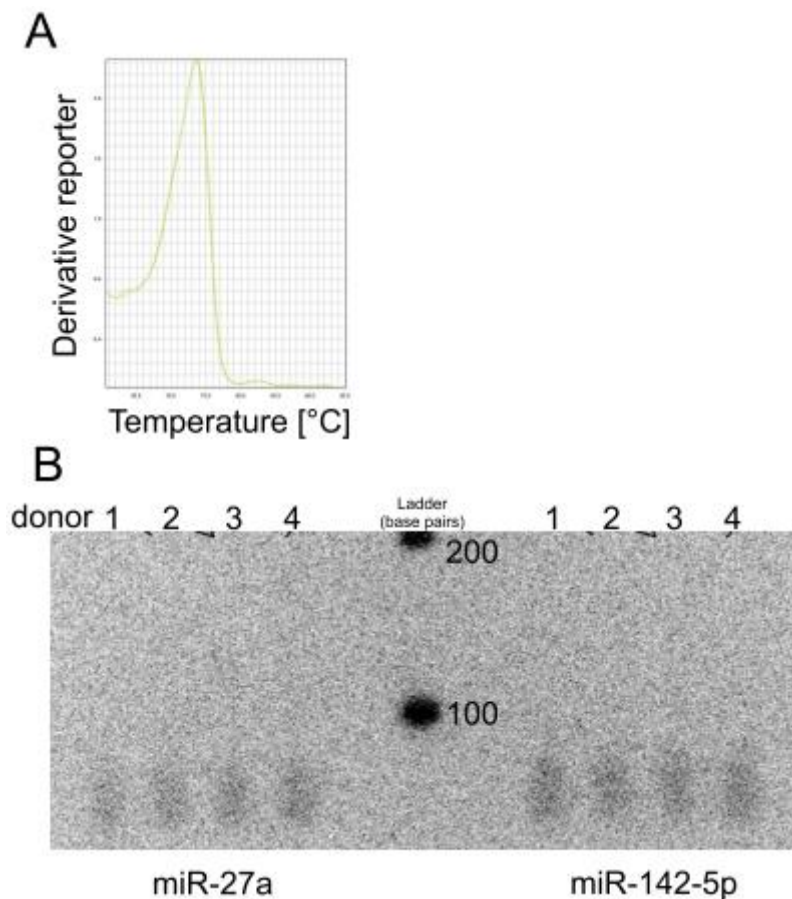


Figure 16. Substantiation of miRNA amplicons. (A) Dissociation (melting) curve of miR-27a generated by the ABI7500 fast software (Applied Biosystems) after amplification of the miRNA. (B) qRT-PCR products were run on a 3% agarose gel and visualized under UV-light.

Only the 3 members of the miR-23a cluster namely miR-23a, miR-27a and miR-24 were consistently upregulated by TGF- β . This upregulation was further upheld when tested in 2 more donors (totally n=5) (**Figure 17**). Conversely, inhibition of TGF- β signaling by SD-208 reduced their expression of the miR-23a cluster. Although there were slight regulations for the

other miRNAs, donor variability was pronounced and thus they were not considered for functional validations.

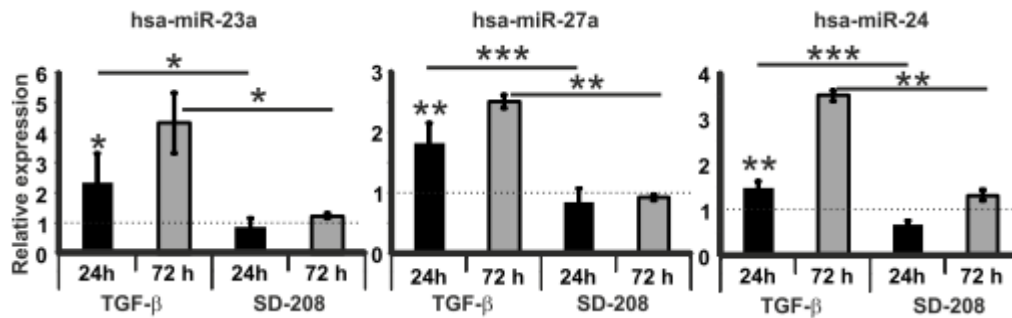


Figure 17. Regulation of miR-23a cluster in CD8⁺ T cells after treatment with TGF-β. CD8⁺ T cells were isolated, activated and either left untreated (control) or treated with TGF-β (5 ng/ml) or SD-208 (1 μM) for 24 or, respectively, 72 hours. miRNA expression was quantified by qRT-PCR using U6 snRNA as internal reference. Relative expression was normalized to control. Average levels of induction (± SD) from different donors are shown (n=5 for 24 h, n=3 for 72 h time-point). p-values were determined using unpaired Student's *t*-test (* *p*<0.05, ** *p*<0.01, *** *p*<0.001).

miR-23a, miR-27a and miR-24 were upregulated by TGF-β in murine CD8⁺ T cells.

TGF-β signaling involving SMADs is highly conserved in metazoans (136). The similarities in molecular targets (including those involved with immune responses) of TGF-β signaling have been extensively compared in mouse and human systems. To confirm the link between TGF-β signaling and induction of the miR-23a cluster, we further used CD8⁺ T cells obtained from the spleen of either wild-type Balb/cJ mice or from mice overexpressing a dominant negative TGF-β type II receptor under control of the human CD2 promoter (hCD2-ΔkTβRII) (123). This presented us a system with genetically impaired TGF-β signaling. Similar to human cells, also CD8⁺ T cells from wild type mice showed an induction of miR-23a, miR-27a and miR-24 upon TGF-β treatment. However, cells from hCD2-ΔkTβRII mice (which lack the intracellular kinase domain) did not show an induction of these miRNAs (**Figure 18**). Due to the low number of animals available for this experiment (4 wild-type and 3 transgenic mice), this induction did not reach statistical significance for individual miRNAs (*p*>0.05). Nevertheless, when z-scores of respective CT values of the miRNAs from the qRT-PCR were taken, ANOVA analysis showed that the miR-23a cluster as a whole was significantly (*p*<0.05) upregulated in CD8⁺ T cells from wild type mice, but not in cells from hCD2-ΔkTβRII mice. Thus, the TGF-β dependent induction of the miRNA-23a cluster which had been found in activated and resting human CD8⁺ T cells could also be confirmed *ex vivo* in transgenic mice expressing a dominant-negative receptor for TGF-β. As basal levels of the

miR-23a cluster members were not reduced in hCD2- Δ kT β RII mice, TGF- β might act as an inducer of these miRNAs without being required for baseline expression. Alternatively, compensatory mechanisms could be operational in mice expressing the dominant-negative TGF- β receptor.

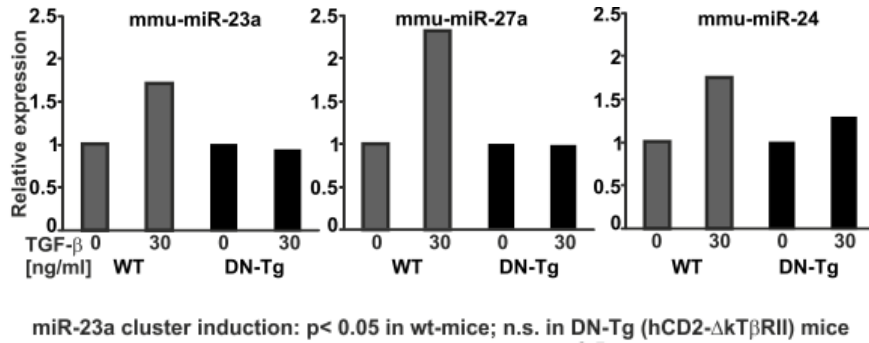


Figure 18. Induction of mouse miR-23a cluster by TGF- β . CD8⁺ T cells were purified from the spleen of hCD2- Δ kT β RII mice overexpressing a dominant negative form of the TGF- β type 2 receptor (DN-Tg) (n=3) and from wild-type mice (WT) (n=4). These cells were activated for 24 h using anti-CD3 and anti-CD28 antibodies in the presence or absence of 30 ng/ml TGF- β 1. Cells were lysed and total RNA was isolated, poly-adenylated and cDNA was prepared. qRT-PCR was performed to quantify miRNA expression using SNORD70 RNA as an internal reference. Relative expression was averaged within the WT or DN-Tg groups and is shown. To analyze the regulation of the miR-23a cluster, z-scores of mean CT values were taken and analyzed by ANOVA ($p < 0.05$).

5.4 The 3'UTRs of LAMP1 and IFN- γ contain binding sites for members of the miR-23a cluster

To search for putative targets of the miR-23a cluster, online miRNA target prediction tools, namely Targetscan (www.targetscan.org), miRanda (www.mirna.org) and DIANA-microT-CDS (diana.cslab.ece.ntua.gr/micro-CDS/?r=search) were employed. Among the predicted target mRNAs CD107a/LAMP1 and IFN- γ stood out as they are both involved in TGF- β sensitive immunological pathways (73, 137), and may hence be of particular relevance for miRNA-mediated, TGF- β dependent immunomodulation. CD107a/LAMP1 has two putative binding sites for miR-23a in its 3'UTR and the 3'UTR of IFN- γ contains complementary regions for both miR-27a and miR-24 (**Figure 19**).

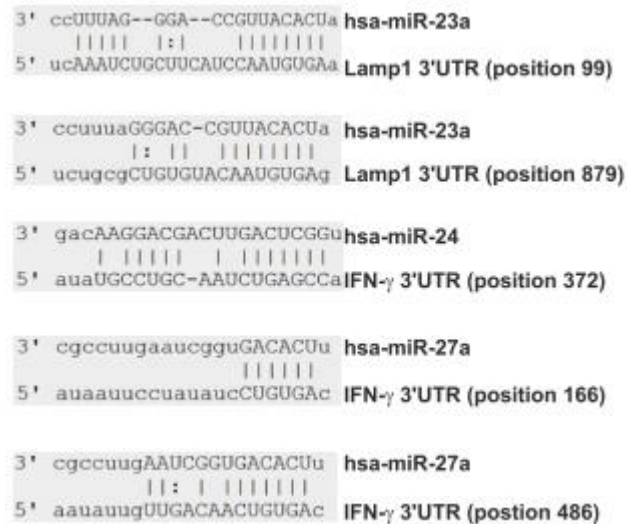


Figure 19. Predicted binding sites of the miR-23a cluster on IFN- γ and LAMP1 3' UTRs. Shown are the alignments of miR-23a, miR-27a and miR-24 on the respective mRNA 3'UTRs (Figure source: miRanda (microRNA.org)).

5.4.1 Cloning reporter gene constructs

The respective 3'UTRs of IFN- γ and LAMP1 were amplified from CD8⁺ T cell cDNA using primers with Pme1 or Spe 1 restriction sites (**Figure 20**). The amplified 3'UTRs were then fused to the firefly luciferase gene in the modified pMIR-RL plasmid to generate pMIR-LAMP1-3'UTR and pMIR-IFN- γ -3'UTR.

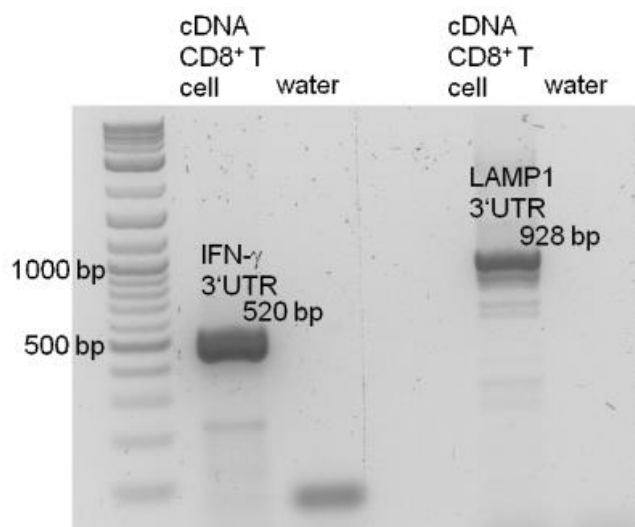


Figure 20. 3' UTR of IFN- γ and LAMP1. RNA from CD8⁺ T cells was isolated using Tri Reagent (Sigma-Aldrich) following the manufacturer's instructions. 0.5 μ g of total RNA was reverse transcribed using iScript Reverse Transcription kit (Biorad). Using 25 ng of cDNA as template, the 3'UTRs of IFN- γ and LAMP1 mRNA were amplified with the respective primers using the Crimson LongAmp polymerase (NEB). The figure shows the 3' UTRs after resolving them on a 1.5% agarose gel.

In order to further confirm the specificity of the miRNA binding to the respective 3' UTRs, we mutated nucleotides within the miRNA binding site to eliminate complementarity (**Figure 21**). Such mutated 3'UTRs were chemically synthesized and fused to the firefly luciferase gene to generate pMIR-LAMP1-mut 3'UTR and pMIR-IFN- γ -mut 3'UTR constructs. This was achieved by introducing 3 to 6 point mutations into each binding site. To maximize repulsion between the miRNA and the 3'UTR at these mutated sites, purines were replaced by pyrimidines and *vice versa*.

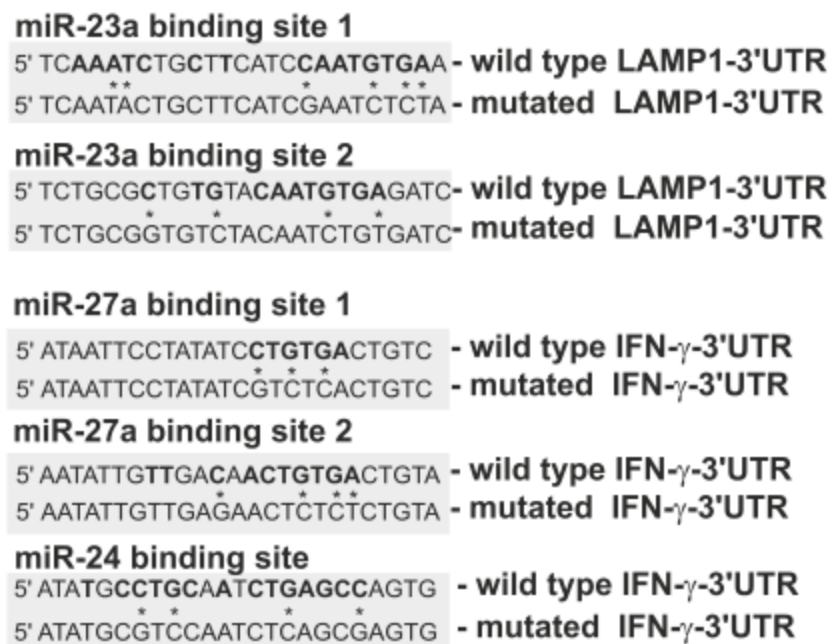


Figure 21. Mutated seed sequences. The illustration shows an alignment of the miRNA binding regions of wild type URT with the mutated 3'UTR. '*' sign indicates a mutation at that point.

5.4.2 miRNA-23a targets the 3'UTR of LAMP1

We performed reporter gene assays using modified pMIR-RL constructs containing the 3' UTR of the putative target mRNA fused to the coding sequence of firefly luciferase which is expressed under a *herpes simplex* virus thymidine kinase (HSV-TK) promoter. As a robust transfection system, we used HEK293T cells. HEK293T cells were transfected with a luminescent miRNA reporter construct containing the 3'UTR of LAMP1 (pMIR-LAMP1-3'UTR). Increased firefly luciferase activity was observed when endogenous miR-23a was blocked by the respective antagomir whereas blockade of miR-27a or miR-24 or addition of an antagomir against the non-expressed (brain-specific) miR-9 (138) showed no significant effect (**Figure 22A, left**). Conversely, overexpression of miR-23a reduced the luciferase signal while miR-27a and miR-24 or addition of control RNA did not affect luminescence (**Figure 22A, right**). These data support the *in silico* prediction that miR-23a binds to the

3'UTR of LAMP1 and thereby leads to inhibition of protein synthesis. Moreover, miR-23a overexpression failed to silence firefly luciferase expression from the pMIR-LAMP1-mut 3'UTR construct. This assay confirmed the specificity of the predicted miRNA binding (Figure 22 B).

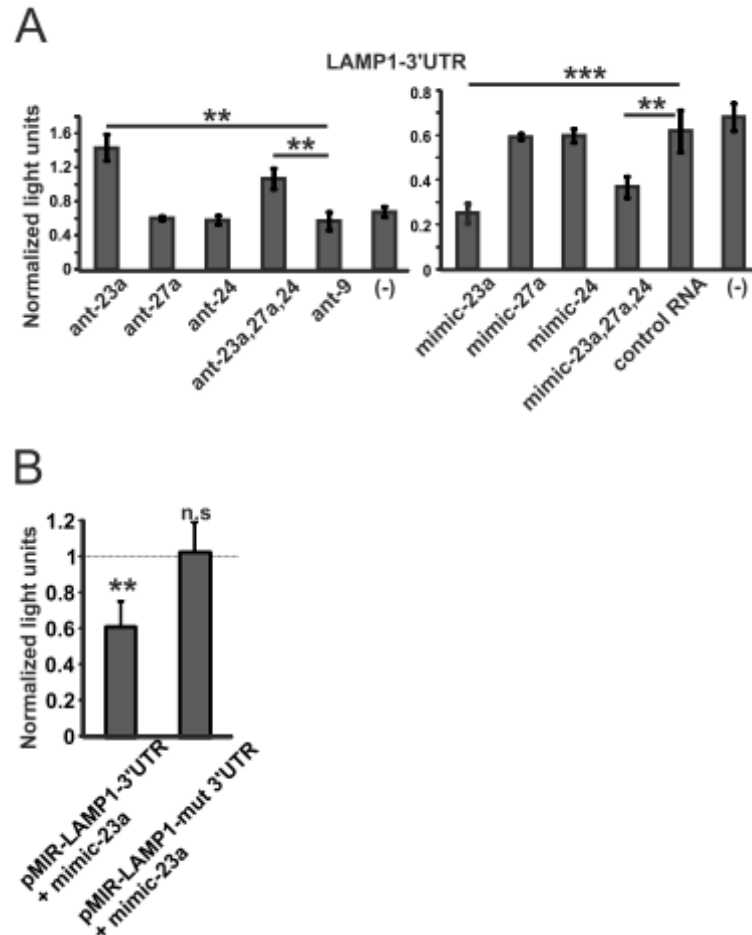
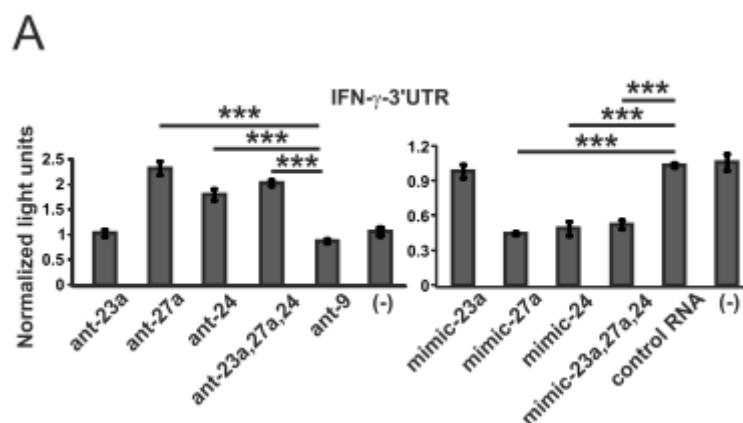


Figure 22. miR-23a can target LAMP1-3'UTR. Reporter gene assays were performed using unmodified or mutated 3'UTRs of LAMP1. HEK293T cells were thus transfected with either pMIR-RL, pMIR-LAMP1-3'UTR or pMIR-LAMP1-mut 3'UTR alone (-) or in combination with antagomirs against miR-9 (ant-9) as control, miR-23a (ant-23a), miR-27a (ant-27a), miR-24 (ant-24) or all 3 together (ant-23a, 27a, 24) respectively. Likewise, mimics for miR-23a (mimic-23a), miR-27a (mimic-27a), miR-24 (mimic-24), all 3 together (mimic-23a, 27a, 24) or negative control RNA (control RNA) were co-transfected with the reporter plasmids as indicated. 24 hours after transfection, the cells were lysed in Reporter Lysis Buffer (Promega) and a dual luciferase assay was performed. Relative light units (RLU) were calculated by taking the ratio of background-subtracted firefly to *renilla* luciferase light units. The RLUs from the various constructs were then normalized to those obtained with pMIR-RL (in **A**) or to the group co-transfected with the respective construct and the irrelevant control RNA (in **B**). Transfections were performed in triplicates and a representative out of 3 independent experiments is shown (\pm SD). p-values were determined using Student's *t*-test (* $p < 0.05$, ** $p < 0.01$, *** $p < 0.001$).

5.4.3 miR-24 and miR-27a target the 3'UTR of IFN- γ

When HEK293T cells were transfected with a luminescent miRNA reporter construct containing the 3'UTR of IFN- γ (pMIR-IFN- γ -3'UTR), increased firefly luciferase activity was observed upon suppression of endogenous miR-27a and miR-24. Inhibition of miR-23a or control transfection with an antagomir against miRNA-9 had no such effect (**Figure 23 A left**). On the other hand, over-expression of miR-27a and miR-24 significantly lowered firefly luciferase activity whereas the over-expression of miR-23a or transfection with control RNA did not affect luciferase activity (**Figure 23A, right**). The apparent lack of synergy between miR-27a and miR-24 which both bind to the same 3'-UTR may be explained by the total amount of mimics or antagomirs which was always kept constant. In addition, it is not clear whether independent binding of two different miRNAs can further enhance the transcriptional blockade achieved by binding of a single miRNA or whether limited availability of accessory proteins may restrict the total effect of miRNAs. Still, the reporter assay data clearly show that miR-27a and miR-24 both bind to the 3'UTR of IFN- γ and block protein synthesis. Again, mutation of the predicted binding sites on the IFN- γ 3' UTR prevented the silencing of firefly luciferase gene upon overexpression of miR-27a and miR-24 (**Figure 23B**) confirming the specificity of miRNA binding to the proposed sites on the respective 3'UTRs which will then inhibit protein synthesis.



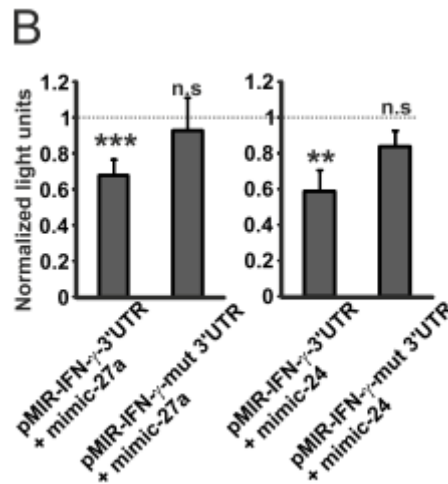


Figure 23. miR-27a and miR-24 can target IFN- γ 3'UTR. HEK293T cells were transfected with either pMIR-RL, pMIR-IFN- γ -3'UTR or pMIR-IFN- γ -mut 3'UTR alone (-) or in combination with antagomirs against miR-9 (ant-9) as control, miR-23a (ant-23a), miR-27a (ant-27a), miR-24 (ant-24) or all 3 together (ant-23a, 27a, 24) respectively. Likewise, mimics for miR-23a (mimic-23a), miR-27a (mimic-27a), miR-24 (mimic-24), all 3 together (mimic-23a, 27a, 24) or negative control RNA (control RNA) were co-transfected with the reporter plasmids as indicated. 24 hours after transfection, the cells were lysed in Reporter Lysis Buffer (Promega) and a dual luciferase assay was performed. Relative light units (RLU) were calculated by taking the ratio of background-subtracted firefly to *renilla* luciferase light units. The RLU from the various constructs were then normalized to those obtained with pMIR-RL (in A) or to the group co-transfected with the respective construct and the irrelevant control RNA (in B). Transfections were performed in triplicates and a representative out of 3 independent experiments is shown (\pm SD). p-values were determined using Student's *t*-test (* $p < 0.05$, ** $p < 0.01$, *** $p < 0.001$).

5.5 The miR-23a cluster inhibits LAMP1 surface expression on activated CD8⁺ T cells

TGF- β mediated inhibition of activation and degranulation of cytotoxic CD8⁺ T cells has been described earlier (137). Since degranulation causes transient integration of CD107a/LAMP1 into the outer cell membrane, lytic activity can be quantified via surface staining for LAMP1. However, the mechanism by which TGF- β inhibits degranulation has not been described yet. As for potential direct miRNA-mediated effects on LAMP1, miRNAs can only inhibit synthesis of new LAMP1 protein through the 3'UTR. Hence, miRNAs are unlikely to be involved in rapid regulations which occur mainly by translocation. Therefore we first investigated the dynamics of LAMP1 expression during activation of CD8⁺ T cells. To this aim, we added the translation inhibitor cycloheximide (CHX) to a stimulation experiment. Immunoblotting revealed that CHX prevents the activation-dependent increase in total

LAMP1 expression. Basal LAMP1 levels, however, were hardly affected (**Figure 24**) indicating a very low turnover of LAMP1 protein (139, 140). (Immunoblot-based quantification is affected by the effect of CHX on the loading control (GAPDH) and thus mainly qualitative).

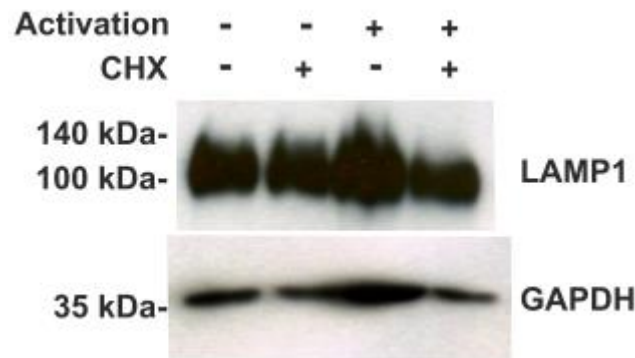


Figure 24. Total LAMP1 levels after activation. In order to quantify total LAMP1, untouched CD8⁺ T cells were isolated and either rested or activated with anti-CD2, anti-CD3 and anti-CD28 coated beads, in the absence or presence of cycloheximide (CHX). After 48 h, cells were lysed and the protein was quantified using immunoblotting as described.

We then attempted to study the kinetics of LAMP1 surface expression on CD8⁺ T cells after activation in the presence of CHX. As expected, non-activated CD8⁺ T cells express very little LAMP1 on the cell surface while activated cells showed a progressive increase of surface LAMP1 expression with time. However, when we stimulated cells in the presence of CHX, it showed little effect on surface LAMP1 at 6 h, but prevented the activation-induced display of LAMP1 at later time points (**Figure 25**).

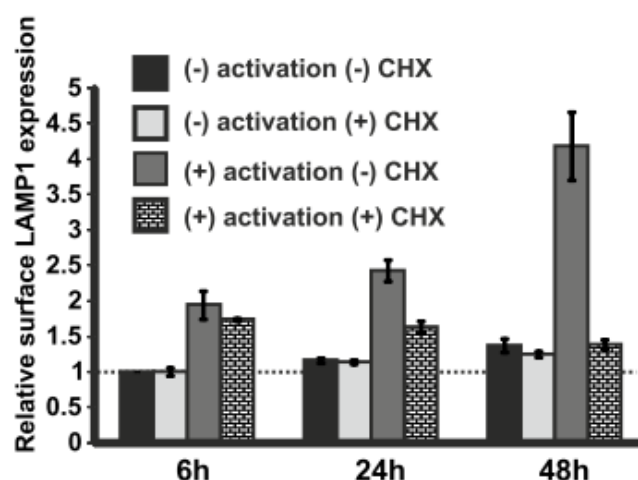


Figure 25. Effect of CHX on LAMP1 surface expression. CD8⁺ T cells were isolated and treated as in (**Figure 24**). After 2 h, 20 h and 44 h, respectively, PE-conjugated anti-LAMP1 antibody or an isotype control antibody was added to the cells followed by monensin. 4 hours later, surface expression of LAMP1 was determined by flow cytometry. To obtain specific fluorescence intensity (SFI) values, the median fluorescence values obtained

with PE-conjugated anti-CD107a were divided by the median fluorescence values obtained with a PE-labeled isotype control antibody.

While this effect of CHX could imply that surface LAMP1 expression is contributed by freshly translated LAMP1 (which would be sensitive to both miR-23a and CHX), it could also imply an effect of CHX on the myriad of proteins that are required for degranulation and/or vesicular transport. As LAMP1 is a highly abundant glycosylated protein with a rather long half life (nearly 2 days), Even the complete blockade of protein synthesis by cycloheximide affected its expression levels in activated T cells only slightly. Therefore, it was unlikely that the miRNAs could affect total LAMP1 pools in the cell in such a short period (139, 140). We put our hypothesis to the test by quantifying the effect of the miR-23a cluster on the activation-induced surface expression of LAMP1. Having found that the percentage of bead-activated CD8⁺ T cells expressing CD107a/LAMP1 on the surface increased from about 20% at 6 h after stimulation to almost 70% after 48 h, we chose this later time point as a potential read-out for miRNA regulation. While this may appear rather late for the measurement of CD107a/LAMP1, any inhibition of translation (whether by CHX or by miRNAs) can only become relevant with time. As implied by the reporter gene assays, LAMP1 surface expression on T cells decreased when the miR-23a cluster was over-expressed, whereas higher LAMP1 surface expression was observed when the cells were nucleofected with antagonists against the miR-23a cluster (**Figure 26A**).

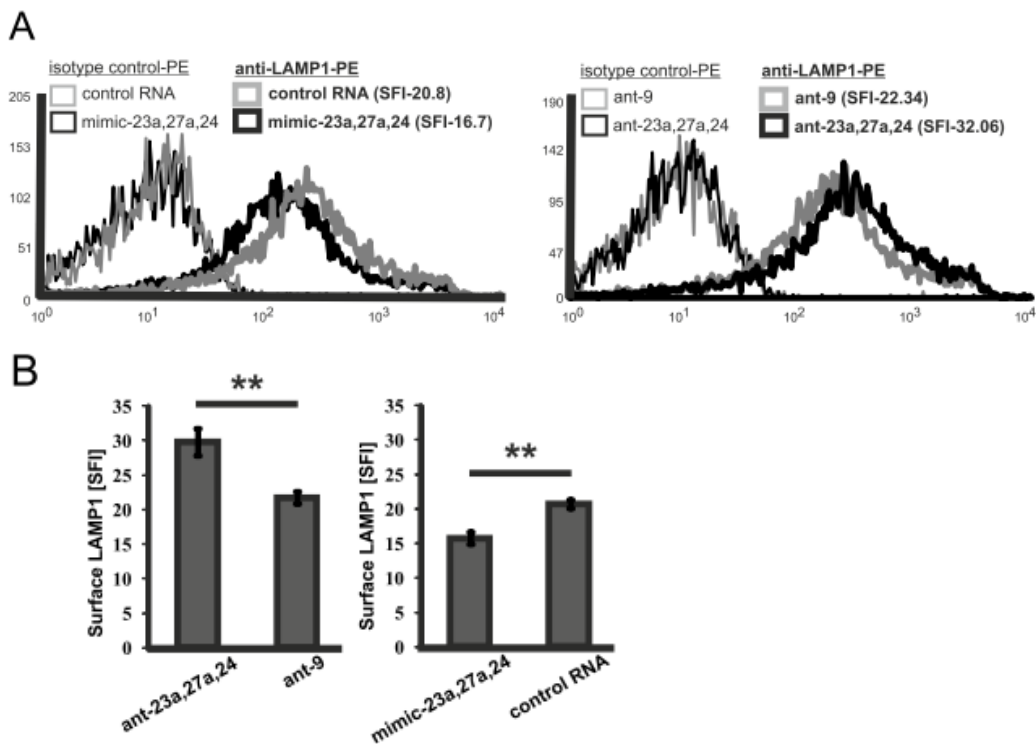


Figure 26. Effect of miR-23a cluster on surface LAMP1 expression. CD8⁺ T cells were isolated and split up into 4 groups. Each group was nucleofected with either a cocktail of mimics for miR-23a, miR-27a and miR-24 (mimic-23a, 27a, 24) or negative control RNA (control RNA) or a cocktail of antagomirs against miR-23a, miR-27a and miR-24 (ant-23a,27a,24) or antagomirs against miR-9 (ant-9). The total concentration of nucleotides was kept constant at 300 nM. 12 h after nucleofection, the cells were activated with beads as in (Figure 12). After 48 hours, anti-LAMP1 PE antibody or an isotype control antibody was added to the cells followed by monensin. 4 hours later, the cells were analyzed for LAMP1 expression by flow cytometry. (A) A histogram from a representative experiment (n=3) is shown. In (B), fluorescence values from 3 independent experiments were plotted (\pm SD). p-values were determined using Student's *t*-test. ($p > 0.05$, * $p < 0.05$, ** $p < 0.01$, *** $p < 0.001$)

While this suggests that granule exocytosis by activated T cells requires additional production of LAMP1 which could be affected by miR-23a, we did not see any significant effect of the miRNAs on total LAMP1 in the cells. Alternatively, the probability of a yet unidentified protein (involved in granule trafficking or plasma membrane fusion) being additionally targeted by miR-23a would also lead to decreased LAMP1 cell surface expression. In both cases, induction of miR-23a will impair CD8⁺ T cell degranulation and thus contribute to the known effects of TGF- β . However, considering that the effect was only moderate, we did not investigate the multitude of transport proteins which could additionally be targeted by miR-23a.

5.6 miR-23a cluster inhibits IFN- γ expression in activated CD8⁺ T cells

While TGF- β is already known to control IFN- γ on transcriptional level (73), post transcriptional regulations are poorly understood. Our results from reporter gene assays (see Figure 23A and 23B) suggest that the miR-23a cluster (which can be induced by TGF- β) could potentially modulate IFN- γ translation. Activation of CD8⁺ T cells with bead-bound agonistic antibodies against CD2, CD3 and CD28 led to IFN- γ secretion which could be detected after 6 h, reaching a maximum between 24 and 48 h (Figure 27).

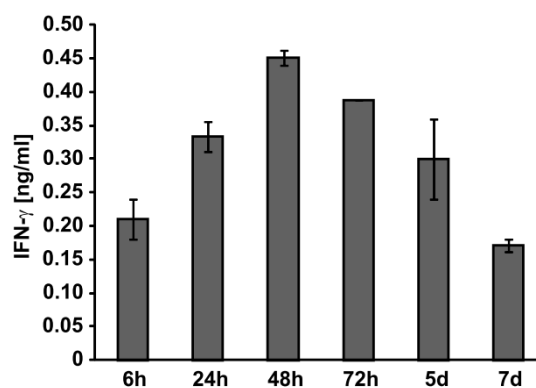


Figure 27. Kinetics of IFN- γ secretion in activated CD8⁺ T cells. CD8⁺ T cells isolated from a healthy human donor were stimulated anti-CD2, anti-CD3 and anti-CD28 coated beads. Supernatant from these cells were collected after 6 h, 24 h, 48 h, 72 h, 5 days and 7 days. Concentration of IFN- γ in technical duplicates was quantified in these supernatants by sandwich ELISA as described in the Methods section. Experiment was performed twice using different donors and a representative experiment is shown.

Nucleofection negatively affected the ability of cells to produce IFN- γ . We observed that nucleofected cells produced about $\frac{1}{2}$ to $\frac{1}{3}$ of that was produced by non-nucleofected cells. In order to allow sufficient time for the antagonists to silence the respective miRNAs and the mimics to inhibit newly synthesized IFN- γ , we assessed effects of miRNAs on IFN- γ expression after 48 h of activation. ELISA measurements revealed significantly less IFN- γ in supernatants from CD8⁺ T cells in which the miR-23a cluster had been overexpressed compared to cells transfected with control RNA (**Figure 28A**). A shift in IFN- γ -FITC fluorescence further showed that overexpression of the miR-23a cluster reduces the average amount of IFN- γ per cell (**Figure 28B**) without necessarily lowering the percentage of IFN- γ ⁺ cells – which would be compatible with a miRNA-mediated effect that may attenuate rather than abrogate protein production.

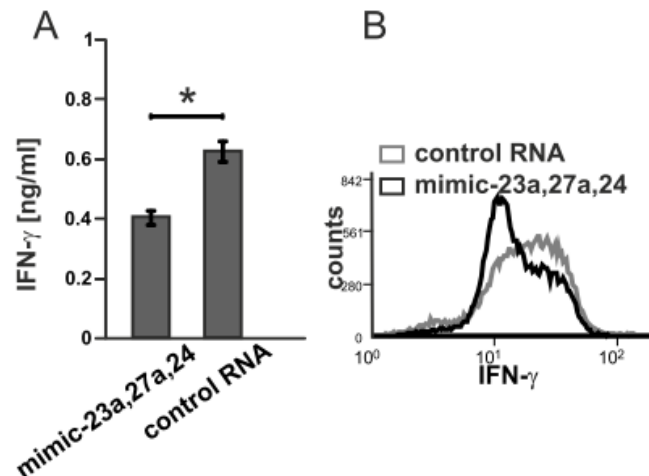


Figure 28. miR-23a cluster overexpression inhibits IFN- γ production. To analyze the effects of miR-23a cluster overexpression, CD8⁺ T cells were isolated and nucleofected either with control RNA or a combination of mimics for miR-23a, miR-27a and miR-24, always keeping the RNA concentration constant at 300 nM. 12 h after nucleofection, the CD8⁺ T cells were activated using anti-CD2, anti-CD3 and anti-CD28 coated beads. p-values were determined using Student's *t*-test (* $p < 0.05$, ** $p < 0.01$, *** $p < 0.001$) from triplicate wells. (A) Following 48 h of activation, supernatants were collected and IFN- γ levels were quantified by ELISA as described in the Methods section. The nucleofected and stimulated cells were incubated with monensin for an additional 4 h before IFN- γ expression was determined by intracellular flow cytometry. A histogram overlay of the intracellular IFN- γ staining in the cells is shown in (B).

In line with the pMIR reporter gene assays which had shown that miR-27a and miR-24, but not miR-23a, can target IFN- γ via its 3'UTR, intracellular cytokine staining indicated significantly lower IFN- γ levels in cells when either miR-27a or miR-24 was overexpressed whereas no change was observed upon overexpression of miR-23a (**Figure 29**).

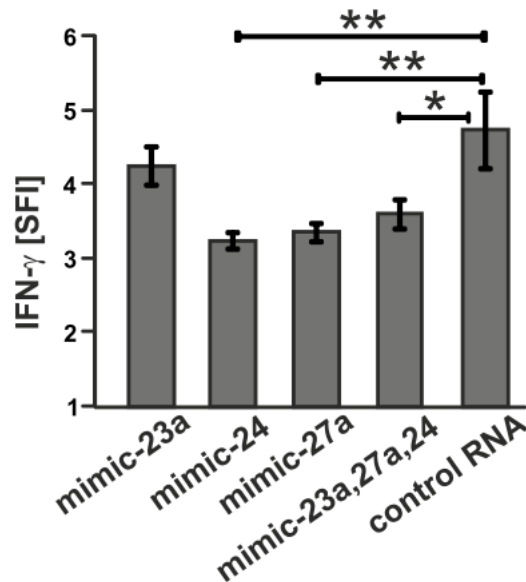


Figure 29. IFN- γ expression is specifically inhibited by miR-27a and miR-24 but not by miR-23a. To analyze the effects of overexpression of individual members of the miR-23a cluster, CD8⁺ T cells were isolated and nucleofected either with control RNA or with mimics for individual miR-23a cluster members or with their combination, always keeping the RNA concentration constant at 300 nM. 12 h after nucleofection, the CD8⁺ T cells were activated using anti-CD2, anti-CD3 and anti-CD28 coated beads. Following 48 h of activation, cells were incubated with monensin for an additional 4 h before IFN- γ expression was determined by intracellular flow cytometry. Specific fluorescence intensities from 3 independent experiments were determined by normalizing the median fluorescence of the IFN- γ antibody staining to that of an isotype control antibody and are plotted (\pm SD). p-values were determined using Student's *t*-test (* $p < 0.05$, ** $p < 0.01$, *** $p < 0.001$).

Surprisingly, we did not see any difference in secreted IFN- γ when the miR-23a cluster was silenced (**Figure 30 A**) using antagomirs against the cluster. However, when we analyzed the fairly small amount of residual IFN- γ protein in cell lysates, levels were significantly elevated after silencing of the miR-23a cluster. Again, cells transfected with the antagomir against the non-expressed miR-9 served as control (**Figure 30 B**).

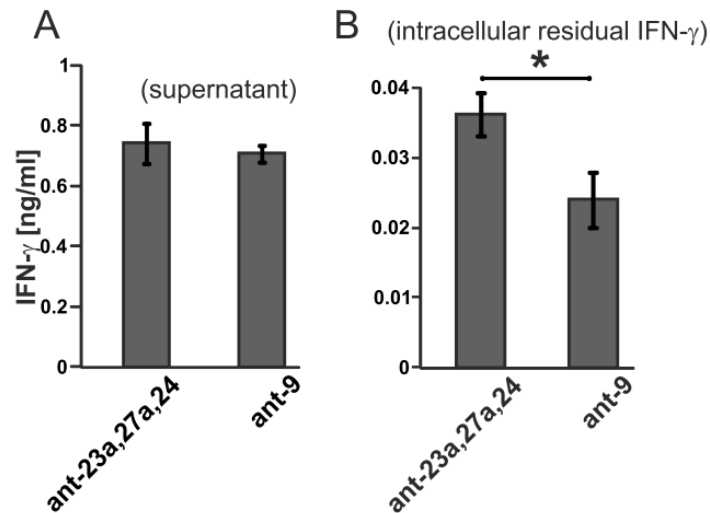


Figure 30. Inhibition of the miR-23a cluster affects residual IFN- γ within the CD8⁺ T cells. To analyze the effect of silencing the miR-23a cluster on IFN- γ expression, CD8⁺ T cells were isolated and nucleofected with either 300 nM of combined antagomirs against miR-23a cluster members (ant-23a,27a,24) or with 300 nM of an irrelevant control antagomir against miR-9. 12 h after nucleofection, the cells were activated with anti-CD2, anti-CD3 and anti-CD28 coated beads. Following 48 h of activation, supernatants were collected and secreted IFN- γ was quantified by ELISA. Tests were performed in 2 technical replicates and a representative experiment (of n=3) is shown (A). At the same time, the cells were lysed and IFN- γ contained in the lysates was also determined via sandwich ELISA (B). Data are shown \pm SD and p-values were determined using Student's *t*-test (* $p < 0.05$, ** $p < 0.01$, *** $p < 0.001$).

Additionally, we observed a significantly higher percentage of IFN- γ positive cells after silencing of the miR-23a cluster (Figure 31). Thus, endogenous levels of miR-24 and miR-27a in CD8⁺ T cells could be sufficient to prevent IFN- γ production in slightly activated cells, but may have little effect on cells producing a large amount of IFN- γ .

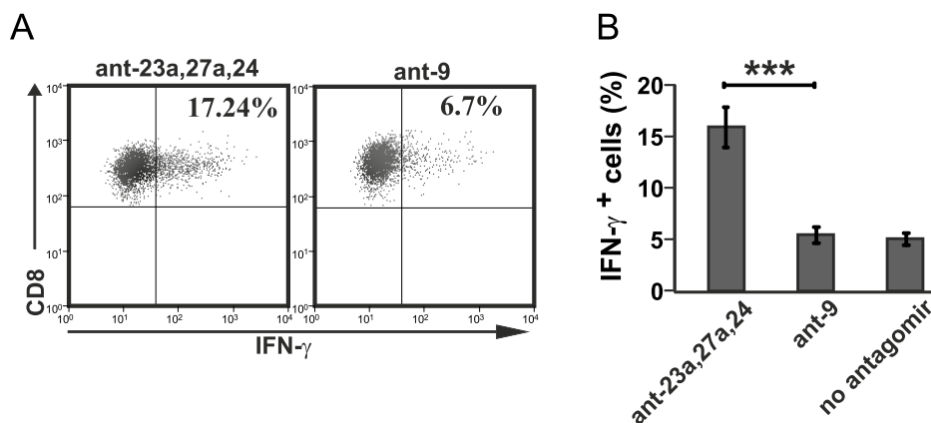


Figure 31. Inhibition of miR-23a cluster increased the number of IFN- γ producing cells. CD8⁺ T cells were isolated and were treated as done in Figure 30. After 44 h these cells were further incubated with monensin for 4 h and the percentage of IFN- γ ⁺ cells was determined by intracellular flow cytometry as described in the Methods section. A representative dot plot is shown in (A) while the percentage of IFN- γ ⁺ cells (\pm SD) from 3

independent experiments is indicated in (B). p-values were determined using Student's *t*-test (* $p < 0.05$, ** $p < 0.01$, *** $p < 0.001$).

Since we had found the miR-23a cluster to be induced by TGF- β , we asked whether inhibition of these miRNAs also influences IFN- γ production in the presence of TGF- β . In fact, while TGF- β treatment reduced the number of IFN- γ positive cells in all groups, the percentage of cells remaining positive for IFN- γ was significantly increased when the cells had been transfected with antagonists before being exposed to TGF- β (Figure 32).

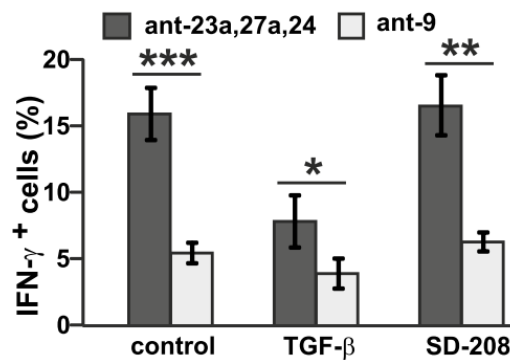


Figure 32. Inhibition of miRNAs could not rescue the effect of TGF- β on IFN- γ expression. CD8⁺ T cells were isolated and treated as done in Figure 30. Additionally, following nucleofection with antagonists, each group was divided and treated with either TGF- β (5 ng/ml), SD-208 (1 μ M) or left untreated for 12 h. After 48 h of activation, IFN- γ ⁺ cells were determined by intracellular flow cytometry and their respective percentages were plotted. p-values were determined using Student's *t*-test (* $p < 0.05$, ** $p < 0.01$, *** $p < 0.001$).

Considering that antagonists do not affect the known repression of IFN- γ transcription by TGF- β (73, 141), more than this partial rescue would have appeared implausible. Thus, inhibition of IFN- γ translation by the TGF- β -inducible miR-23a cluster apparently constitutes a second, indirect mechanism by which TGF- β suppresses IFN- γ production. Nevertheless, the miR-23a cluster can inhibit translation of IFN- γ also in the absence of TGF- β .

5.7 miRNAs from the miR-23a cluster inhibit IFN- γ expression in Melan-A-specific CD8⁺ T cells

So far, we had only analyzed T cells that had been activated by a non-specific TCR-trigger via antibody-coated beads. To understand the role of the miR-23a cluster on IFN- γ production following a more physiological and antigen-specific stimulus, we analyzed activation patterns of Melan-A-specific CD8⁺ T cells. These cells are derived from purified naïve T cells that were primed *in vitro* using peptide-pulsed dendritic cells and subsequently expanded to yield high numbers of T cells with an early effector memory phenotype (129).

First we tested whether TGF- β was able to induce the miR-23a cluster in these activated and expanded cells. Melan-A-specific CD8⁺ T cells were treated with TGF- β or SD208 and the miR-23a cluster expression was quantified relative to U6 snRNA. Similar to our results with non-specific T cell stimuli in CD8⁺ T cells from peripheral blood, miR-23a, miR-27a and miR-24 were also induced by TGF- β in this antigen-specific T cell population (**Figure 33**).

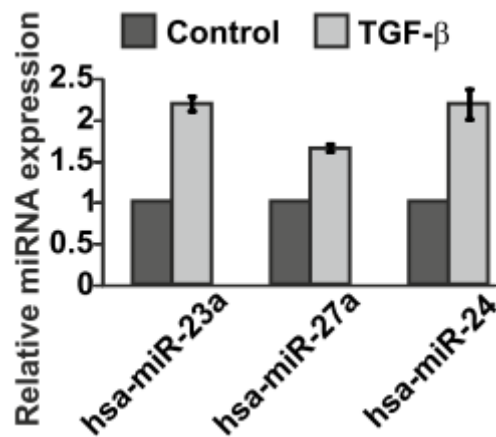


Figure 33. miR-23a cluster is induced by TGF- β in Melan-A specific CD8⁺ T cells. In order to confirm the induction of the miR-23a cluster, Melan-A-specific T cells were generated and treated with TGF- β (5ng/ml) or left untreated (control) for 24 h. miRNA was isolated and the expression of miR-23a, miR-27a and miR-24 was determined relative to U6 snRNA by qRT-PCR. Expression levels were normalized to the control and the mean normalized expression from 3 experiments is shown.

To functionally investigate the effect of the miR-23a cluster on antigen-specific T cells, expanded Melan-A-specific CD8⁺ T cells (purity of 30-50%) were restimulated with monocytes pulsed with the Melan-A26-35(A27L) (ELA) peptide, the Melan-A-overexpressing FM55 cell line or the FM55 cell line pulsed with ELA peptide. Melan-A-specific CD8⁺ T cells that had been restimulated with the irrelevant WT1 antigen (the HLA-A2 restricted epitope of Wilms Tumor antigen 1 (126-134)) on monocytes served as negative control. Intracellular cytokine staining 4 h after restimulation showed an increased percentage of IFN- γ ⁺ cells when the miR-23a cluster had been suppressed (**Figure 34A and 34B**) whereas overexpression of the cluster did not affect the proportion of IFN- γ -producing cells.

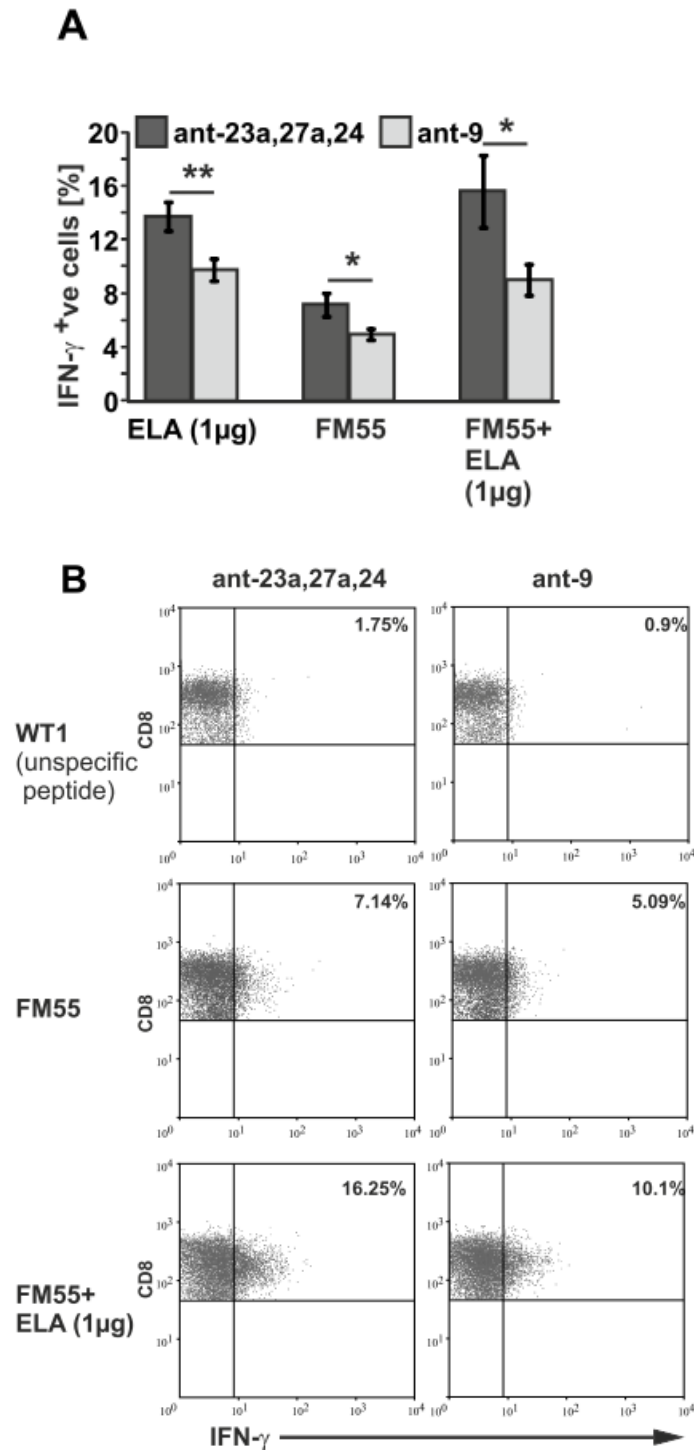


Figure 34. Suppression of the miR-23a cluster in restimulated Melan-A specific cells reduces the number of IFN- γ producers. (A) Melan-A specific CD8⁺ T cells were divided into 2 groups, and nucleofected with either 300 nM of antagomir cocktail (containing 100 nM each of antagomirs against miR-23a, miR-27a and miR-24) or 300 nM antagomir against miR-9. After 48 h, the cells were re-stimulated either with monocytes loaded with 1 μ g/ml ELA peptide (ELA 1 μ g), with monocytes loaded with WT1 (unspecific peptide) (WTI), with the Melan-A-expressing FM55 (FM55) cell line or with FM55 cells loaded with 1 μ g/ml ELA peptide (FM55+ ELA1 μ g). The percentage of IFN- γ positive cells was quantified by intracellular flow cytometry 4 hours after re-stimulation in the presence of monensin. Data from 3 independent experiments were pooled and the mean of

percentage of IFN- γ positive cells (\pm SD) is indicated. Representative dot-plots are shown in (B). p-values were determined using Student's *t*-test (* $p < 0.05$, ** $p < 0.01$, *** $p < 0.001$).

We also attempted a prolonged restimulation for 18 h and collected the supernatant from these cells. Here we detected significantly higher amounts of IFN- γ when the miR-23a cluster had been inhibited. Conversely, overexpression of the miR-23a cluster reduced the levels of secreted IFN- γ (Figure 35). Controls included the irrelevant antagomir against the non-expressed miR-9 and the control RNA.

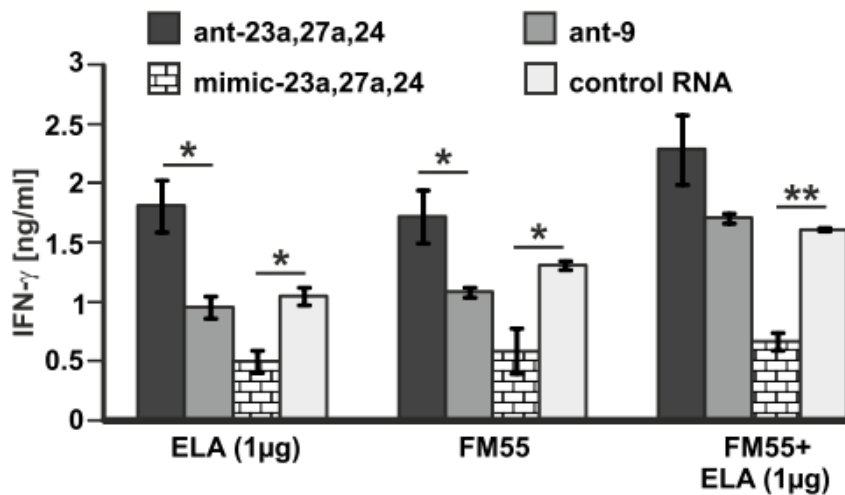


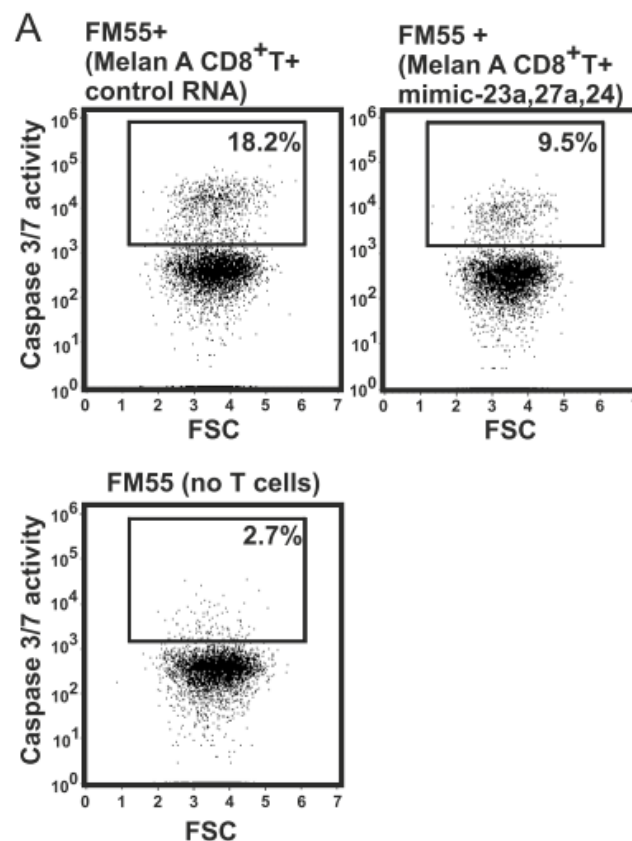
Figure 35. Modulation of the miR-23a cluster affects the levels of secreted IFN-g in Melan-A specific CD8⁺ T cells. Melan-A specific CD8⁺ T cells were divided into 4 groups, and nucleofected with either 300 nM of antagomir cocktail (containing 100 nM each of antagomirs against miR-23a, miR-27a and miR-24) or 300 nM antagomir against miR-9 or 300 nM of miRNA mimic cocktail (containing 100 nM each of mimic-23a, mimic-27a and mimic-24) or 300 nM of control RNA. After 48 h, the cells were re-stimulated with monocytes loaded with 1 μ g/ml ELA peptide (ELA 1 μ g), with the Melan-A-expressing FM55 (FM55) cell line or with FM55 cells loaded with 1 μ g/ml ELA peptide (FM55+ ELA1 μ g). Supernatants were collected 18 h after re-stimulation and secreted IFN- γ was quantified by ELISA. Shown are mean concentrations of IFN- γ measured in a representative experiment (n=3 independent experiments, measurements performed in triplicate). p-values were determined using Student's *t*-test (* $p < 0.05$, ** $p < 0.01$, *** $p < 0.001$).

Thus, the experiments performed in this system (which seeks to recapitulate the physiological mode of T cell activation) confirmed the previously observed pattern that inhibition of the miR-23a cluster increases the percentage of IFN- γ ⁺ cells whereas transfection with mimics for miR-24 and miR-27a reduces the amount of IFN- γ secreted by highly stimulated CD8⁺ T cells. Moreover, the amount of IFN- γ detected by ELISA was also increased by the antagomirs (which had not been observed with bead-stimulated CD8⁺ T cells). Accordingly,

the miR-23a cluster serves as a TGF- β -inducible set of miRNAs involved in the fine tuning of IFN- γ production in CD8⁺ T cells.

5.8 The miR-23a cluster inhibits the cytotoxic activity of antigen-specific CD8⁺ T cells

To study the effect of the miR-23a cluster on the cytotoxic activity of CD8⁺ T cells, we analyzed the killing of FM55 (target) cells by Melan-A-specific CD8⁺ T (effector) cells. We used the CellEventTM Caspase 3/7 Green detection reagent to detect dying cells. This cell permeable reagent is cleaved by caspases and rendering it fluorescent, enabling us to quantify dying cells by flow cytometry. To this aim, both effector and target cells were co-cultured for 4 h before the caspase substrate was added. 30 min later, the percentage of FM55 cells showing increased Caspase 3/7 activity was determined by flow cytometry. Overexpression of the miR-23a cluster using mimics for miR-23a, miR-27a and miR-24 significantly reduced the killing capacity of Melan-A-specific T cells when compared to those transfected with the control RNA (**Figure 36A and 36B**). Similar effects on the cytotoxic activity were observed when the miR-23a cluster was overexpressed in STEAP specific CD8⁺ T cells used as effectors against STEAP peptide loaded MCF-7 target cells (**Figure 36C**).



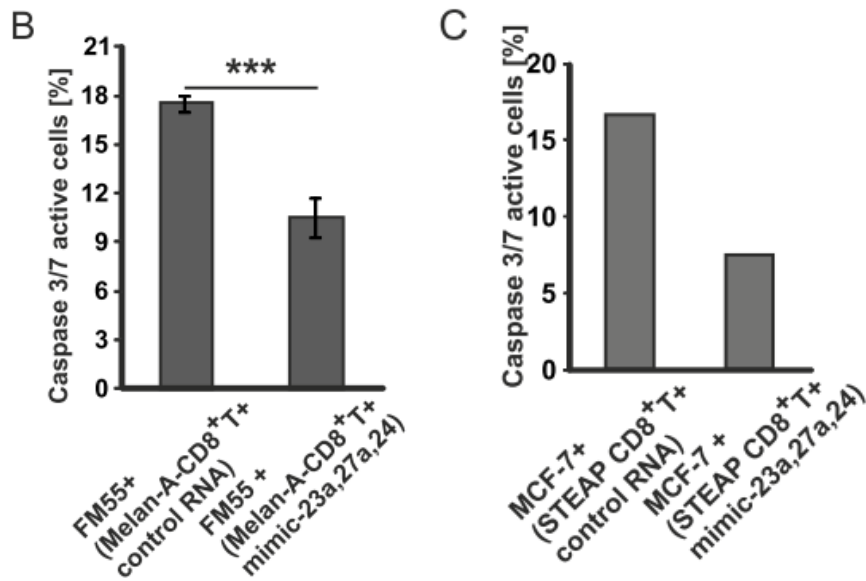


Figure 36. miR-23a cluster inhibits CD8⁺ T cell cytotoxicity. (A,B) Melan-A-specific CD8⁺ T cells (purity >90%) were nucleofected (program U-014) with 300 nM of either mimics for miR-23a, miR-27a and miR-24 or with 300 nM control RNA and seeded in CellGro DC medium with 5% human AB serum and IL-15 (5 ng/ml). 10⁴ FM55 cells were seeded per well in a 96 well plate. 48 h after nucleofecting the T cells and 24 h after seeding the FM55 cells, 10⁴ CD8⁺ T cells from each nucleofected group were harvested, washed and added to the wells containing FM55 cells. 4 h later, CellEvent™ Caspase 3/7 Green detection reagent was added at a final conc. of 4 μM and incubated for an additional 30 minutes. Wells with only FM55 cells served as a control for the basal caspase 3/7 activity in these cells. Cells were harvested, stained with anti-CD8β PE-Cy7 and Caspase 3/7 activity was measured by flow cytometry. Each condition was assayed in 4 technical replicates and 3 independent experiments were conducted. The percentage of CD8^{low} cells (± SD) showing caspase 3/7 activity in a representative experiment is indicated in (B). (C) The effect of the miR-23a cluster on the cytotoxicity of a STEAP-specific CD8⁺ T cell clone (purity > 90%) against STEAP peptide (5 μg/ml) loaded MCF-7 cells was assessed using the same experimental protocol as in (A).

5.9 Regulation of NKG2D surface expression by TGF- β

Context:

The activating C-type lectin-like receptor natural-killer group 2, member D (NKG2D), expressed on NK cells and certain T cell subsets, is crucial for anti-tumor immune responses (142). Transformed or stressed cells upregulate (induced) self ligands like major histocompatibility complex (MHC) class I chain related (MIC) molecules A and B (MICA, MICB) and UL16 binding proteins (ULBP1-6) which can bind and activate NKG2D. In humans, activated NKG2D cannot signal on its own but require DAP10. As mentioned earlier, NKG2D is expressed on the cell surface complexed to DAP10. Little or no NKG2D surface expression is seen without the co-expression of DAP10. Downregulation of NKG2D surface expression by tumor secreted TGF- β seems to be one of the mechanisms by which tumors evade NK and T cell cytotoxicity. However, the mechanisms that drive NKG2D suppression are poorly understood.

Results

5.9.1 NKG2D surface expression on CD8⁺ T cells and NK cells is reduced by TGF- β

It has been shown that TGF- β downregulates NKG2D receptor on CD8⁺ T cells and NK cells in glioma patients (143). Furthermore, serum from colorectal and lung cancer patients, with elevated levels of TGF- β , reduced NKG2D surface expression and severely impaired NK cell functions. In order to test the effect of exogenous TGF- β on NKG2D expression of CD8⁺ T cells and NK cells ex vivo, we treated human PBMCs with increasing concentrations (0.15 ng/ml to 20 ng/ml) of TGF- β for 48 h and assessed the levels of NKG2D surface expression by flow cytometry. TGF- β reduced the surface expression of NKG2D on CD8⁺ T cells in PBMCs in a dose dependent manner (**Figure 37**). Downregulation of NKG2D reached saturation at TGF- β concentrations of 2.5 ng/ml and above on both CD8⁺ T cells and NK cells. Hence 5 ng/ml TGF- β was used for all experiments.

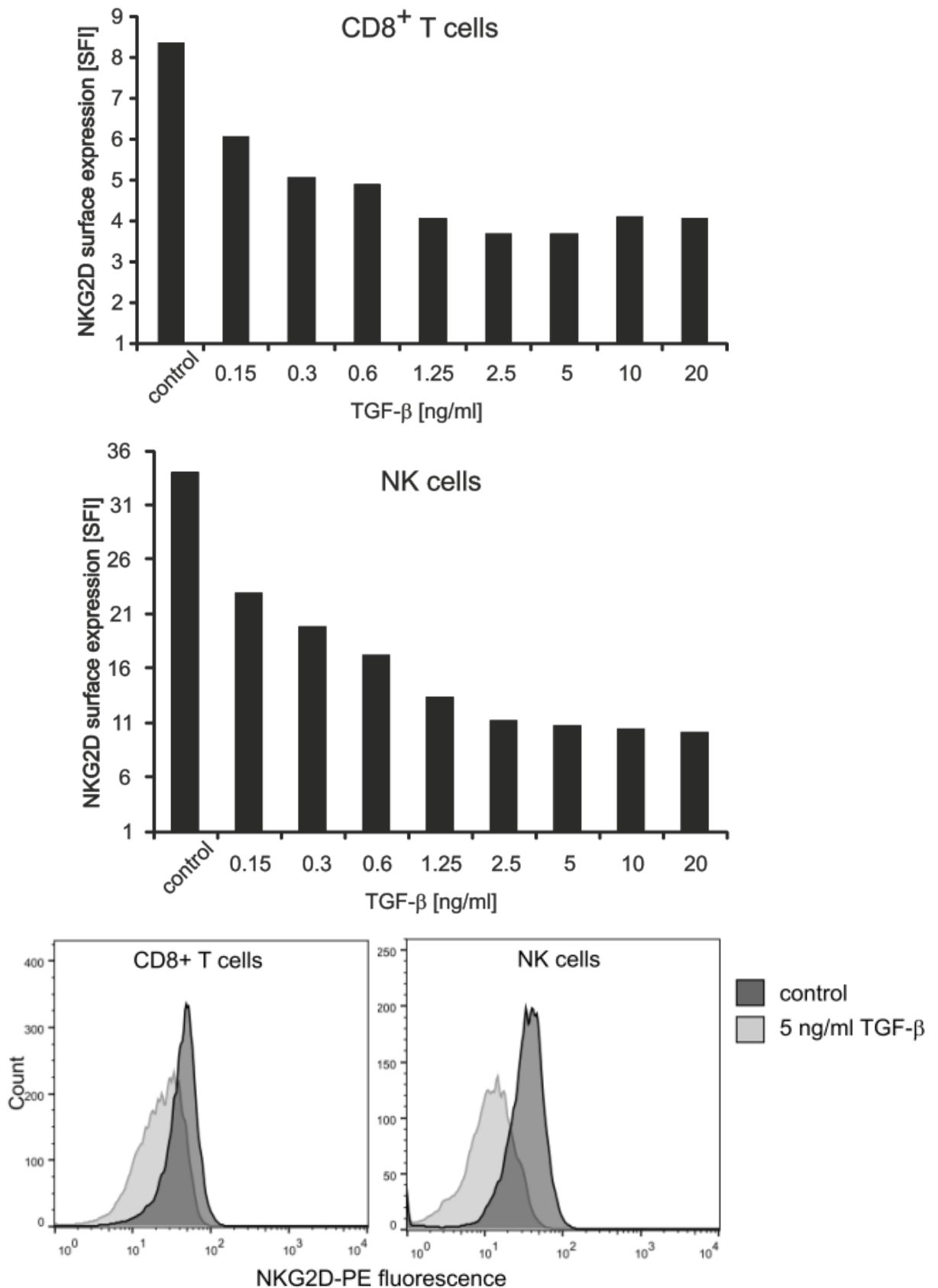


Figure 37: Dose dependent downregulation of NKG2D surface expression by TGF-β. PBMCs were freshly isolated and were rested overnight (15 h). 1×10^6 cells were treated with the indicated concentrations of TGF-β. After 48 h, cells were harvested and split into 2 parts. Each part was stained with NKG2D-PE antibody (or an

isotype antibody) along with CD3-PE Cy5 and either CD8-FITC or CD56 FITC and analyzed by flow cytometry. NK cells were gated on the CD3^{low} CD56^{high} population while CD8⁺ cells were gated on the CD3^{high} CD8^{high} population and the expression of NKG2D was determined. SFI values were determined by taking the ratio of NKG2D-PE median fluorescence to the isotype-PE median fluorescence and are shown for CD8⁺ cells and NK cells in the top and middle panels. Bottom panel shows the histogram overlay of control cells and 5ng/ml TGF- β treated cells.

5.9.2 NKG2D mRNA expression is largely un-altered by TGF- β

To test the effect of TGF- β on NKG2D mRNA expression, I isolated and purified CD8⁺ T cells and NK cells (85% to 90% purity) from healthy donor peripheral blood. Cells were treated with 5ng/ml TGF- β or nothing and were cultured for 24 h. Cells were lysed and cDNA was prepared. NKG2D mRNA expression was quantified relative to 18S rRNA. Consistent with the findings reported earlier by our group (77) and others (144), NKG2D mRNA expression was only slightly affected by TGF- β in both CD8⁺ T cells ($p = 0.12$) and NK cells ($p = 0.52$) (**Figure 38**). This pointed towards several possible means of post transcriptional inhibition of NKG2D surface expression by TGF- β .

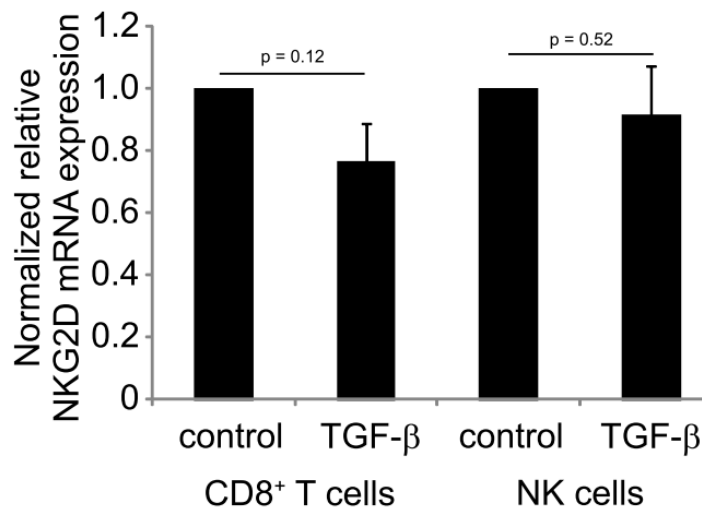


Figure 38. NKG2D mRNA regulation by TGF- β . CD8⁺ T cells and NK cells were purified from peripheral blood using antibody conjugated magnetic beads as described. Cells were treated with 5 ng/ml TGF- β or were left untreated. After 24 h, cells were lysed, total RNA was isolated and reverse transcribed into cDNA. Expression of NKG2D mRNA was quantified relative to 18S rRNA using SybrGreen based quantitative PCR. The experiment was performed using 2 donors and each PCR reaction was done in duplicates. Representative data from one of the donors are shown.

5.9.3 TGF- β signaling does not interfere with reporter gene fused to NKG2D 3'UTR

Our first guess for post transcriptional regulation of NKG2D was the involvement of miRNAs that could bind the 3'UTR of its mRNA. To this end, a pMIR-NKG2D 3'UTR construct was cloned and generated by Dr. Lasse Weinmann at the Max Planck Institute of Biochemistry, Martinsried, Munich, Germany. In short, NKG2D 3'UTR was amplified from the cDNA of human lymphocytes using primers containing restriction sites for either SacI or NaeI.

NKG2D 3'UTR SacI fwd: ATCTGAGCTCAGATGATCAACCATCTCAATAAAAAGC

NKG2D 3'UTR NaeI rev: ATCT GCCGGCGCATGAGACTCAAGATTCTATTTATTC.

The amplified 776 bp 3'UTR fragment was then fused to the pMIR-RL (modified with HSV-TK promoter) plasmid between the NaeI and SacI sites. PBLs from healthy donors were nucleofected with either pMIR-NKG2D or with the control plasmid pMIR-RL. Cells were then treated with TGF- β (5 ng/ml), SD208 (1 μ M) or were left untreated for 24 h. No reduction of firefly luciferase activity was observed after TGF- β treatment and thus we dismissed the hypothesis that TGF- β induced miRNAs were interfering with the 3'UTR of NKG2D (**Figure 39**).

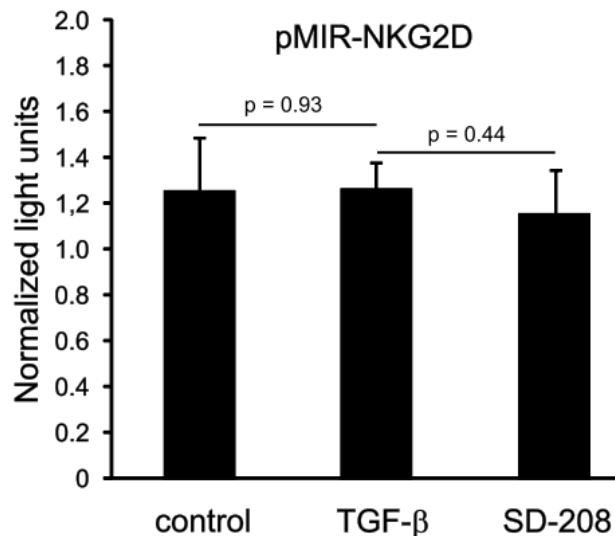


Figure 39: TGF- β does not target NKG2D 3'UTR. 5×10^6 PBMCs were nucleofected with 1 μ g/100 μ l of either pMIR-NKG2D or pMIR-RL plasmids. After 1 h, 1×10^6 cells were treated in triplicates with TGF- β (5 ng/ml), SD-208 (1 μ M) or were left untreated for 24 h. Cells were harvested and lysed in 100 μ l 1X Reporter lysis buffer (Promega). After one freeze-thaw cycle at -20°C , firefly and *Renilla* luciferase activities were measured. Ratio of background subtracted firefly to *Renilla* luciferase counts was calculated to normalize transfection efficiency. Luciferase counts from the pMIR-NKG2D transfected cells were then normalized to those transfected with pMIR-RL. Experiment was performed 3 times and a representative experiment is shown

5.9.4 TGF- β inhibits DAP10 mRNA and protein expression

Due to the fact that NKG2D is rarely expressed without DAP10 on the cell surface we turned our focus towards the accessory signaling protein DAP10, which is associated with NKG2D in human cells. Microarrays comparing TGF- β treated vs untreated NK cells, prepared by my former colleague (Dr. Yvonne Dombrowski), showed that DAP10 mRNA was downregulated in TGF- β treated NK cells (**Figure 40A**). To further confirm this effect, we quantified DAP10 mRNA using qRT-PCR on NK cells treated with or without TGF- β and found that DAP10 mRNA was indeed less after TGF- β treatment (**Figure 40B**). We then checked whether the negative effect of TGF- β on mRNA was reflected in DAP10 protein expression. Protein lysates from TGF- β treated (48 h) or untreated NK cells when analyzed by immunoblotting indicated that DAP10 protein expression was in fact inhibited by TGF- β (**Figure 40C**).

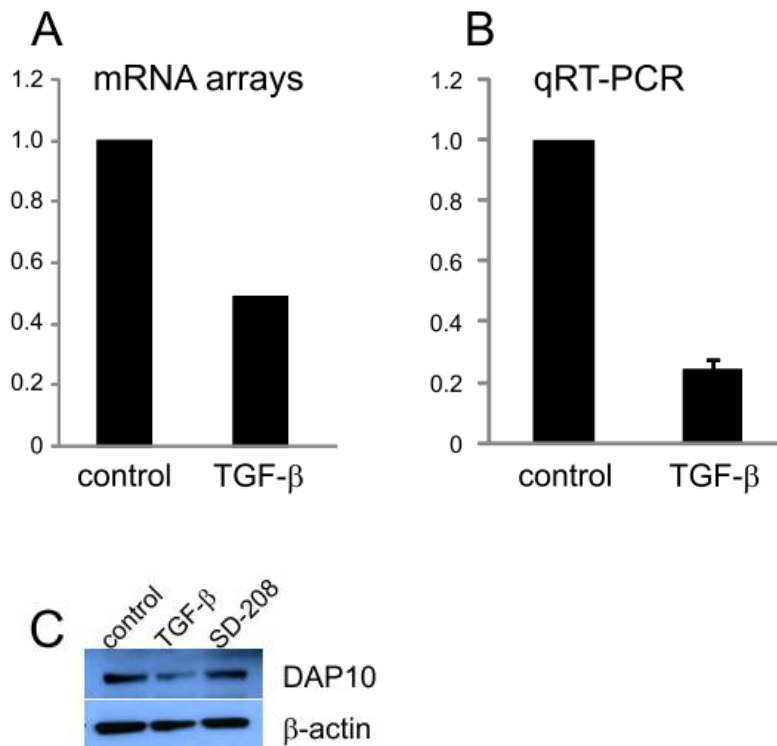


Figure 40: Regulation of DAP10 by TGF- β . (A). NK cell microarrays were prepared as described in *Materials and methods*. The fold expression change of DAP10 mRNA after TGF- β treatment relative to the untreated group is shown. (B) NK cells were magnetically purified from peripheral blood of healthy donors (n=3) and were treated with 5 ng/ml TGF- β or were left untreated. RNA was isolated after 24 h and the level of DAP10 mRNA was quantified relative to 18S rRNA as described. qRT-PCR was performed using duplicates and representative results from 1 of 3 donors are shown. (C) Purified NK cells were either treated with either TGF- β (5ng/ml) or SD-208 (1 μ M) or were left untreated for 48 h. Protein lysates were prepared and DAP10 protein expression was visualized by immunoblotting.

5.9.5 Does TGF- β inhibit NKG2D surface expression by downregulating DAP10?

To answer this question, we tried to ectopically overexpress DAP10 to rescue NKG2D expression in the presence of TGF- β in primary NK cells as well as NKL and NK92 cell lines. Given the difficulty of transfecting these cells, instead of conventional reagents and nucleofection techniques, we decided to use retroviral and lentiviral transductions. We received pLPCX-DAP10-GFP (145) plasmid from Prof. Dr. Hugh Reyburn (Division of Immunology, University of Cambridge, UK). This plasmid was co-precipitated along with pHIT60 and pVSV-G and transfected into HEK293T cells to generate the retrovirus which was then used for retroviral transduction of NK cells and NKL cell lines (146). We also subcloned DAP10-GFP into a pCDNA3.1 backbone and nucleofected these cells with it. Analyzing the expression of GFP using flow cytometry, both retroviral transduction and nucleofection of NK and NKL cells yielded < 5% efficiency. We are also unsuccessful in infecting NK cells using lentiviral vectors. Since our lab does not meet S2 safety regulations, viral transductions were conducted at the Institute for Virology and Immunology, Würzburg, under the supervision of Prof. Thomas Hermann and at the Department of Dermatology, Würzburg with the help of Dr. Roland Houben. However due to several practical difficulties, we were unsuccessful in ectopically expressing DAP10 in NK cells. Still, the idea and hypothesis are testable once robust NK cell transfection techniques have been developed.

6 Discussion

6.1 Induction of the miR-23a cluster by TGF- β and functional characterization of its immunomodulatory functions.

Within and around our body are an overwhelming amount of pathogens and foreign particles which can potentially kill us. On top of this are our own cells that can transform to enter uncontrollable cell divisions thereby causing life threatening cancers. Yet we are kept alive as a result of controlled interactions of our immune system with those external and internal agents. Equally important is the control of self antigen reactions through peripheral tolerance mechanisms, the most pronounced being displayed towards the maintenance of our gut microbiota (147). T cell mediated immunity essentially has evolved into a fine-tuned multi-level system which enables us to interact and adjust ourselves with our environment. T cells and NK cells mediate anti-cancer immune responses by eliminating cancer cells through different ways; T cells mediate anti-cancer antigen specific responses while NK cells detect and eliminate cells that show signs of transformation or stress. Cancers also evolve mechanisms of immune evasion by mutating or shedding stress activated ligands, downregulating HLA-A molecules and secreting immunosuppressive cytokines. Lately, miRNAs have been identified to play a role in the cancer vs immune system battle. Many solid tumors are infiltrated by immune cells that are often unable to mount functional responses. Immunosuppressive miRNAs that are induced by the tumor microenvironment in tumor infiltrating immune cells can dampen responses of activated T cells. This study mainly focused on immunosuppressive miRNAs induced by TGF- β .

In the initiation of a T cell response, naïve CD8⁺ T cells get primed by antigen-presenting cells in the lymph node, expand in an antigen-specific manner and differentiate while gaining effector functions. After migration towards peripheral tissues, renewed antigen-contact should lead to IFN- γ production (148), to activation of further cytotoxic effector mechanisms and to the elimination of the antigen-expressing cell. At immune-privileged sites or in a tumor microenvironment, however, peripheral tolerance mechanisms need to be considered. In fact, the ability to escape from immune-mediated destruction has recently been named as a hallmark of cancer (149). In this context, the most potent of all immunosuppressive cytokines, namely TGF- β , deserves special attention as it is frequently secreted by tumor cells (150). Transcriptional effects of TGF- β on CD8⁺ T cells have already been analyzed in great detail (73). Still, we hypothesized that TGF- β -dependent immunomodulation might operate at

several levels and thus explored a potential contribution of miRNAs in this context. Hence, we investigated miRNA changes induced by TGF- β in pre-activated CD8⁺ T cells *in vitro*, using both bead-based stimulation via CD3, CD28 and CD2 and antigen-specific CD8⁺ T cell activation and expansion via peptide-loaded antigen-presenting cells.

To obtain an overview over miRNA regulations induced by TGF- β , we first analyzed miRNA profiles in activated CD8⁺ T cells that had been treated or not with TGF- β for 24 h. In order to recognize effects from endogenous TGF- β signaling, a further control treated with the TGF- β receptor I kinase inhibitor SD-208 (125) was included. For sequencing or microarray analysis, the total amount of RNA was increased by pooling of several donors which also helped to even out extreme individual responses, to facilitate the detection of rare miRNA species and to keep costs at an affordable level. To ensure that the TGF- β that we added was functional we checked the phosphorylation of SMAD-2/3 by immunoblotting as well as tested for the downregulation of NKG2D surface expression (Figure 12).

While a recent systematic cross-platform comparison (134) showed that different techniques lead to different results, the comparison between the different techniques was not a primary aim of our study. Hence, the cross-validation was based on biological rather than merely technical replicates. 13 miRNAs that were found to be regulated in both microarrays and sequencing libraries (displaying a similar tendency) (Table 3) were then further validated by qRT-PCR, using individual T cell samples from various donors (Table 4). Accordingly, we could focus on those miRNAs that showed consistent regulations by all three approaches. Next generation sequencing of CD8⁺ T cell miRNAs also enabled us to detect new miRNA candidates based on their abundance, secondary structure patterns and free energy of folding (see 5.1.3). While most these sequences still have to be further evaluated, one has meanwhile been added to the Sanger miRNA database as miR-1280 and later retracted. One of the sequences showed about 80% homology to cer-miR-248 stem loop.

However, our primary focus was on the miR-23a cluster. Among all miRNAs that were regulated by TGF- β , the miR-23a cluster stood out since all three co-transcribed miRNAs (miR-23a, miR-27a and miR-24) were present in reasonable copy numbers (relative abundance was 2.25% for miR-23a, 3.5% for miR-27a and 0.67% for miR-24) and were uniformly increased after addition of TGF- β , irrespective of the detection method, the donor and the mode and extent of T cell pre-activation. Hence, these regulations are unaffected by the Ago-dependent global changes in miRNA expression during T cell activation which have recently been described (151). Moreover, similar regulations were also found in murine CD8⁺ T cells from Balb/cJ wild-type mice, but not in CD8⁺ T cells from hCD2- Δ kT β R11 mice

which express a dominant-negative TGF- β receptor under the control of the CD2 promoter (Figure 18). Though the level of induction may appear rather low (and would hardly appear relevant for mRNAs) after 24 h of TGF- β treatment, similar changes in miRNA expression have repeatedly been observed to yield functionally significant effects (152, 153). Furthermore, the induction of the miR-23a cluster when monitored over 72 h indicated a continued accumulation of all 3 cluster members within CD8⁺ T cells (Figure 17). This can cause a compounding and persistent effect on the known early transcriptional regulations of TGF- β target genes (significance of which is discussed later). Known effects of the miR-23a cluster include the modulation of apoptosis and proliferation via targeting of XIAP, FADD and PTEN (154-156). While these proteins are also interesting in connection with TGF- β , we screened >1,000 potential targets predicted by computational methods for candidates that could contribute to the effects of TGF- β on CD8⁺ T cell effector functions and focused our attention on CD107a/LAMP1 and IFN- γ . Although not predicted by the various mentioned tools, we also tested the effect of miR-23a cluster on other T cell effector molecules like granzyme B, perforin and Fas-L. However, the miR-23a cluster members did not affect the expression of granzyme B, perforin and Fas-L upon T cell activation.

Significant effort was put into selecting an appropriate transfection method for T cells that was minimally toxic yet sufficiently effective in delivering plasmid DNA and small RNA molecules like antagomirs and miRNA mimics. Nucleofection proved the best with >70% transfection efficiency by preserving the ability of cells to respond to activation stimuli. Still, to study molecular interactions of miRNAs to complementary regions on target mRNA 3'UTRs, we performed luciferase-reporter gene assays using the HEK293 T cell line for its relative ease of culture and transfection using conventional reagents.

LAMP1 is an essential component of the cytotoxic granule membrane which prevents the granule content from damaging the host cell. While little is known about the regulation of LAMP1, TGF- β reduces the cytotoxic potential of CD8⁺ T cells (73) which would be consistent with a miRNA effect on LAMP1 translation. Moreover, the 3'-UTR of LAMP1 contains two putative binding sites for the TGF- β -inducible miR-23a. The 3'-UTR of IFN- γ , in contrast, contains predicted binding sites for the further members of the miR-23a cluster: two for miR-27a and one binding site for miR-24 (Figure 19). In addition, IFN- γ is known to be affected by TGF- β . A transcriptional mechanism of inhibition operating via Smad2/3 and ATF1 has already been dissected on molecular level (73) and a TGF- β -dependent reduction of IFN- γ mRNA stability has been observed in the murine NK cell line LNK5E6 (157). Using

luciferase-based reporter gene assays, we could show direct effects of miR-23a on the 3'-UTR of LAMP1 and of miR-24 and miR-27a on the 3'-UTR of IFN- γ (Figure 22 and 23). Specificity was further confirmed by mutation of the predicted binding sites. Thus, the *in silico* predictions could be experimentally validated. Synergy effects between the two miRNAs targeting the 3'-UTR of IFN- γ were not observed which may be due to all transfections being performed with a constant total amount of miRNA mimics. Further, binding of one miRNA to the target 3'UTR should already suffice to inhibit translation. Most importantly, however, simultaneous modulation of all three cluster members is the most physiological approach as the miRNAs in the cluster are co-expressed from a single polycistronic RNA. Here it has to be noted that the pMIR-RL plasmid that we used drives the expression of the miRNA sensitive luciferase gene using the HSV-TK promoter which has a rather modest activity when compared to other viral promoters (e.g. CMV). This enables the detection of subtle miRNA activities.

After these proof-of-principle assays which were performed in HEK293T cells, we sought to explore the functional relevance in primary human CD8⁺ T cells (which display about 8-fold higher endogenous levels of miRNAs than the HEK293 T cells used for reporter gene assays). However, while primary CD8⁺ T cells are clearly most relevant for our study (and unaffected by compensation or adaptation processes that could obscure effects in genetic models), they are relatively difficult to transfect. Control experiments were performed to ensure that the delivery of antagomirs and miRNA mimics could be achieved by nucleofection. Consequently, these tools were found to be suitable for further assays, although nucleofection is somewhat stressful for the cells and miRNA inhibition by antagomirs is never more than partial. In particular, one has to be aware that effects can be “diluted” by the contribution of cells which do not take up the nucleofected oligonucleotides. Furthermore, we included antagomirs against the non-expressed miR-9 as well as the *All stars negative control RNA* alongside the experimental nucleofections as relevant controls.

With regard to LAMP1, functional results were somewhat equivocal: A degranulation assay in the presence of anti-CD107a/LAMP1 antibody and monensin revealed that inhibition of the miR-23a cluster can indeed increase the amount of LAMP1 at the surface of degranulating cells. Moreover, total LAMP1 levels were hardly modulated during T cell activation when monitored by immunoblotting (Figure 24). This could be due to a low turnover of LAMP1 protein and to the presence of large intracellular reservoirs – which was confirmed by addition of the translation inhibitor cycloheximide to stimulated CD8⁺ T cells (Figure 25). Considering that nucleofected T cells can't be maintained much longer *in vitro*, effects of miR-23a on

LAMP1 should ultimately be clarified in (ideally T cell specific and inducible) miR-23a knock-out animals *in vivo*. Based on the *in vitro* data obtainable from human cells, the selective effect on cell surface LAMP1 could be explained by the co-existence of different pools of LAMP1 in the cell, with granule formation requiring freshly translated LAMP1. Alternatively, the highly promiscuous nature of miRNAs would also allow for an additional interaction of miR-23a with a factor required for granule trafficking or fusion with the plasma membrane. Irrespective of these considerations, our data show that miR-23a interacts with the 3'UTR of LAMP1 and decreases LAMP1 cell surface expression.

Clearer results were obtained on the regulation of IFN- γ in CD8⁺ T cells. Interestingly, in bead-stimulated polyclonal CD8⁺ T cells inhibition of autocrine miR-23a cluster expression increased the number of IFN- γ -positive cells upon stimulation and the amount of intracellular IFN- γ , though there was no effect on the much higher IFN- γ levels in the supernatant (Figure 30). Conversely, overexpression of miR-23a cluster led to a considerable reduction of total IFN- γ levels whereas the number of IFN- γ -producing CD8⁺ T cells remained unchanged (Figure 28). These findings invite for speculations on the dynamics of IFN- γ production in heterogeneous polyclonally activated T cell populations. Clearly, some cells do not produce IFN- γ , and these non-producers cannot respond to miRNA inhibition. However, a proportion of cells may be at the brink of getting activated. In these cells, small amounts of IFN- γ mRNA might already be present while translation could still be prevented by autocrine miR-23a cluster expression. Inhibition of endogenous miR-24 and miR-27a could then initiate IFN- γ production and thus explain the increase in IFN- γ producing cells after transfection with antagomirs. Finally, a further population of highly activated cells may have overcome inhibitory effects of endogenous miR-24 and miR-27a expression, possibly by producing IFN- γ mRNA in excess. In these, IFN- γ mRNA might simply outcompete the number of miRNA transcripts. As these cells will secrete large quantities of IFN- γ , they will largely be responsible for the amount of IFN- γ in the supernatant. Transfection of such IFN- γ “high producers” with miRNA mimics would then reduce the amount of IFN- γ in the supernatant without altering the percentage of IFN- γ -positive cells. Such a pattern could be due to the simultaneous occurrence of different activation stages in the polyclonal culture and/or to the simultaneous presence of different subtypes of CD8⁺ T cells with different capacities for producing IFN- γ (158). This invites further experiments to analyze the effect of the miR-23a cluster on different T cell subsets.

We then chose *in vitro* expanded antigen-specific T cells with a well characterized early effector memory phenotype (129). In this system, the effect of the miRNA mimics on IFN- γ secretion and the increase in the number of IFN- γ^+ CD8 $^+$ T cells after transfection with the antagomirs was confirmed. Moreover, while endogenous expression levels of miR-23a cluster members were very similar between bead-stimulated and antigen-specifically expanded CD8 $^+$ T cells, assays in this more physiological setting revealed a previously unrecognized effect of the antagomirs on the total amount of secreted IFN- γ (Figure 35). An explanation might be found by investigating IFN- γ mRNA and miR-23a cluster expression on an individual per cell basis which, however, would have been beyond the scope of this study.

We further assessed the effect of inhibiting the miR-23a cluster in CD8 $^+$ T cells that were subsequently treated with TGF- β . As TGF- β is known to reduce IFN- γ production via transcriptional repression, antagomirs could not prevent this reduction. Nevertheless, the effect of TGF- β was attenuated in the presence of antagomirs. Induction of the miR-23a cluster by TGF- β thus seems to amplify the transcriptional effect on IFN- γ and may be involved in fine tuning of the response. In addition, miRNAs have a tendency to persist and accumulate. Carrying on from what was discussed earlier, the highest expression of the miR-23a cluster was found from 72h up to 5 days after TGF- β treatment which suggests that induction of the miR-23a cluster and its effect on IFN- γ and LAMP1 can persist well beyond 24 h (when the miRNA arrays and deep sequencing were performed) and can prolong the effect of TGF- β beyond the duration of the transcriptional repression.

Finally, we used both polyclonal Melan-A-specific T cells and a STEAP-specific T cell clone to investigate whether the miR-23a cluster affects CD8 $^+$ T cell cytotoxicity against tumor cell targets. Compared to nucleofection with an irrelevant control RNA, nucleofection with the miR-23a cluster reduced the killing capacity of cytotoxic T cells to approximately half, both for the polyclonal Melan-A-specific T cells and for the cytotoxic T cell clone. Moreover, the effect was observed both with FM55 melanoma cells showing endogenous Melan-A expression and with STEAP peptide loaded MCF-7 breast cancer cells.

Thus, our study led from a broad screening of TGF- β -dependent miRNA regulation in primary human CD8 $^+$ T cells and confirmation in a transgenic mouse model to a previously unrecognized immunomodulatory mechanism of the miR-23a cluster which likely adds to the immunosuppressive properties of TGF- β . Apart from an effect of endogenous miR-23a cluster expression on the proportion of IFN- γ -positive cells in activated CD8 $^+$ T cells, we could also show effects of miR-23a on the availability of LAMP1 on the surface of cytotoxic

granules. Most importantly, overexpression of the miR-23a cluster attenuated the cytotoxic potential of antigen-specific CD8⁺ T cells. Consequently, the role of the miR-23a cluster in CTL and its link to TGF- β signaling deserves further investigation in suitable disease models *in vivo*. Moreover, since distinct miRNA profiles have been associated with several cancers, the changes in the miRome CD8⁺ T cells caused by exogenous TGF- β might correlate with those of cancers which secrete high levels of this cytokine. Hence the deep sequencing data and miRNA arrays that we generated need to be computationally analyzed for such correlations. Apart from miRnome profiles being just biomarkers for diseases, modulation of individual miRNAs has been shown to induce certain diseases. Thus, therapeutic targeting of miRNAs is a promising and upcoming area of research. Direct modulation of miRNAs to effect tumor remissions have already succeeded in mice. Although delivery of miRNAs *in vitro* have been effectively developed, *in vivo* administration and site directivity of miRNA expression modulators is the key issue. miRNAs also hold the potential to act as supporting agents to act as sensitizers in current therapeutic regimens. Having said these, the immunosuppressive functions of the miR-23a cluster make them a therapeutically interesting miRNA cluster which can be targeted to improve anti-tumor immune responses.

6.2 Regulation of NKG2D/DAP10 surface expression by TGF- β

Our experiments indicated that NKG2D mRNA expression was hardly modulated by TGF- β in NK cells (Figure 38). Reporter gene assays showed the lack of any post transcriptional regulations (by miRNAs) targeting NKG2D 3'UTR (Figure 39). Interestingly in NK cells, mRNA arrays as well as qRT-PCR showed a downregulation of DAP10 mRNA upon addition of TGF- β . Thus we hypothesize that TGF- β modulates NKG2D surface expression via suppression of DAP10 rather than NKG2D directly. To validate this, we tried to ectopically overexpress DAP10 in NK cells to rescue NKG2D surface expression in the presence of TGF- β . Unfortunately, we were unable to overcome the difficulties associated with transfecting DAP10 into primary NK cells using nucleofection or retroviral vectors. Among NK cells lines, YT cells could readily be transfected whereas NK-L and NK92 cells resisted the attempted gene transfer. YT cells do, however, lack NKG2D expression which means that they do not represent a suitable model for the posed question. Still, upon availability of an efficient NK cell transfection system, our hypothesis concerning the DAP10-dependent regulation of NKG2D surface expression would deserve further exploration.

7 Publications:

2014

1) The TGF- β -inducible miR-23a cluster attenuates IFN- γ levels and antigen-specific cytotoxicity in human CD8⁺ T cells.

Chandran PA, Keller A, Weinmann L, Adel Seida A, Braun M, Andreev K, Fischer B, Horn E, Schwinn S, Junker M, Houben R, Dombrowski Y, Dietl J, Finotto S, Wölfl M, Meister G, Wischhusen J. *Journal of Leukocyte Biology*. 2014 Oct, PMID: 25030422.

Contribution: This study was designed and performed by me under the supervision of Prof. Dr. Jörg Wischhusen. This manuscript covers most of the study described in my thesis.

2) Omega-3 fatty acid concentrate from *Dunaliella salina* possesses anti-inflammatory properties including blockade of NF- κ B nuclear translocation.

Chitranjali T, **Chandran PA**, G Muraleedhara Kurup. *Immunopharmacology and immunotoxicology* (In revision).

Contribution: I wrote the manuscript and designed the revision experiments.

2012

3) Whole miRNome-wide differential co-expression of microRNAs.

Stähler CF, Keller A, Leidinger P, Backes C, **Chandran A**, Wischhusen J, Meder B, Meese E. *Genomics Proteomics Bioinformatics*. 2012 Oct, PMID: 23200138

2011

4) A specific miRNA signature in the peripheral blood of glioblastoma patients.

Roth P, Wischhusen J, Happold C, **Chandran PA**, Hofer S, Eisele G, Weller M, Keller A. *Journal of Neurochemistry*. 2011 Aug, PMID: 21561454.

Contribution: I quantified the expression of hsa-miR-128 and hsa-miR-342-3p in CD8⁺ T cells and PBMCs in the presence and absence of TGF- β .

5) Ectonucleotidases CD39 and CD73 on OvCA cells are potent adenosine-generating enzymes responsible for adenosine receptor 2A-dependent suppression of T cell function and NK cell cytotoxicity.

Häusler SF, Montalbán del Barrio I, Strohschein J, **Anoop Chandran P**, Engel JB, Hönig A, Ossadnik M, Horn E, Fischer B, Krockenberger M, Heuer S, Seida AA, Junker M, Kneitz H, Kloor D, Klotz KN, Dietl J, Wischhusen J. *Cancer Immunology Immunotherapy*. 2011 Oct, PMID: 21638125

Contribution: I cloned and generated the sh RNA plasmids to silence A2A receptor, CD39, CD73 which were used in this study. I also assisted the experiments performed by Montalbán del Barrio I and Strohschein J.

2010

6) Whole blood-derived miRNA profiles as potential new tools for ovarian cancer screening.

Häusler SF, Keller A, **Chandran PA**, Ziegler K, Zipp K, Heuer S, Krockenberger M, Engel JB, Hönig A, Scheffler M, Dietl J, Wischhusen J. British Journal of Cancer. 2010 Aug, PMID: 20683447.

Contribution: This study involved the screening RNA from whole blood from several ovarian cancer patients and healthy people for ovarian cancer specific miRNA profiles employing machine learning approach. I received and isolated the miRNAs from whole blood samples for the complete study.

8 Abbreviations

°C	degree Celsius	LAMP	lysosome associated membrane protein
µg	microgram	LNA	Locked nucleic acid
µl	microliter	MACS	Magnet assisted cell sorting
µM	micromolar	mg	milligram
APC	Allophycocyanin	MHC	Major histocompatibility complex
BSA	Bovine serum albumin	min	minute (s)
CD	Cluster of differentiation	ml	milliliter
cDNA	complementary DNA	mM	millimolar
CTL	Cytotoxic T lymphocyte	ng	nanogram
DAP	DNAX activation protein	NK cells	Natural Killer cells
dd	double distilled	nm	nanometer
DN	Double negative	PBMC	Peripheral blood mononuclear cell
DNA	Deoxyribonucleic acid	PBS	Phosphate buffered saline
DP	Double positive	PCR	polymerase chain reaction
EDTA	Ethylenediaminetetraacetic acid	PE	Phycoerythrin
ELISA	Enzyme-linked immunosorbent assay	PMSF	phenylmethanesulfonyl fluoride
FBS	Fetal bovine serum	RISC	RNA induced silencing complex
FITC	Fluorescein isothiocyanate	RNA	Ribonucleic acid
h	hour (s)	rpm	revolutions per minute
HRP	horse radish peroxidase	RPMI	Roswell Park Memorial Institute
hsa	Homo sapiens	s	second (s)
HSA	human serum albumin	SDS	Sodium dodecyl sulphate
IFN	Interferon	Smad	Sma mothers against decapentaplegic
IL	Interleukin	TCR	T cell receptor
IMDM	Iscove's Modified Dulbecco's Medium	TGF	Transforming growth factor
IU	International units	UTR	Untranslated region

9 References

1. Pui, J. C., D. Allman, L. Xu, S. DeRocco, F. G. Karnell, S. Bakkour, J. Y. Lee, T. Kadesch, R. R. Hardy, J. C. Aster, and W. S. Pear. 1999. Notch1 expression in early lymphopoiesis influences B versus T lineage determination. *Immunity* 11: 299-308.
2. Michie, A. M., J. R. Carlyle, T. M. Schmitt, B. Ljutic, S. K. Cho, Q. Fong, and J. C. Zuniga-Pflucker. 2000. Clonal characterization of a bipotent T cell and NK cell progenitor in the mouse fetal thymus. *J Immunol* 164: 1730-1733.
3. Germain, R. N. 2002. T-cell development and the CD4-CD8 lineage decision. *Nature reviews. Immunology* 2: 309-322.
4. Klein, L., B. Kyewski, P. M. Allen, and K. A. Hogquist. 2014. Positive and negative selection of the T cell repertoire: what thymocytes see (and don't see). *Nature reviews. Immunology* 14: 377-391.
5. von Boehmer, H., H. S. Teh, and P. Kisielow. 1989. The thymus selects the useful, neglects the useless and destroys the harmful. *Immunology today* 10: 57-61.
6. Ellmeier, W., S. Sawada, and D. R. Littman. 1999. The regulation of CD4 and CD8 coreceptor gene expression during T cell development. *Annual review of immunology* 17: 523-554.
7. Borgulya, P., H. Kishi, U. Muller, J. Kirberg, and H. von Boehmer. 1991. Development of the CD4 and CD8 lineage of T cells: instruction versus selection. *The EMBO journal* 10: 913-918.
8. Chan, S. H., D. Cosgrove, C. Waltzinger, C. Benoist, and D. Mathis. 1993. Another view of the selective model of thymocyte selection. *Cell* 73: 225-236.
9. Robey, E. A., B. J. Fowlkes, J. W. Gordon, D. Kioussis, H. von Boehmer, F. Ramsdell, and R. Axel. 1991. Thymic selection in CD8 transgenic mice supports an instructive model for commitment to a CD4 or CD8 lineage. *Cell* 64: 99-107.
10. Robey, E. A., B. J. Fowlkes, and D. M. Pardoll. 1990. Molecular mechanisms for lineage commitment in T cell development. *Seminars in immunology* 2: 25-34.
11. Girard, J. P., C. Moussion, and R. Forster. 2012. HEVs, lymphatics and homeostatic immune cell trafficking in lymph nodes. *Nature reviews. Immunology* 12: 762-773.
12. Hickman, H. D., K. Takeda, C. N. Skon, F. R. Murray, S. E. Hensley, J. Loomis, G. N. Barber, J. R. Bennink, and J. W. Yewdell. 2008. Direct priming of antiviral CD8+ T

- cells in the peripheral interfollicular region of lymph nodes. *Nature immunology* 9: 155-165.
13. John, B., T. H. Harris, E. D. Tait, E. H. Wilson, B. Gregg, L. G. Ng, P. Mrass, D. S. Roos, F. Dzierszinski, W. Weninger, and C. A. Hunter. 2009. Dynamic Imaging of CD8(+) T cells and dendritic cells during infection with *Toxoplasma gondii*. *PLoS pathogens* 5: e1000505.
 14. Mescher, M. F., J. M. Curtsinger, P. Agarwal, K. A. Casey, M. Gerner, C. D. Hammerbeck, F. Popescu, and Z. Xiao. 2006. Signals required for programming effector and memory development by CD8+ T cells. *Immunological reviews* 211: 81-92.
 15. Parish, I. A., and S. M. Kaech. 2009. Diversity in CD8(+) T cell differentiation. *Current opinion in immunology* 21: 291-297.
 16. Chang, J. T., M. L. Ciocca, I. Kinjyo, V. R. Palanivel, C. E. McClurkin, C. S. Dejong, E. C. Mooney, J. S. Kim, N. C. Steinel, J. Oliaro, C. C. Yin, B. I. Florea, H. S. Overkleeft, L. J. Berg, S. M. Russell, G. A. Koretzky, M. S. Jordan, and S. L. Reiner. 2011. Asymmetric proteasome segregation as a mechanism for unequal partitioning of the transcription factor T-bet during T lymphocyte division. *Immunity* 34: 492-504.
 17. Joshi, N. S., W. Cui, A. Chandele, H. K. Lee, D. R. Urso, J. Hagman, L. Gapin, and S. M. Kaech. 2007. Inflammation directs memory precursor and short-lived effector CD8(+) T cell fates via the graded expression of T-bet transcription factor. *Immunity* 27: 281-295.
 18. Badovinac, V. P., J. S. Haring, and J. T. Harty. 2007. Initial T cell receptor transgenic cell precursor frequency dictates critical aspects of the CD8(+) T cell response to infection. *Immunity* 26: 827-841.
 19. Rudd, C. E., A. Taylor, and H. Schneider. 2009. CD28 and CTLA-4 coreceptor expression and signal transduction. *Immunological reviews* 229: 12-26.
 20. Watts, T. H. 2005. TNF/TNFR family members in costimulation of T cell responses. *Annual review of immunology* 23: 23-68.
 21. Carrio, R., O. F. Bathe, and T. R. Malek. 2004. Initial antigen encounter programs CD8+ T cells competent to develop into memory cells that are activated in an antigen-free, IL-7- and IL-15-rich environment. *J Immunol* 172: 7315-7323.
 22. Pipkin, M. E., J. A. Sacks, F. Cruz-Guilloty, M. G. Lichtenheld, M. J. Bevan, and A. Rao. 2010. Interleukin-2 and inflammation induce distinct transcriptional programs that promote the differentiation of effector cytolytic T cells. *Immunity* 32: 79-90.

23. Groom, J. R., and A. D. Luster. 2011. CXCR3 ligands: redundant, collaborative and antagonistic functions. *Immunology and cell biology* 89: 207-215.
24. Sallusto, F., D. Lenig, R. Forster, M. Lipp, and A. Lanzavecchia. 1999. Two subsets of memory T lymphocytes with distinct homing potentials and effector functions. *Nature* 401: 708-712.
25. Barry, M., and R. C. Bleackley. 2002. Cytotoxic T lymphocytes: all roads lead to death. *Nature reviews. Immunology* 2: 401-409.
26. Mirandola, P., C. Ponti, G. Gobbi, I. Sponzilli, M. Vaccarezza, L. Cocco, G. Zauli, P. Secchiero, F. A. Manzoli, and M. Vitale. 2004. Activated human NK and CD8+ T cells express both TNF-related apoptosis-inducing ligand (TRAIL) and TRAIL receptors but are resistant to TRAIL-mediated cytotoxicity. *Blood* 104: 2418-2424.
27. Takeda, K., M. J. Smyth, E. Cretney, Y. Hayakawa, N. Kayagaki, H. Yagita, and K. Okumura. 2002. Critical role for tumor necrosis factor-related apoptosis-inducing ligand in immune surveillance against tumor development. *The Journal of experimental medicine* 195: 161-169.
28. Smyth, M. J., J. M. Kelly, V. R. Sutton, J. E. Davis, K. A. Browne, T. J. Sayers, and J. A. Trapani. 2001. Unlocking the secrets of cytotoxic granule proteins. *Journal of leukocyte biology* 70: 18-29.
29. Clark, R., and G. M. Griffiths. 2003. Lytic granules, secretory lysosomes and disease. *Current opinion in immunology* 15: 516-521.
30. Veugelers, K., B. Motyka, I. S. Goping, I. Shostak, T. Sawchuk, and R. C. Bleackley. 2006. Granule-mediated killing by granzyme B and perforin requires a mannose 6-phosphate receptor and is augmented by cell surface heparan sulfate. *Molecular biology of the cell* 17: 623-633.
31. Lopez, J. A., O. Susanto, M. R. Jenkins, N. Lukoyanova, V. R. Sutton, R. H. Law, A. Johnston, C. H. Bird, P. I. Bird, J. C. Whisstock, J. A. Trapani, H. R. Saibil, and I. Voskoboinik. 2013. Perforin forms transient pores on the target cell plasma membrane to facilitate rapid access of granzymes during killer cell attack. *Blood* 121: 2659-2668.
32. Atkinson, E. A., M. Barry, A. J. Darmon, I. Shostak, P. C. Turner, R. W. Moyer, and R. C. Bleackley. 1998. Cytotoxic T lymphocyte-assisted suicide. Caspase 3 activation is primarily the result of the direct action of granzyme B. *The Journal of biological chemistry* 273: 21261-21266.
33. Estebanez-Perpina, E., P. Fuentes-Prior, D. Belorgey, M. Braun, R. Kiefersauer, K. Maskos, R. Huber, H. Rubin, and W. Bode. 2000. Crystal structure of the caspase

- activator human granzyme B, a proteinase highly specific for an Asp-P1 residue. *Biological chemistry* 381: 1203-1214.
34. Medema, J. P., R. E. Toes, C. Scaffidi, T. S. Zheng, R. A. Flavell, C. J. Melief, M. E. Peter, R. Offringa, and P. H. Krammer. 1997. Cleavage of FLICE (caspase-8) by granzyme B during cytotoxic T lymphocyte-induced apoptosis. *European journal of immunology* 27: 3492-3498.
 35. He, J. S., and H. L. Ostergaard. 2007. CTLs contain and use intracellular stores of FasL distinct from cytolytic granules. *J Immunol* 179: 2339-2348.
 36. Andrin, C., M. J. Pinkoski, K. Burns, E. A. Atkinson, O. Krahenbuhl, D. Hudig, S. A. Fraser, U. Winkler, J. Tschopp, M. Opas, R. C. Bleackley, and M. Michalak. 1998. Interaction between a Ca²⁺-binding protein calreticulin and perforin, a component of the cytotoxic T-cell granules. *Biochemistry* 37: 10386-10394.
 37. Zhang, M., S. M. Park, Y. Wang, R. Shah, N. Liu, A. E. Murmann, C. R. Wang, M. E. Peter, and P. G. Ashton-Rickardt. 2006. Serine protease inhibitor 6 protects cytotoxic T cells from self-inflicted injury by ensuring the integrity of cytotoxic granules. *Immunity* 24: 451-461.
 38. Eskelinen, E. L., Y. Tanaka, and P. Saftig. 2003. At the acidic edge: emerging functions for lysosomal membrane proteins. *Trends in cell biology* 13: 137-145.
 39. Andrejewski, N., E. L. Punnonen, G. Guhde, Y. Tanaka, R. Lullmann-Rauch, D. Hartmann, K. von Figura, and P. Saftig. 1999. Normal lysosomal morphology and function in LAMP-1-deficient mice. *The Journal of biological chemistry* 274: 12692-12701.
 40. Gamp, A. C., Y. Tanaka, R. Lullmann-Rauch, D. Wittke, R. D'Hooge, P. P. De Deyn, T. Moser, H. Maier, D. Hartmann, K. Reiss, A. L. Illert, K. von Figura, and P. Saftig. 2003. LIMP-2/LGP85 deficiency causes ureteric pelvic junction obstruction, deafness and peripheral neuropathy in mice. *Human molecular genetics* 12: 631-646.
 41. Krzewski, K., A. Gil-Krzewska, V. Nguyen, G. Peruzzi, and J. E. Coligan. 2013. LAMP1/CD107a is required for efficient perforin delivery to lytic granules and NK-cell cytotoxicity. *Blood* 121: 4672-4683.
 42. Beatty, G., and Y. Paterson. 2001. IFN-gamma-dependent inhibition of tumor angiogenesis by tumor-infiltrating CD4⁺ T cells requires tumor responsiveness to IFN-gamma. *J Immunol* 166: 2276-2282.
 43. Beatty, G. L., and Y. Paterson. 2001. Regulation of tumor growth by IFN-gamma in cancer immunotherapy. *Immunologic research* 24: 201-210.

44. Hobeika, A. C., W. Etienne, B. A. Torres, H. M. Johnson, and P. S. Subramaniam. 1999. IFN-gamma induction of p21(WAF1) is required for cell cycle inhibition and suppression of apoptosis. *Journal of interferon & cytokine research : the official journal of the International Society for Interferon and Cytokine Research* 19: 1351-1361.
45. Weber, J. S., and S. A. Rosenberg. 1988. Modulation of murine tumor major histocompatibility antigens by cytokines in vivo and in vitro. *Cancer research* 48: 5818-5824.
46. Tran, E., S. Turcotte, A. Gros, P. F. Robbins, Y. C. Lu, M. E. Dudley, J. R. Wunderlich, R. P. Somerville, K. Hogan, C. S. Hinrichs, M. R. Parkhurst, J. C. Yang, and S. A. Rosenberg. 2014. Cancer immunotherapy based on mutation-specific CD4+ T cells in a patient with epithelial cancer. *Science* 344: 641-645.
47. Assoian, R. K., A. Komoriya, C. A. Meyers, D. M. Miller, and M. B. Sporn. 1983. Transforming growth factor-beta in human platelets. Identification of a major storage site, purification, and characterization. *The Journal of biological chemistry* 258: 7155-7160.
48. Burt, D. W. 1992. Evolutionary grouping of the transforming growth factor-beta superfamily. *Biochemical and biophysical research communications* 184: 590-595.
49. Burt, D. W., and A. S. Law. 1994. Evolution of the transforming growth factor-beta superfamily. *Progress in growth factor research* 5: 99-118.
50. Newfeld, S. J., R. G. Wisotzkey, and S. Kumar. 1999. Molecular evolution of a developmental pathway: phylogenetic analyses of transforming growth factor-beta family ligands, receptors and Smad signal transducers. *Genetics* 152: 783-795.
51. Govinden, R., and K. D. Bhoola. 2003. Genealogy, expression, and cellular function of transforming growth factor-beta. *Pharmacology & therapeutics* 98: 257-265.
52. Dubois, C. M., M. H. Laprise, F. Blanchette, L. E. Gentry, and R. Leduc. 1995. Processing of transforming growth factor beta 1 precursor by human furin convertase. *The Journal of biological chemistry* 270: 10618-10624.
53. Annes, J. P., J. S. Munger, and D. B. Rifkin. 2003. Making sense of latent TGFbeta activation. *Journal of cell science* 116: 217-224.
54. Crawford, S. E., V. Stellmach, J. E. Murphy-Ullrich, S. M. Ribeiro, J. Lawler, R. O. Hynes, G. P. Boivin, and N. Bouck. 1998. Thrombospondin-1 is a major activator of TGF-beta1 in vivo. *Cell* 93: 1159-1170.

55. Munger, J. S., X. Huang, H. Kawakatsu, M. J. Griffiths, S. L. Dalton, J. Wu, J. F. Pittet, N. Kaminski, C. Garat, M. A. Matthay, D. B. Rifkin, and D. Sheppard. 1999. The integrin alpha v beta 6 binds and activates latent TGF beta 1: a mechanism for regulating pulmonary inflammation and fibrosis. *Cell* 96: 319-328.
56. Nunes, I., R. L. Shapiro, and D. B. Rifkin. 1995. Characterization of latent TGF-beta activation by murine peritoneal macrophages. *J Immunol* 155: 1450-1459.
57. Allison, R. S., M. L. Mumy, and L. M. Wakefield. 1998. Translational control elements in the major human transforming growth factor-beta 1 mRNA. *Growth Factors* 16: 89-100.
58. Brown, C. B., A. S. Boyer, R. B. Runyan, and J. V. Barnett. 1999. Requirement of type III TGF-beta receptor for endocardial cell transformation in the heart. *Science* 283: 2080-2082.
59. Massague, J. 1998. TGF-beta signal transduction. *Annual review of biochemistry* 67: 753-791.
60. Huse, M., T. W. Muir, L. Xu, Y. G. Chen, J. Kuriyan, and J. Massague. 2001. The TGF beta receptor activation process: an inhibitor- to substrate-binding switch. *Molecular cell* 8: 671-682.
61. Inman, G. J., F. J. Nicolas, and C. S. Hill. 2002. Nucleocytoplasmic shuttling of Smads 2, 3, and 4 permits sensing of TGF-beta receptor activity. *Molecular cell* 10: 283-294.
62. Kavsak, P., R. K. Rasmussen, C. G. Causing, S. Bonni, H. Zhu, G. H. Thomsen, and J. L. Wrana. 2000. Smad7 binds to Smurf2 to form an E3 ubiquitin ligase that targets the TGF beta receptor for degradation. *Molecular cell* 6: 1365-1375.
63. Nakao, A., M. Afrakhte, A. Moren, T. Nakayama, J. L. Christian, R. Heuchel, S. Itoh, M. Kawabata, N. E. Heldin, C. H. Heldin, and P. ten Dijke. 1997. Identification of Smad7, a TGFbeta-inducible antagonist of TGF-beta signalling. *Nature* 389: 631-635.
64. Attisano, L., and J. L. Wrana. 2000. Smads as transcriptional co-modulators. *Current opinion in cell biology* 12: 235-243.
65. Massague, J., and D. Wotton. 2000. Transcriptional control by the TGF-beta/Smad signaling system. *The EMBO journal* 19: 1745-1754.
66. Shi, Y., and J. Massague. 2003. Mechanisms of TGF-beta signaling from cell membrane to the nucleus. *Cell* 113: 685-700.
67. Genestier, L., S. Kasibhatla, T. Brunner, and D. R. Green. 1999. Transforming growth factor beta1 inhibits Fas ligand expression and subsequent activation-induced cell

- death in T cells via downregulation of c-Myc. *The Journal of experimental medicine* 189: 231-239.
68. Ruegemer, J. J., S. N. Ho, J. A. Augustine, J. W. Schlager, M. P. Bell, D. J. McKean, and R. T. Abraham. 1990. Regulatory effects of transforming growth factor-beta on IL-2- and IL-4-dependent T cell-cycle progression. *J Immunol* 144: 1767-1776.
 69. Wolfrain, L. A., T. M. Walz, Z. James, T. Fernandez, and J. J. Letterio. 2004. p21Cip1 and p27Kip1 act in synergy to alter the sensitivity of naive T cells to TGF-beta-mediated G1 arrest through modulation of IL-2 responsiveness. *J Immunol* 173: 3093-3102.
 70. Cottrez, F., and H. Groux. 2001. Regulation of TGF-beta response during T cell activation is modulated by IL-10. *J Immunol* 167: 773-778.
 71. Gorelik, L., S. Constant, and R. A. Flavell. 2002. Mechanism of transforming growth factor beta-induced inhibition of T helper type 1 differentiation. *The Journal of experimental medicine* 195: 1499-1505.
 72. Kitani, A., I. Fuss, K. Nakamura, F. Kumaki, T. Usui, and W. Strober. 2003. Transforming growth factor (TGF)-beta1-producing regulatory T cells induce Smad-mediated interleukin 10 secretion that facilitates coordinated immunoregulatory activity and amelioration of TGF-beta1-mediated fibrosis. *The Journal of experimental medicine* 198: 1179-1188.
 73. Thomas, D. A., and J. Massague. 2005. TGF-beta directly targets cytotoxic T cell functions during tumor evasion of immune surveillance. *Cancer cell* 8: 369-380.
 74. Ahmadzadeh, M., and S. A. Rosenberg. 2005. TGF-beta 1 attenuates the acquisition and expression of effector function by tumor antigen-specific human memory CD8 T cells. *J Immunol* 174: 5215-5223.
 75. Massague, J. 2008. TGFbeta in Cancer. *Cell* 134: 215-230.
 76. Shipitsin, M., L. L. Campbell, P. Argani, S. Weremowicz, N. Bloushtain-Qimron, J. Yao, T. Nikolskaya, T. Serebryiskaya, R. Beroukhim, M. Hu, M. K. Halushka, S. Sukumar, L. M. Parker, K. S. Anderson, L. N. Harris, J. E. Garber, A. L. Richardson, S. J. Schnitt, Y. Nikolsky, R. S. Gelman, and K. Polyak. 2007. Molecular definition of breast tumor heterogeneity. *Cancer cell* 11: 259-273.
 77. Krockenberger, M., Y. Dombrowski, C. Weidler, M. Ossadnik, A. Honig, S. Hausler, H. Voigt, J. C. Becker, L. Leng, A. Steinle, M. Weller, R. Bucala, J. Dietl, and J. Wischhusen. 2008. Macrophage migration inhibitory factor contributes to the immune escape of ovarian cancer by down-regulating NKG2D. *J Immunol* 180: 7338-7348.

78. Garrity, D., M. E. Call, J. Feng, and K. W. Wucherpfennig. 2005. The activating NKG2D receptor assembles in the membrane with two signaling dimers into a hexameric structure. *Proceedings of the National Academy of Sciences of the United States of America* 102: 7641-7646.
79. Rosen, D. B., M. Araki, J. A. Hamerman, T. Chen, T. Yamamura, and L. L. Lanier. 2004. A Structural basis for the association of DAP12 with mouse, but not human, NKG2D. *J Immunol* 173: 2470-2478.
80. Gilfillan, S., E. L. Ho, M. Cella, W. M. Yokoyama, and M. Colonna. 2002. NKG2D recruits two distinct adapters to trigger NK cell activation and costimulation. *Nature immunology* 3: 1150-1155.
81. Lee, R. C., R. L. Feinbaum, and V. Ambros. 1993. The *C. elegans* heterochronic gene *lin-4* encodes small RNAs with antisense complementarity to *lin-14*. *Cell* 75: 843-854.
82. Borchert, G. M., W. Lanier, and B. L. Davidson. 2006. RNA polymerase III transcribes human microRNAs. *Nature structural & molecular biology* 13: 1097-1101.
83. Cai, X., C. H. Hagedorn, and B. R. Cullen. 2004. Human microRNAs are processed from capped, polyadenylated transcripts that can also function as mRNAs. *RNA* 10: 1957-1966.
84. Lee, Y., M. Kim, J. Han, K. H. Yeom, S. Lee, S. H. Baek, and V. N. Kim. 2004. MicroRNA genes are transcribed by RNA polymerase II. *The EMBO journal* 23: 4051-4060.
85. Staehler, C. F., A. Keller, P. Leidinger, C. Backes, A. Chandran, J. Wischhusen, B. Meder, and E. Meese. 2012. Whole miRNome-wide differential co-expression of microRNAs. *Genomics, proteomics & bioinformatics* 10: 285-294.
86. Athanasiadis, A., A. Rich, and S. Maas. 2004. Widespread A-to-I RNA editing of Alu-containing mRNAs in the human transcriptome. *PLoS biology* 2: e391.
87. Luciano, D. J., H. Mirsky, N. J. Vendetti, and S. Maas. 2004. RNA editing of a miRNA precursor. *RNA* 10: 1174-1177.
88. Davis, B. N., A. C. Hilyard, G. Lagna, and A. Hata. 2008. SMAD proteins control DROSHA-mediated microRNA maturation. *Nature* 454: 56-61.
89. Yi, R., Y. Qin, I. G. Macara, and B. R. Cullen. 2003. Exportin-5 mediates the nuclear export of pre-microRNAs and short hairpin RNAs. *Genes & development* 17: 3011-3016.

90. Diederichs, S., and D. A. Haber. 2007. Dual role for argonautes in microRNA processing and posttranscriptional regulation of microRNA expression. *Cell* 131: 1097-1108.
91. Ameres, S. L., J. Martinez, and R. Schroeder. 2007. Molecular basis for target RNA recognition and cleavage by human RISC. *Cell* 130: 101-112.
92. Haley, B., and P. D. Zamore. 2004. Kinetic analysis of the RNAi enzyme complex. *Nature structural & molecular biology* 11: 599-606.
93. Liu, J., M. A. Carmell, F. V. Rivas, C. G. Marsden, J. M. Thomson, J. J. Song, S. M. Hammond, L. Joshua-Tor, and G. J. Hannon. 2004. Argonaute2 is the catalytic engine of mammalian RNAi. *Science* 305: 1437-1441.
94. Lewis, B. P., C. B. Burge, and D. P. Bartel. 2005. Conserved seed pairing, often flanked by adenosines, indicates that thousands of human genes are microRNA targets. *Cell* 120: 15-20.
95. Meister, G. 2007. miRNAs get an early start on translational silencing. *Cell* 131: 25-28.
96. Wang, B., T. M. Love, M. E. Call, J. G. Doench, and C. D. Novina. 2006. Recapitulation of short RNA-directed translational gene silencing in vitro. *Molecular cell* 22: 553-560.
97. Kiriakidou, M., G. S. Tan, S. Lamprinaki, M. De Planell-Saguer, P. T. Nelson, and Z. Mourelatos. 2007. An mRNA m7G cap binding-like motif within human Ago2 represses translation. *Cell* 129: 1141-1151.
98. Maroney, P. A., Y. Yu, J. Fisher, and T. W. Nilsen. 2006. Evidence that microRNAs are associated with translating messenger RNAs in human cells. *Nature structural & molecular biology* 13: 1102-1107.
99. Hausler, S. F., A. Keller, P. A. Chandran, K. Ziegler, K. Zipp, S. Heuer, M. Krockenberger, J. B. Engel, A. Honig, M. Scheffler, J. Dietl, and J. Wischhusen. 2010. Whole blood-derived miRNA profiles as potential new tools for ovarian cancer screening. *British journal of cancer* 103: 693-700.
100. Keller, A., P. Leidinger, A. Bauer, A. Elsharawy, J. Haas, C. Backes, A. Wendschlag, N. Giese, C. Tjaden, K. Ott, J. Werner, T. Hackert, K. Ruprecht, H. Huwer, J. Huebers, G. Jacobs, P. Rosenstiel, H. Dommisch, A. Schaefer, J. Muller-Quernheim, B. Wullich, B. Keck, N. Graf, J. Reichrath, B. Vogel, A. Nebel, S. U. Jager, P. Staehler, I. Amarantos, V. Boisguerin, C. Staehler, M. Beier, M. Scheffler, M. W. Buchler, J. Wischhusen, S. F. Haeusler, J. Dietl, S. Hofmann, H. P. Lenhof, S.

- Schreiber, H. A. Katus, W. Rottbauer, B. Meder, J. D. Hoheisel, A. Franke, and E. Meese. 2011. Toward the blood-borne miRNome of human diseases. *Nature methods* 8: 841-843.
101. Lu, J., G. Getz, E. A. Miska, E. Alvarez-Saavedra, J. Lamb, D. Peck, A. Sweet-Cordero, B. L. Ebert, R. H. Mak, A. A. Ferrando, J. R. Downing, T. Jacks, H. R. Horvitz, and T. R. Golub. 2005. MicroRNA expression profiles classify human cancers. *Nature* 435: 834-838.
102. Pritchard, C. C., H. H. Cheng, and M. Tewari. 2012. MicroRNA profiling: approaches and considerations. *Nature reviews. Genetics* 13: 358-369.
103. Creighton, C. J., J. G. Reid, and P. H. Gunaratne. 2009. Expression profiling of microRNAs by deep sequencing. *Briefings in bioinformatics* 10: 490-497.
104. Shendure, J., and H. Ji. 2008. Next-generation DNA sequencing. *Nature biotechnology* 26: 1135-1145.
105. Zheng, H., R. Fu, J. T. Wang, Q. Liu, H. Chen, and S. W. Jiang. 2013. Advances in the Techniques for the Prediction of microRNA Targets. *International journal of molecular sciences* 14: 8179-8187.
106. Krutzfeldt, J., M. N. Poy, and M. Stoffel. 2006. Strategies to determine the biological function of microRNAs. *Nature genetics* 38 Suppl: S14-19.
107. Karube, Y., H. Tanaka, H. Osada, S. Tomida, Y. Tatematsu, K. Yanagisawa, Y. Yatabe, J. Takamizawa, S. Miyoshi, T. Mitsudomi, and T. Takahashi. 2005. Reduced expression of Dicer associated with poor prognosis in lung cancer patients. *Cancer science* 96: 111-115.
108. Esquela-Kerscher, A., and F. J. Slack. 2006. Oncomirs - microRNAs with a role in cancer. *Nature reviews. Cancer* 6: 259-269.
109. Johnson, S. M., H. Grosshans, J. Shingara, M. Byrom, R. Jarvis, A. Cheng, E. Labourier, K. L. Reinert, D. Brown, and F. J. Slack. 2005. RAS is regulated by the let-7 microRNA family. *Cell* 120: 635-647.
110. Calin, G. A., C. Sevignani, C. D. Dumitru, T. Hyslop, E. Noch, S. Yendamuri, M. Shimizu, S. Rattan, F. Bullrich, M. Negrini, and C. M. Croce. 2004. Human microRNA genes are frequently located at fragile sites and genomic regions involved in cancers. *Proceedings of the National Academy of Sciences of the United States of America* 101: 2999-3004.
111. Calin, G. A., C. D. Dumitru, M. Shimizu, R. Bichi, S. Zupo, E. Noch, H. Aldler, S. Rattan, M. Keating, K. Rai, L. Rassenti, T. Kipps, M. Negrini, F. Bullrich, and C. M.

- Croce. 2002. Frequent deletions and down-regulation of micro- RNA genes miR15 and miR16 at 13q14 in chronic lymphocytic leukemia. *Proceedings of the National Academy of Sciences of the United States of America* 99: 15524-15529.
112. Cimmino, A., G. A. Calin, M. Fabbri, M. V. Iorio, M. Ferracin, M. Shimizu, S. E. Wojcik, R. I. Aqeilan, S. Zupo, M. Dono, L. Rassenti, H. Alder, S. Volinia, C. G. Liu, T. J. Kipps, M. Negrini, and C. M. Croce. 2005. miR-15 and miR-16 induce apoptosis by targeting BCL2. *Proceedings of the National Academy of Sciences of the United States of America* 102: 13944-13949.
113. Iorio, M. V., M. Ferracin, C. G. Liu, A. Veronese, R. Spizzo, S. Sabbioni, E. Magri, M. Pedriali, M. Fabbri, M. Campiglio, S. Menard, J. P. Palazzo, A. Rosenberg, P. Musiani, S. Volinia, I. Nenci, G. A. Calin, P. Querzoli, M. Negrini, and C. M. Croce. 2005. MicroRNA gene expression deregulation in human breast cancer. *Cancer research* 65: 7065-7070.
114. Michael, M. Z., O. C. SM, N. G. van Holst Pellekaan, G. P. Young, and R. J. James. 2003. Reduced accumulation of specific microRNAs in colorectal neoplasia. *Molecular cancer research : MCR* 1: 882-891.
115. Ciafre, S. A., S. Galardi, A. Mangiola, M. Ferracin, C. G. Liu, G. Sabatino, M. Negrini, G. Maira, C. M. Croce, and M. G. Farace. 2005. Extensive modulation of a set of microRNAs in primary glioblastoma. *Biochemical and biophysical research communications* 334: 1351-1358.
116. Eis, P. S., W. Tam, L. Sun, A. Chadburn, Z. Li, M. F. Gomez, E. Lund, and J. E. Dahlberg. 2005. Accumulation of miR-155 and BIC RNA in human B cell lymphomas. *Proceedings of the National Academy of Sciences of the United States of America* 102: 3627-3632.
117. O'Donnell, K. A., E. A. Wentzel, K. I. Zeller, C. V. Dang, and J. T. Mendell. 2005. c-Myc-regulated microRNAs modulate E2F1 expression. *Nature* 435: 839-843.
118. Schwarzenbach, H., N. Nishida, G. A. Calin, and K. Pantel. 2014. Clinical relevance of circulating cell-free microRNAs in cancer. *Nature reviews. Clinical oncology* 11: 145-156.
119. Wang, J., K. Y. Zhang, S. M. Liu, and S. Sen. 2014. Tumor-associated circulating microRNAs as biomarkers of cancer. *Molecules* 19: 1912-1938.
120. Yong, F. L., C. W. Law, and C. W. Wang. 2013. Potentiality of a triple microRNA classifier: miR-193a-3p, miR-23a and miR-338-5p for early detection of colorectal cancer. *BMC cancer* 13: 280.

121. Griveau, A., J. Bejaud, S. Anthiya, S. Avril, D. Autret, and E. Garcion. 2013. Silencing of miR-21 by locked nucleic acid-lipid nanocapsule complexes sensitize human glioblastoma cells to radiation-induced cell death. *International journal of pharmaceuticals* 454: 765-774.
122. Trang, P., J. F. Wiggins, C. L. Daige, C. Cho, M. Omotola, D. Brown, J. B. Weidhaas, A. G. Bader, and F. J. Slack. 2011. Systemic delivery of tumor suppressor microRNA mimics using a neutral lipid emulsion inhibits lung tumors in mice. *Molecular therapy : the journal of the American Society of Gene Therapy* 19: 1116-1122.
123. Schramm, C., M. Protschka, H. H. Kohler, J. Podlech, M. J. Reddehase, P. Schirmacher, P. R. Galle, A. W. Lohse, and M. Blessing. 2003. Impairment of TGF-beta signaling in T cells increases susceptibility to experimental autoimmune hepatitis in mice. *American journal of physiology. Gastrointestinal and liver physiology* 284: G525-535.
124. Sauer, K. A., P. Scholtes, R. Karwot, and S. Finotto. 2006. Isolation of CD4+ T cells from murine lungs: a method to analyze ongoing immune responses in the lung. *Nature protocols* 1: 2870-2875.
125. Uhl, M., S. Aulwurm, J. Wischhusen, M. Weiler, J. Y. Ma, R. Almirez, R. Mangadu, Y. W. Liu, M. Platten, U. Herrlinger, A. Murphy, D. H. Wong, W. Wick, L. S. Higgins, and M. Weller. 2004. SD-208, a novel transforming growth factor beta receptor I kinase inhibitor, inhibits growth and invasiveness and enhances immunogenicity of murine and human glioma cells in vitro and in vivo. *Cancer research* 64: 7954-7961.
126. Friese, M. A., J. Wischhusen, W. Wick, M. Weiler, G. Eisele, A. Steinle, and M. Weller. 2004. RNA interference targeting transforming growth factor-beta enhances NKG2D-mediated antiglioma immune response, inhibits glioma cell migration and invasiveness, and abrogates tumorigenicity in vivo. *Cancer research* 64: 7596-7603.
127. Tarasov, V., P. Jung, B. Verdoodt, D. Lodygin, A. Epanchintsev, A. Menssen, G. Meister, and H. Hermeking. 2007. Differential regulation of microRNAs by p53 revealed by massively parallel sequencing: miR-34a is a p53 target that induces apoptosis and G1-arrest. *Cell Cycle* 6: 1586-1593.
128. Hurteau, G. J., S. D. Spivack, and G. J. Brock. 2006. Potential mRNA degradation targets of hsa-miR-200c, identified using informatics and qRT-PCR. *Cell Cycle* 5: 1951-1956.

129. Wolfl, M., K. Merker, H. Morbach, S. W. Van Gool, M. Eyrich, P. D. Greenberg, and P. G. Schlegel. 2011. Primed tumor-reactive multifunctional CD62L+ human CD8+ T cells for immunotherapy. *Cancer immunology, immunotherapy : CII* 60: 173-186.
130. Beitzinger, M., L. Peters, J. Y. Zhu, E. Kremmer, and G. Meister. 2007. Identification of human microRNA targets from isolated argonaute protein complexes. *RNA biology* 4: 76-84.
131. Dyer, B. W., F. A. Ferrer, D. K. Klinedinst, and R. Rodriguez. 2000. A noncommercial dual luciferase enzyme assay system for reporter gene analysis. *Analytical biochemistry* 282: 158-161.
132. Crane, C. A., S. J. Han, J. J. Barry, B. J. Ahn, L. L. Lanier, and A. T. Parsa. 2010. TGF-beta downregulates the activating receptor NKG2D on NK cells and CD8+ T cells in glioma patients. *Neuro-oncology* 12: 7-13.
133. Willenbrock, H., J. Salomon, R. Sokilde, K. B. Barken, T. N. Hansen, F. C. Nielsen, S. Moller, and T. Litman. 2009. Quantitative miRNA expression analysis: comparing microarrays with next-generation sequencing. *RNA* 15: 2028-2034.
134. Aldridge, S., and J. Hadfield. 2012. Introduction to miRNA profiling technologies and cross-platform comparison. *Methods Mol Biol* 822: 19-31.
135. Oliveros, J. C. 2007. An interactive tool for comparing lists with Venn Diagrams. <http://bioinfogp.cnb.csic.es/tools/venny/index.html>.
136. Huminiecki, L., L. Goldovsky, S. Freilich, A. Moustakas, C. Ouzounis, and C. H. Heldin. 2009. Emergence, development and diversification of the TGF-beta signalling pathway within the animal kingdom. *BMC evolutionary biology* 9: 28.
137. Mempel, T. R., M. J. Pittet, K. Khazaie, W. Weninger, R. Weissleder, H. von Boehmer, and U. H. von Andrian. 2006. Regulatory T cells reversibly suppress cytotoxic T cell function independent of effector differentiation. *Immunity* 25: 129-141.
138. Xu, X. L., R. Zong, Z. Li, M. H. Biswas, Z. Fang, D. L. Nelson, and F. B. Gao. 2011. FXR1P but not FMRP regulates the levels of mammalian brain-specific microRNA-9 and microRNA-124. *The Journal of neuroscience : the official journal of the Society for Neuroscience* 31: 13705-13709.
139. Isaac, E. L., L. E. Karageorgos, D. A. Brooks, J. J. Hopwood, and P. J. Meikle. 2000. Regulation of the lysosome-associated membrane protein in a sucrose model of lysosomal storage. *Experimental cell research* 254: 204-209.

140. Meikle, P. J., M. Yan, E. M. Ravenscroft, E. L. Isaac, J. J. Hopwood, and D. A. Brooks. 1999. Altered trafficking and turnover of LAMP-1 in Pompe disease-affected cells. *Molecular genetics and metabolism* 66: 179-188.
141. Trotta, R., J. Dal Col, J. Yu, D. Ciarlariello, B. Thomas, X. Zhang, J. Allard, 2nd, M. Wei, H. Mao, J. C. Byrd, D. Perrotti, and M. A. Caligiuri. 2008. TGF-beta utilizes SMAD3 to inhibit CD16-mediated IFN-gamma production and antibody-dependent cellular cytotoxicity in human NK cells. *J Immunol* 181: 3784-3792.
142. Guerra, N., Y. X. Tan, N. T. Joncker, A. Choy, F. Gallardo, N. Xiong, S. Knoblauch, D. Cado, N. M. Greenberg, and D. H. Raulet. 2008. NKG2D-deficient mice are defective in tumor surveillance in models of spontaneous malignancy. *Immunity* 28: 571-580.
143. Eisele, G., J. Wischhusen, M. Mittelbronn, R. Meyermann, I. Waldhauer, A. Steinle, M. Weller, and M. A. Friese. 2006. TGF-beta and metalloproteinases differentially suppress NKG2D ligand surface expression on malignant glioma cells. *Brain : a journal of neurology* 129: 2416-2425.
144. Park, Y. P., S. C. Choi, P. Kiesler, A. Gil-Krzewska, F. Borrego, J. Weck, K. Krzewski, and J. E. Coligan. 2011. Complex regulation of human NKG2D-DAP10 cell surface expression: opposing roles of the gammac cytokines and TGF-beta1. *Blood* 118: 3019-3027.
145. Roda-Navarro, P., M. Vales-Gomez, S. E. Chisholm, and H. T. Reyburn. 2006. Transfer of NKG2D and MICB at the cytotoxic NK cell immune synapse correlates with a reduction in NK cell cytotoxic function. *Proceedings of the National Academy of Sciences of the United States of America* 103: 11258-11263.
146. Soneoka, Y., P. M. Cannon, E. E. Ramsdale, J. C. Griffiths, G. Romano, S. M. Kingsman, and A. J. Kingsman. 1995. A transient three-plasmid expression system for the production of high titer retroviral vectors. *Nucleic acids research* 23: 628-633.
147. Lathrop, S. K., S. M. Bloom, S. M. Rao, K. Nutsch, C. W. Lio, N. Santacruz, D. A. Peterson, T. S. Stappenbeck, and C. S. Hsieh. 2011. Peripheral education of the immune system by colonic commensal microbiota. *Nature* 478: 250-254.
148. Schenkel, J. M., K. A. Fraser, V. Vezys, and D. Masopust. 2013. Sensing and alarm function of resident memory CD8(+) T cells. *Nature immunology* 14: 509-513.
149. Hanahan, D., and R. A. Weinberg. 2011. Hallmarks of cancer: the next generation. *Cell* 144: 646-674.

150. Derynck, R., R. J. Akhurst, and A. Balmain. 2001. TGF-beta signaling in tumor suppression and cancer progression. *Nature genetics* 29: 117-129.
151. Bronevetsky, Y., A. V. Villarino, C. J. Eisley, R. Barbeau, A. J. Barczak, G. A. Heinz, E. Kremmer, V. Heissmeyer, M. T. McManus, D. J. Erle, A. Rao, and K. M. Ansel. 2013. T cell activation induces proteasomal degradation of Argonaute and rapid remodeling of the microRNA repertoire. *The Journal of experimental medicine* 210: 417-432.
152. Taylor, M. A., K. Sossey-Alaoui, C. L. Thompson, D. Danielpour, and W. P. Schiemann. 2013. TGF-beta upregulates miR-181a expression to promote breast cancer metastasis. *The Journal of clinical investigation* 123: 150-163.
153. Smith, A. L., R. Iwanaga, D. J. Drasin, D. S. Micalizzi, R. L. Vartuli, A. C. Tan, and H. L. Ford. 2012. The miR-106b-25 cluster targets Smad7, activates TGF-beta signaling, and induces EMT and tumor initiating cell characteristics downstream of Six1 in human breast cancer. *Oncogene* 31: 5162-5171.
154. Chhabra, R., Y. K. Adlakha, M. Hariharan, V. Scaria, and N. Saini. 2009. Upregulation of miR-23a-27a-24-2 cluster induces caspase-dependent and -independent apoptosis in human embryonic kidney cells. *PloS one* 4: e5848.
155. Siegel, C., J. Li, F. Liu, S. E. Benashski, and L. D. McCullough. 2011. miR-23a regulation of X-linked inhibitor of apoptosis (XIAP) contributes to sex differences in the response to cerebral ischemia. *Proceedings of the National Academy of Sciences of the United States of America* 108: 11662-11667.
156. Tan, X., S. Wang, L. Zhu, C. Wu, B. Yin, J. Zhao, J. Yuan, B. Qiang, and X. Peng. 2012. cAMP response element-binding protein promotes gliomagenesis by modulating the expression of oncogenic microRNA-23a. *Proceedings of the National Academy of Sciences of the United States of America* 109: 15805-15810.
157. Hayashi, H., Y. Inoue, H. Tsutsui, H. Okamura, K. Nakanishi, and K. Onozaki. 2003. TGFbeta down-regulates IFN-gamma production in IL-18 treated NK cell line LNK5E6. *Biochemical and biophysical research communications* 300: 980-985.
158. Hamann, D., P. A. Baars, M. H. Rep, B. Hooibrink, S. R. Kerkhof-Garde, M. R. Klein, and R. A. van Lier. 1997. Phenotypic and functional separation of memory and effector human CD8+ T cells. *The Journal of experimental medicine* 186: 1407-1418.

10. Curriculum vitae

Anoop Chandran P



Currently	Post Doc (since Mar 2014)	Department of Immunology, University of Tübingen.	
Education	PhD (Feb 2008- Jan 2014)	Department of Obstetrics and Gynecology, University of Würzburg. International Fellowship, Graduate School of Life Sciences (GSLS), Würzburg.	
	Master degree (2005-2007)	MSc Biotechnology University of Madras, Chennai, India. CGPA: 5.06 Grade: A+ Overall weighted marks: 72.55%	
	Bachelor degree (2002-2005)	BSc Biochemisty+Chemistry& Zoology University of Kerala, Trivandrum, India. First class Overall marks: 90.2%	
	School Year-12 (2002)	Indian School Certificate Loyola School, Trivandrum, India. Overall marks: 81.5%	
	School Year-10 (2000)	Indian Certificate of Secondary Education Loyola School, Trivandrum, India. Overall marks: 88.4%	
	Research experience	PhD thesis:	Identification and functional characterization of TGF- β inducible, immunosuppressive miRNAs in human CD8+ T cells
Supervisors:		¹ PD Dr. rer. nat. Jörg Wischhusen, Department of Obstetrics and Gynecology, University of Würzburg. ² Prof. Dr. Gunter Meister, Department of Biochemistry, University of Regensburg. ³ Prof. Dr. Utz Fischer, Department of Biochemistry, University of Würzburg.	
BMBF project: (10/2011- 01/2014)		Disorazol-Z conjugates (AEZS125) for targeted (LHRH) receptor dependent therapy of solid tumors.	
MSc thesis: (01/2007-07/2007)		Identification of a transcriptional target of the novel non-coding RNA, M3TR. Dr. Anjali Shiras, National Center for Cell Science (NCCS), Pune, India.	
Summer project: (2006)		Cloning and expression of Bmi-1 in mouse embryonic fibroblast (3T3) cell line. Dr. Anjali Shiras, National Center for Cell Science (NCCS), Pune, India.	
Technical expertise	Molecular biology	DNA, RNA and protein isolation, PCR (single cell, nested, qRT), Northern blotting, Immunoblotting, gene cloning, purification, functional evaluation and CDR cloning of antibodies, site-directed mutagenesis.	
	Immunology	Purification, activation, expansion and culture of peripheral blood cell subsets, hybridoma culture, ELISA, flow cytometry, immunocytochemistry, Antigen-specific CD8 ⁺ T cell & NK cell degranulation and cytotoxicity assays, T cell proliferation assays, ELISPOT, multimer stainings.	
	miRNA biology	Isolation and quantification (qRT-PCR, Northern blotting), deep sequencing- data processing and analysis, miRNA arrays, target prediction, 3' UTR cloning and reporter gene assay, functional assays using miRNA mimics and antagomirs.	
	Cell biology	Animal cell culture, solid tumor & ascites handling, cell cycle analysis, metabolic activity assay (XTT, WST) viral transduction, transfection & nucleofection, gene overexpression and silencing, Luciferase assays.	
	Computer skills	Flowjo, Past, Prism (Graphpad), MS office, CorelDRAW X5, MacOS, Linux and Windows.	

Research papers

'The TGF- β -inducible miR-23a cluster attenuates IFN- γ levels and antigen-specific cytotoxicity in human CD8⁺ T cells', **Chandran P.A**, Wischhusen J and colleagues. *Journal of Leukocyte Biology*. 2014 Oct.

Omega-3 fatty acid concentrate from *Dunaliella salina* possesses anti-inflammatory properties including blockade of NF- κ B nuclear translocation. Chitransjali T, **Chandran PA**, Kurup GM. *Immunopharmacology and immunotoxicology* (In revision).

Whole miRNome-wide differential co-expression of microRNAs. Stähler CF, Keller A, Leidinger P, Backes C, **Chandran A**, Wischhusen J, Meder B, Meese E. *Genomics Proteomics Bioinformatics*. 2012 Oct

Ectonucleotidases CD39 and CD73 on OvCA cells are potent adenosine-generating enzymes responsible for adenosine receptor 2A-dependent suppression of T cell function and NK cell cytotoxicity. Häusler SF, Montalbán del Barrio I, Strohschein J, **Chandran P A**, Engel JB, Höning A, Ossadnik M, Horn E, Fischer B, Krockenberger M, Heuer S, Seida AA, Junker M, Kneitz H, Kloor D, Klotz KN, Diel J, Wischhusen J. *Cancer Immunol Immunother*. 2011 Oct

A specific miRNA signature in the peripheral blood of glioblastoma patients. Roth P, Wischhusen J, Happold C, **Chandran PA**, Hofer S, Eisele G, Weller M, Keller A. *J Neurochem*. 2011 Aug

Whole blood-derived miRNA profiles as potential new tools for ovarian cancer screening. Häusler SF, Keller A, **Chandran PA**, Ziegler K, Zipp K, Heuer S, Krockenberger M, Engel JB, Höning A, Scheffler M, Diel J, Wischhusen J. *Br J Cancer*. 2010 Aug

Relevant activities

Oral presentation: 'Role of miRNAs in TGF- β signaling in immune cells', Fellow Retreat 2008, Graduate School of Life Sciences at Schloss Zeilitzheim, Germany.

'miRNA profile in human CD8⁺ T cells after TGF- β treatment', GP Immunomodulation annual retreat 2010, Kloster Schöntal, Germany.

Poster presentation: Brupbacher Symposium 2013, Zurich, Switzerland.

15th International Summer School on Immunology, Immune System: Genes, Receptors and Regulation by Federation of European Biochemical Societies (FEBS) 05-12/09/2009, Hvar, Croatia.

Summer School on Gene regulation, cell differentiation and tolerance by Medizinische Hochschule, Hannover. 12-14/09/2010, Hessenkopf, Goslar

5th International Symposium 'CHIASMA- on the crossroads of research', by Graduate School of Life Sciences, University of Würzburg. 13-14/10/2010, Würzburg, Germany.

International Symposium on Frontiers in Tumor Immunology: Innovative Immunotherapies. University of Tübingen, 02-03/05/2011, Tübingen, Germany.

Workshops & conferences: 3rd International Symposium by Graduate School of Life Sciences, University of Würzburg. 08/10/2007, Würzburg, Germany

International Symposium, 'Living with Pathogens- Never lose control'. Collaborative Research Center SFB 479, 16-18/07/2009, University of Würzburg, Würzburg, Germany.

Compact course on laboratory animals, animal experiments and alternatives 05-11/03/2008, Charité- Universitätsmedizin Berlin and ZEBET/BfR, Berlin Germany.

Skills & Hobbies

Soft skill courses: Workshop on Presentation Technique, 4-5/12-2007, Würzburg. Catalogue and Database Research course, 15/05/2008, Würzburg. Workshop on Writing for Publication, with Amy Scammell, 15/01/2010.

Languages: English, Malayalam, Hindi, Tamil, German (Intensivkurs Grundstufe)

Sports: Badminton (TSG 1, Tübingen), Table tennis, Frisbee.

Hobbies: Shrimp and fish keeping, movies, Indian music.

Others: Driving license (Class B- Germany)

Date:

Place:

Anoop Chandran P